Università degli Studi di Padova

DIPARTIMENTO DI INGEGNERIA INDUSTRIALE
Corso di Laurea Magistrale in Ingegneria Elettrica

Tesi di laurea magistrale

Earth fault current distribution on transmission networks

Candidato:
Matteo Celin
Matricola 1058214

Relatore:
Prof. Roberto Turri

Correlatore:
Dr. Huw Griffiths

Anno Accademico 2014-2015

Contents

Abstract

Ensure the safety of people is of primary importance during the design of substation earthing systems; in particular due to the electrocution risk which may occur during the clearing of possible faults within the electrical transmission network.
Short-circuit faults, during the normal operation of the high voltage system, may occur at a single unknown point of the grid or at the same time, at more points, making even harder to ensure the safety.
The current flow created during a line-to-earth short-circuit is distributed around the fault point, through the soil, metal structures, along passive conductors and also through parts of the network far away from the fault point, such as other substation earthing systems.
The line-to-earth short-circuit is the most frequent type of fault which occurs on transmission networks and due to its unbalance nature, involves the use of the theory of symmetrical components. The short-circuit current value and its distribution depends on:

- Power sources
- Short-circuit impedances
- Fault resistance
- Impedances of the network and its components as transformers, overhead lines or cables
- System configuration

The effects of the earth fault current flow during a short-circuit, may cause the rising of potential in the soil and between earth and metal structures as towers along the overhead lines, or electrical equipment within the high voltage substation areas; the voltage drop in the soil surrounding a grounding system, caused by the soil resistivity variation, may present hazards for personnel standing in the vicinity and personnel stepping in the direction of the voltage gradient.
Knowledge of the earth fault current effects, allows a clear evaluation of possible devices to reduce the risk for the people and to increase the safety level.

Chapter 1

Introduction

The aim of this thesis was the study of the earth fault current distribution and its effects on the UK transmission network, evaluating the partition of the current through the soil, earth wires and tower pylons which carry the three phase conductors in the overhead lines.
When a ground fault occurs on a substation or along an overhead transmission line in a power network with a grounded neutral, the fault current returns through the tower structures, ground return paths and earth wires as shown in fig. 1.1.
Knowledge of this distribution is important at least for two reasons:

- Size selection of an overhead earth wire in order to withstand anticipated fault currents
- Evaluation of voltage rise of faulted structures and related potential safety problem (EPR, Earth Potential Rise)

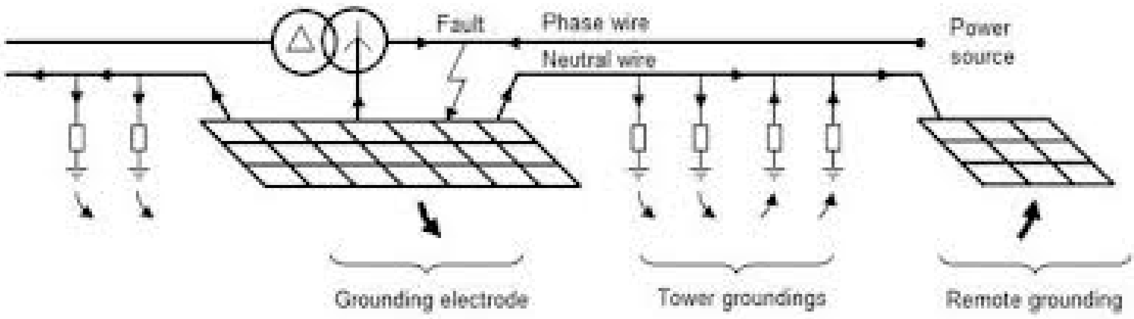

Figure 1.1: Earth fault current distribution on transmission networks

Using software tools as NEPLAN and ATPDraw, in this thesis it was possible:

- Study the UK transmission network behaviour during two different types of fault (line-to-earth and three-phase short-circuit) and analyse the voltage distribution at network substation nodes during the fault
- Analyse the earth current distribution on different network configurations, changing electrical parameters such as soil and tower footing resistance
- Evaluation of earth fault current flows magnitudes, phase angle, contribution of the generators and voltage distribution at the network elements as pylons and earth wires
- Statistic study of Earth Potential Rise (EPR)
- Analysis of fault current distribution through the substation earthing systems in a meshed network

Chapter 2

Transmission network

2.1 Introduction

National Grid Electricity Transmission plc owns the electricity transmission system in England and Wales; its assets comprise a route length of over 7200 kilometers of overhead lines, mainly consisting of double circuits, about 700 kilometers of underground cables and 338 substations at 242 sites. As

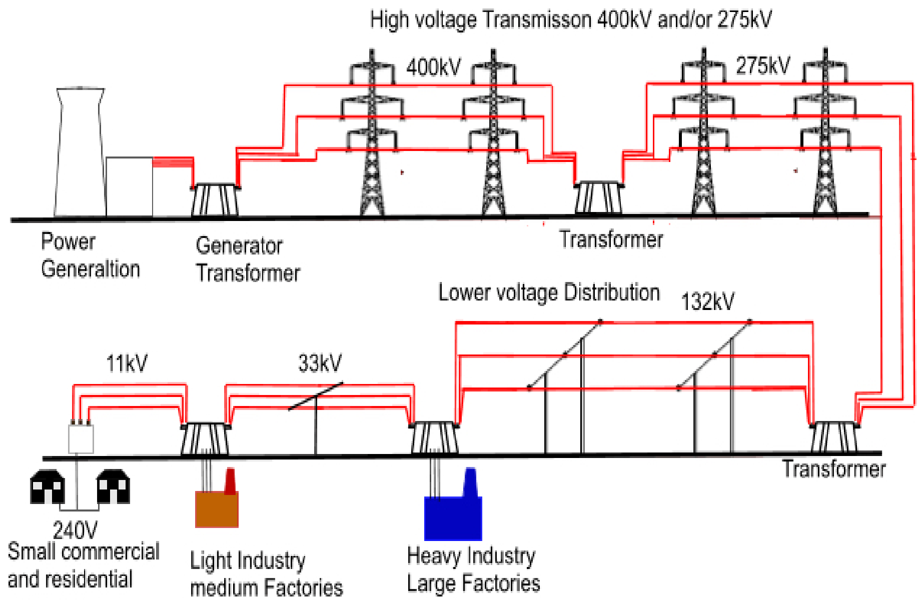

Figure 2.1: Simplified UK electrical power transmission system

an electricity transmission owner, National Grid Electricity Transmission plc owns and maintains the physical assets, development of the networks to accommodate new connections and disconnections, and manage a programme of asset replacement and investments; it is also the national electricity transmission system operator, responsible for managing the operation of both the England and Wales transmission systems and of the two high voltage electricity transmission networks in Scotland, which National Grid does not own.

Day-to-day operation of the Great Britain electricity transmission system involves the continuous realtime matching of demand and generation output, ensuring the stability and security of the power system and the maintenance of satisfactory voltage and frequency.

2.2 Details and components of UK transmission network

The electricity network comprises a mixture of overhead lines and underground cables; in addition there are points on the system, called substations, where voltage transformation takes place and switching and control equipment are located. The interface between electricity transmission and the distribution network operators (DNOs) takes place within these grid substations normally at 132 kV as shown in fig 2.1.
These networks are designed to provide an excellent level of service within a regulatory framework; network design also takes account normal load growth which has historically been around an average of 1.5% to 2% per annum. The main components of a high voltage transmission system are the following:

- **Overhead lines (OHL)** In the UK, transmission networks are constructed using steel towers to support the conductors; these are often referred to as pylons. The OHL support insulators that carry conductors which are usually made of copper or aluminium, based on different sizes to provide different current carrying capabilities. Overhead lines normally connect one large substation to another, with no intermediate connections, and are referred to as routes and these routes connect the network together from generators, at grid supply points to the grid supply substations.

- **Cables** In the UK electricity system cables are installed and operated at all the common voltages used on the electricity network from low voltage (400/230 V) to 400 kV. Lower voltage cables may be installed 0.45 m below the surface while higher voltage cables may be buried at depths of 1 m or more. The length of cables used at the highest transmission voltages is limited due to the substantial costs involved, however as cable voltages reduce, the cost premium compared to an equivalent overhead line falls.

- **Substations** A transmission substation connects two or more transmission lines. The simplest case is where all transmission lines have the same voltage. In such cases, the substation contains high-voltage switches that allow lines to be connected or isolated for fault clearance or maintenance. A transmission substation may have transformers to convert between two transmission voltages, voltage control devices such as capacitors, reactors and equipment such as phase transformers to control power flow. Transmission substations can range from simple to complex; grid transmission substations can cover a large area with multiple voltage levels, many circuit breakers (high voltage switches) and a large amount of protection and control equipment.
  All the high voltage substations are composed by a large earth substation systems with a very low resistance value which has a function of earth potential distribution in case of fault and ensure people safety reducing the Earth Potential Rise (EPR).

- **Transformers** Used to transform voltage from one level to another. Within the transmission systems the most common transformation steps are 400 kV to 275 kV, to 132 kV which supplies the distribution networks which in turn further reduce the voltage to end user requirements. Transformers comprise basically an iron core with copper or aluminium insulated wire coils wrapped around that, further insulated with a mineral oil and housed in a steel tank, with external connection points to the system. The passage of current through the wire coils (windings) causes heating, since no wire is a perfect conductor therefore the insulating oil plays a major part in conducting that heat away. The load carrying capability of the transformer is primarily dictated by the maximum temperature at which the windings and insulation can be operated without causing damage and fault. The greater is the external ambient temperature less heating can be permitted from the windings and consequently the rating is reduced.

- **Earth wire** On the highest part of the tower pylons there are one or more conductors, usually with a lower section then phase conductors, which have two main functions. The first is the lightning protection; the earth wire protects the three-phase system against the lighting strikes which can causes important damages either to the transmission network and to the people who are standing at the overhead line proximity. The second is reducing the global earth resistance of the overhead line; earth wire is usually connected at both sides to the substation earthing systems, this operation ensures a good reducing of fault current and earth substation total impedance which yields a better reduction of the earth potential rise.

2.3 UK transmission system data and interconnection

In the UK there are four transmission systems; one in England and Wales, two in Scotland and one in Northern Ireland each separately and owned. The largest, in terms of line length and share of total transmission is the National Grid Company system, covering England and Wales as shown in fig. 1.3 and 1.2 .

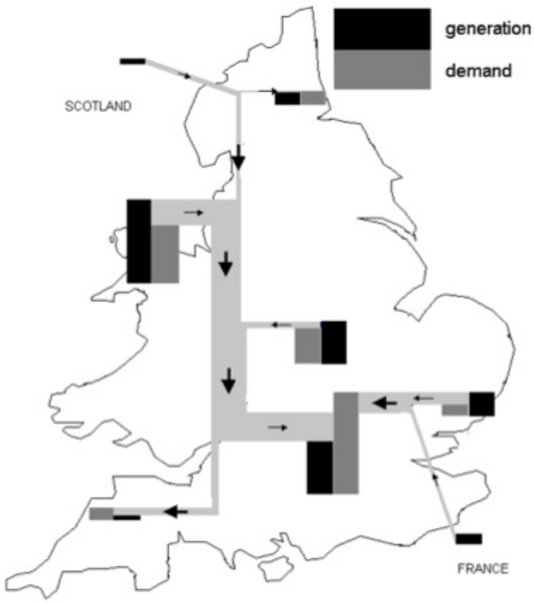

Figure 2.2: Electricity UK flow pattern

Network size

The following data represent the main characteristics of the UK network, all the data were taken according with the Electric Ten Year Statement:

- Maximum demand (2005/2006): 63 GW (approx)(81,39 of capacity)
- Annual electrical energy used in the UK is around 360 TWh
- Capacity: 79,9 GW
- Number of large power stations connected to it: 181
- Length of 400 kV grid: 11.500 km
- Length of 275 kV grid: 9.800 km

Total generating capacity is supplied roughly equally by nuclear, coal fired and gas fired power stations.

Losses

- Joule heating in cables and overhead lines: 857,8 MW
- Fixed losses: 266 MW (consist of corona and iron losses)
- Substation transformer heating losses: 142,4 MW
- Generator transformer heating losses: 157,3 MW

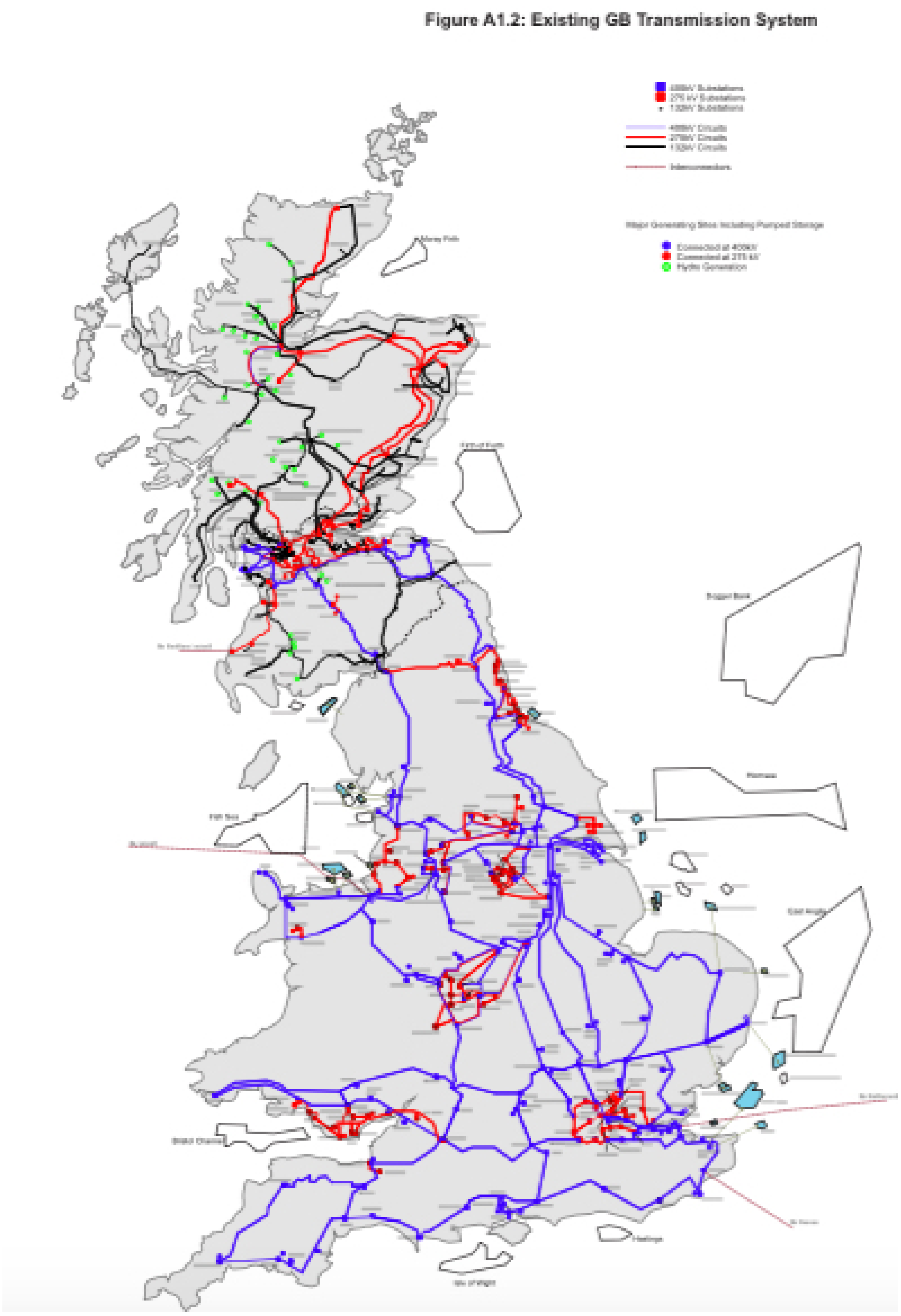

Figure 2.3: Geography UK electric line disposition

Interconnections

The UK grid is connected to adjacent European and Irish electrical grids by submarine power cables, including four links to northern France (HVDC Cross-Channel), Northern Ireland (HVDC Moyle), Republic of Ireland (EastWest Interconnector), the Isle of Man (Isle of Man to England Interconnector), and the Netherlands (BritNed) as shown on fig 2.4. There are also plans to lay cables to link the UK with Iceland and Norway (ScotlandNorway interconnector) in the future.

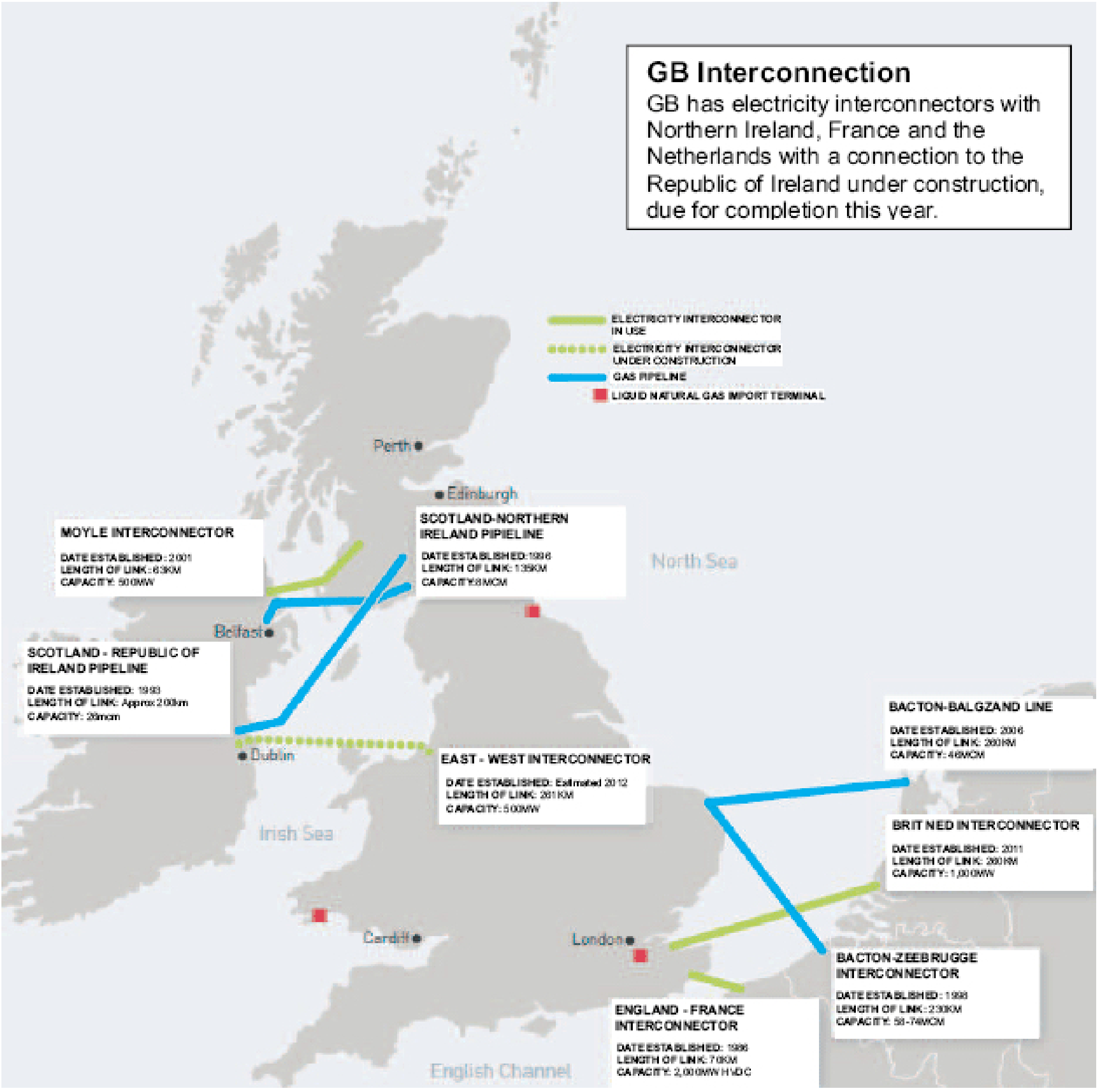

Figure 2.4: UK transmission power system interconnections

Chapter 3

Earthing system

3.1 Introduction

The current during a short circuit can flow, as we know, through the earthing system of the faulted substation but can flow back through the soil, up through the tower pylons and the earth wire which is connected to both substations as shown in fig. 3.1.

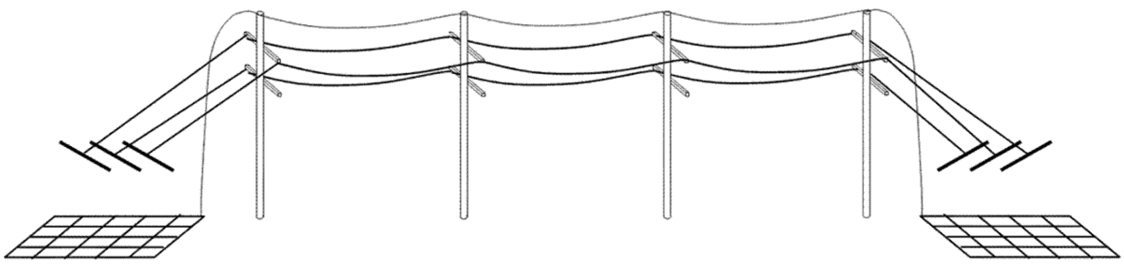

Figure 3.1: Overhead earth-wire connected to the substation earthing systems

Overhead earth wire, as said previously, has two important functions. It carries away a percentage of the fault current (more or less 30-40 %) from the fault point, which depends on the overhead earth wire type, tower footing resistances of adjacent pylons and it also reduces the total earth substation impedance which yields a reducing of the EPR (Earth Potential Rise) in case of fault at a high voltage substation. A grounding system generally comprises several horizontal, vertical or inclined electrodes buried or driven into the earth to reduce the 50 Hz power-frequency earth resistance. The grounding system design of a substation depends largely on the voltage level and the size of the station, and the most common types of electrodes are vertical rods, horizontal earth conductors radiating from one common point, or a meshed network. It is common to combine these types of design if the soil conditions within the substation area changes substantially, and to optimize the performance of the grounding system. The most common grounding design for outdoor substations is a meshed network, often combined with vertical rods as shown in fig. 3.2.

The grounding system shall be dimensioned to withstand corrosion and mechanical stress throughout the lifetime of the electrical installation.
Relevant parameters for the design of grounding systems are:

- Value of fault current
- Fault duration
- Soil properties

Fault current value and fault duration are dependent on the neutral point connection to earth of the high voltage installation; the grounding system comprises earth electrodes, earth conductors and protective bonding conductors.

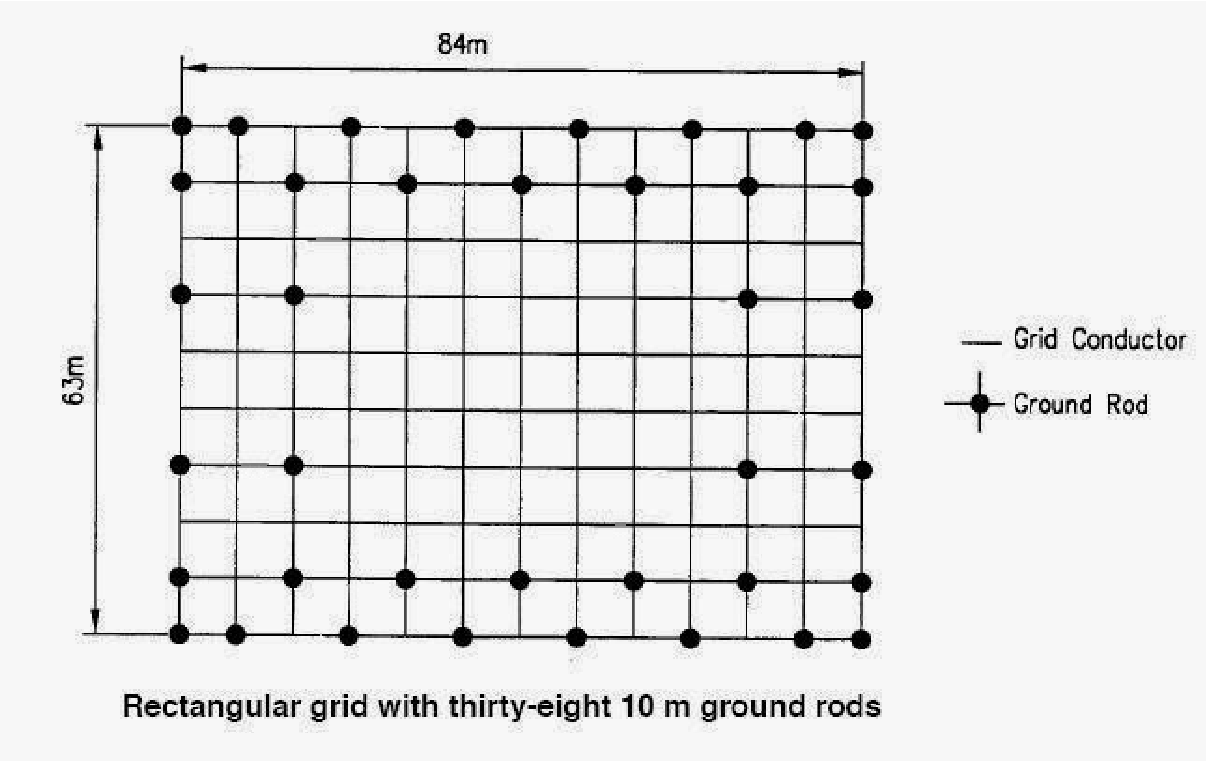

Figure 3.2: Top view of a common grounding system design for HV substations

3.2 EPR, Earth Potential Rise

Earth Potential Rise (EPR) or Ground Potential Rise (GPR) is a phenomenon that occurs when large amounts of electricity enters the earth. This is typically caused when substations or high-voltage towers fault, or when lightning strikes occurs. When currents of large magnitude enters the earth from a grounding system, not only the grounding system will rise in electrical potential, but the surrounding soil as well; the voltages produced by a Earth Potential Rise event can be hazardous to both personnel and equipment.
Soil has resistance known as soil resistivity ρ which will allow an electrical potential gradient or voltage drop to occur along the path of the fault current in the soil; the resulting potential differences cause currents to flow into any and all nearby grounded conductive bodies, including concrete, pipes, copper wires and people. The earth potential rise (EPR) is defined as the voltage between a grounding system to remote earth; the initial design of a grounding system can be based on the EPR, which can be calculated from the formula here reported below :

$$U_E = R_E * I_E$$

- R_E Resistance to earth, calculated or measured [Ω]
- I_E Earth fault current [A]

3.3 Substation grounding theory

The substation earthing system shall be dimensioned and installed in such a way that during a fault in the electrical installation, no danger o life, health or material shall occur neither inside nor outside the installation.
The grounding system shall be constructed to fulfill the following demands, which are applied to all voltage levels:

- Provide the ground connection for the grounded neutral transformers, reactors and capacitors

- Provide a means of discharging and de-energizing equipment to proceed with maintenance on the equipment
- Provide personnel safety against dangerous touch voltages at highest earth fault current
- Prevent damage to property and installations
- Be dimensioned to withstand corrosion and mechanical stress during the entire lifetime of the installation
- Be dimensioned to withstand the thermal stress from fault currents
- Provide a sufficiently low resistance path to ground to minimize rise in ground potential respect to remote ground

The risk connected to electric shock to human beings depends on the current flowing through the heart region and on the magnitude which may cause auricular fibrillation.
The "current-through-body" limit, is transformed into voltage limits shown in fig. 3.3, in order to be compared to the step and touch voltage values considering the following factors:

- The amount of the current flowing through the heart region
- The body impedance along the current path
- The resistance between the contact spot of the body, for example a metal construction against the hand including glove or feet including shoes
- The duration of fault

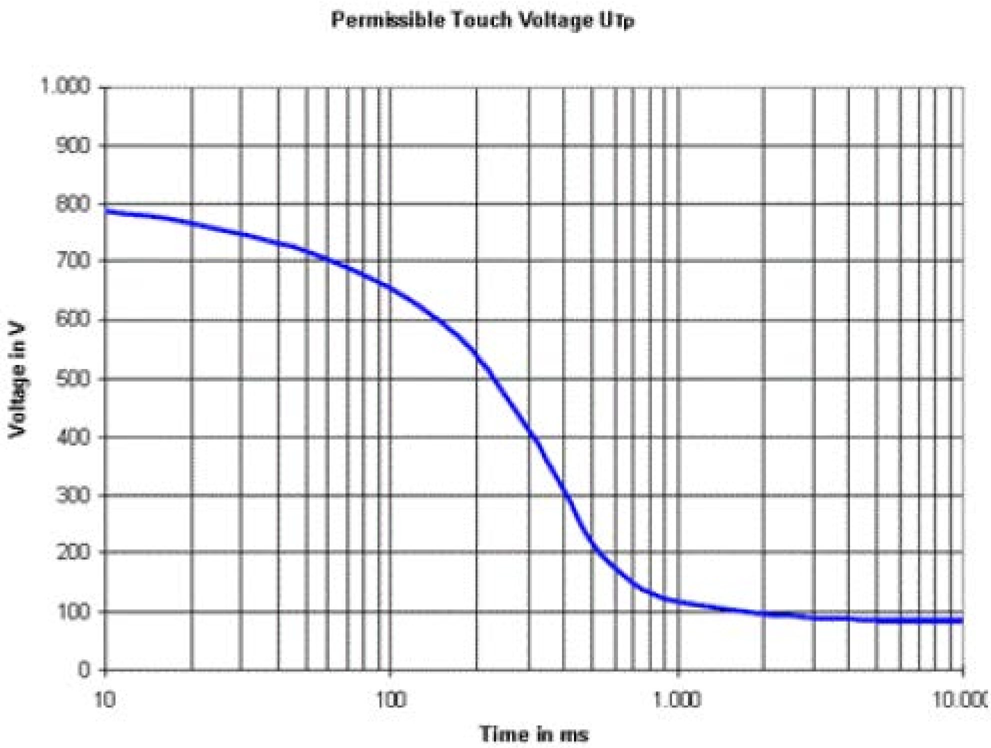

Figure 3.3: Permissible touch voltage

Many factors determine the level of hazard including:

- Available fault current
- Soil type
- Soil structure
- Temperature
- Underlying rock layers
- Clearing time to interrupt the fault

3.3.1 Soil resistivity

Soil resistivity is a measure of how much the soil resists to the flow of electricity; it is a critical factor in design of systems that rely passing current through the earth surface. Knowledge of the soil resistivity and how it varies with depth in the soil is necessary to design the grounding system in an electrical high voltage substation or lightning conductors.
In most substation, the earth is used to conduct fault current when there are ground fault within the system; in single wire earth return power transmission system, the earth itself is used as the path of conduction and in general there is some value above which the impedance of the earth connection must not rise.
The specific resistance (ρ_E) of the soil varies considerably depending on the type of soil, granularity, temperature and density-fluidity content. As can be seen in tab. 3.1. quite large deviations in specific resistance can be observed due to temperature changes and humidity content throughout a year.
The soil at any given substation site is often non-homogeneous due to the fact that the soil consist of several layers; the specific resistance of soil can normally be measured by using a four probe method to determine the resistance to earth (R_E) for earth electrodes. Figure 3.4 shows the distribution of the soil resistance values in all the UK, identifying the range values by different colours.

Formation	Electrical resistivity range
Sea water	0.1 0.3 Ωm
Salted water	0.3 0.9 Ωm
Brackish water	0.9 5 Ωm
Leachate	0.9 5 Ωm
Fresh water	5 80 Ωm
Clay	5 30 Ωm
Wet sand	20 150 Ωm
Sandstone	30 300 Ωm
Limestone	100 800 Ωm
Dry sand	250 4000 Ωm
Granite	1000 20,000 Ωm

Table 3.1: Soil resistance ranges

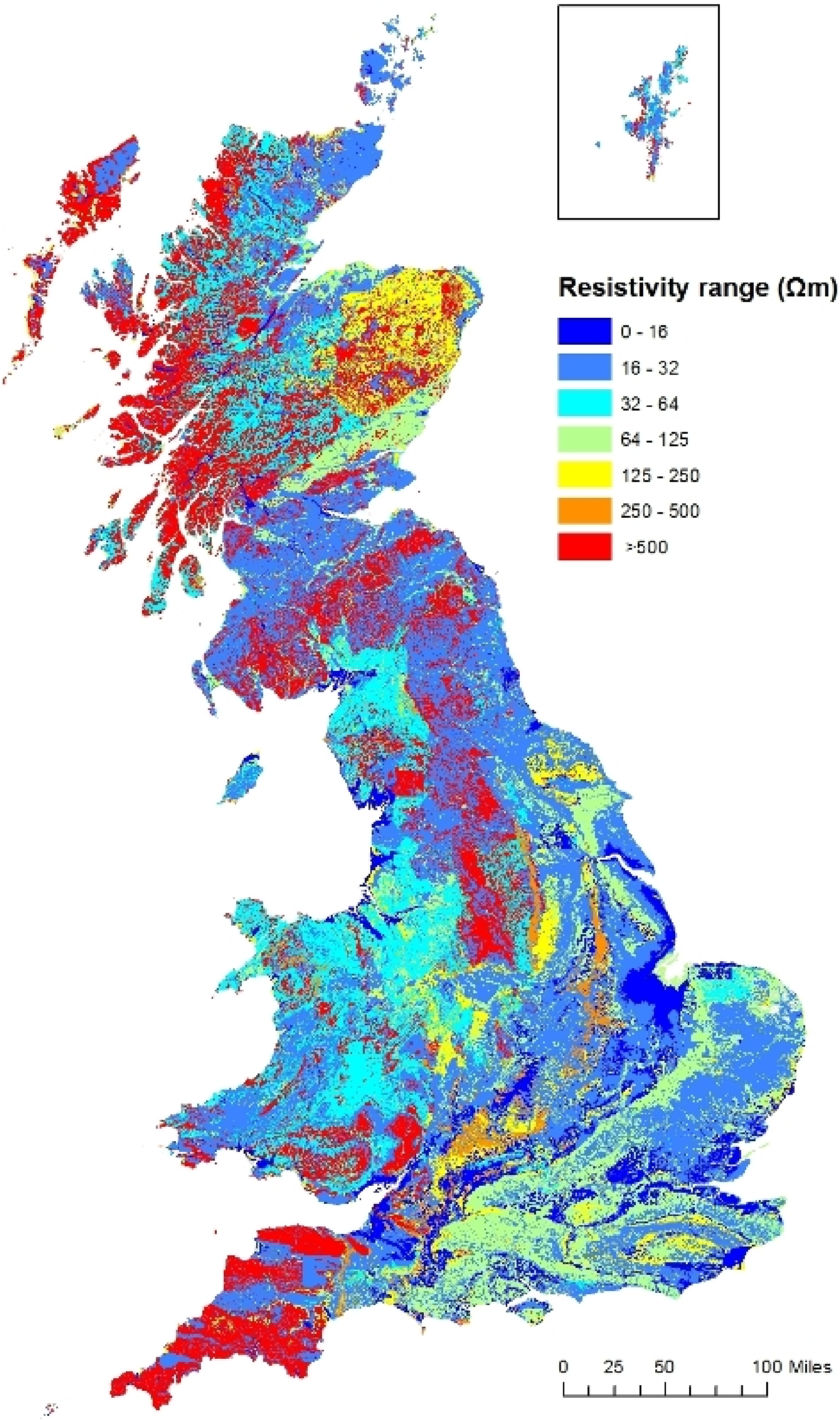

Figure 3.4: UK soil resistance distribution

3.4 Step and touch voltage

Step and touch voltage related to the earth potential rise, play an important role, designing high voltage substations to limit the risk of danger for people who are in proximity or around them or they are touching electrical equipment during a short-circuit fault. Figures 3.5 and 3.6 give an example of touch and step voltage within a substation and how the current splits through the soil and the body.

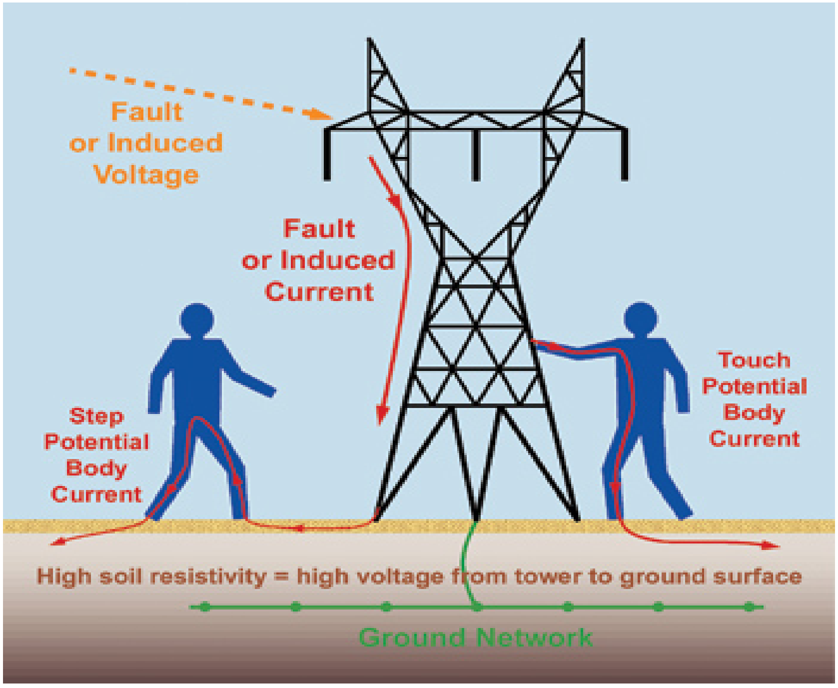

Figure 3.5: Current flows during a line-to-earth short-circuit in case of touch or step voltage

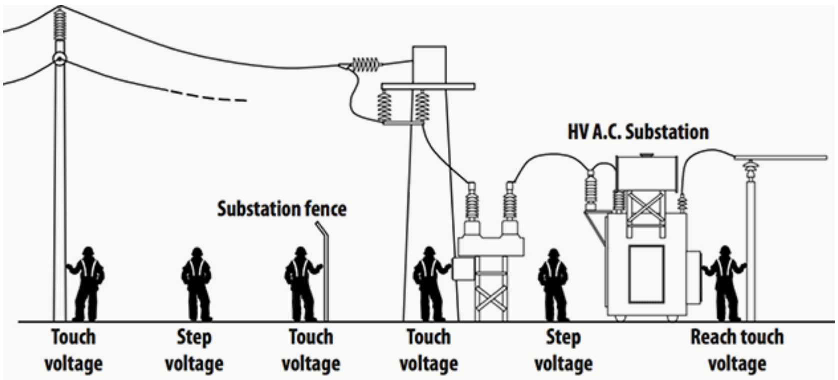

Figure 3.6: Step and touch voltage examples within HV substation and nearby of it

If an electric current passes through the body it can destruct the tiny electrical impulses that travel through the body's nervous system to control the heart and muscles motion.

3.4.1 Step voltage

Step voltage is the voltage between the feet of a person standing near an energized ground object shown in fig. 3.7. It is equal to the difference in voltage, given by the voltage distribution curve, between two points at different distance from the electrode; a person could be a risk of injury during a fault simply by standing near the grounding point.

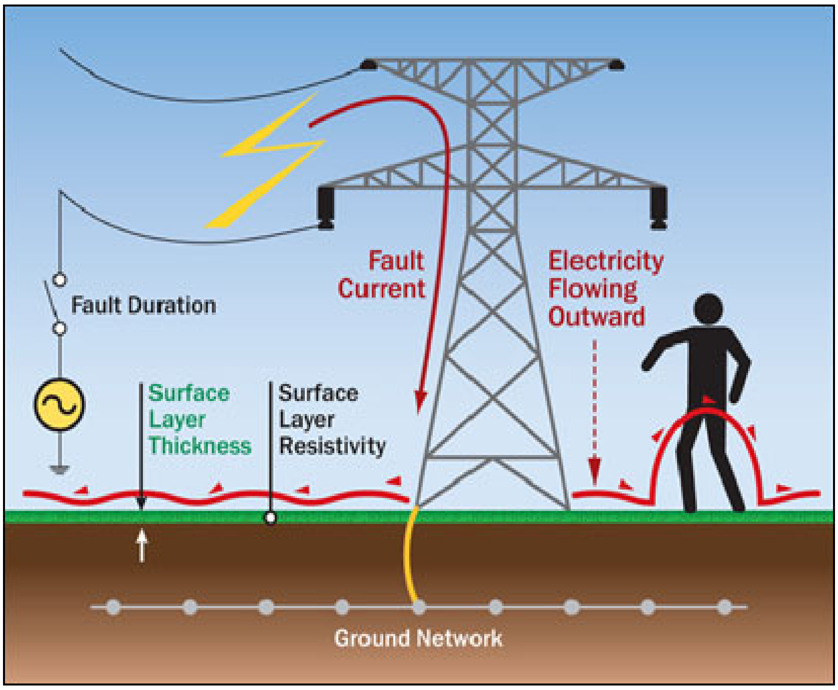

Figure 3.7: Step voltage during a phase-to-earth short-circuit

In the case of step potentials or step voltages, electricity flows if a difference in potential exists between the two legs of a person; the calculations must be performed to determine how great are the tolerable step potentials and then they have to be compared to the step voltages expected at the site.
Hazardous step potentials or step voltage can occur a significant distance away from any given site; more current that is pumped into the ground, the greater is the hazard and soil resistivity and layering plays a major role in how hazardous a fault occurring on a specific site may be.
High soil resistivity tend to increase step voltages; the worst case scenario occurs when the soil has conductive top layers and resistive bottom layers. In this case, the fault current remains in the conductive top layer for much greater distances away from the electrode.

3.4.2 Touch voltage

Touch voltage is the voltage between the energized object and the feet of a person in contact with the object as shown in fig. 3.8. It is equal to the difference in voltage between the object and a point some distance away. The touch potential or touch voltage could be nearly the full voltage across the grounded object if that object is grounded at a point remote from the place where the person is in contact with it.

Engineering standards use a one-meter reach distance for calculating Touch Potentials. A two-meter reach distance is used when two or more objects are inside the EPR event area. For example, a person could be out-stretching both arms and touching two objects at once such as a tower leg and a metal cabinet. The selection of where to place the reference points used in the touch potential or touch voltage calculations are critical in getting an accurate understanding of the level of hazard at a given site. The actual calculation of touch potentials uses a specified object (such as a tower leg) as the first reference point; this means that the further away from the tower the other reference point is located, the greater the difference in potential is.

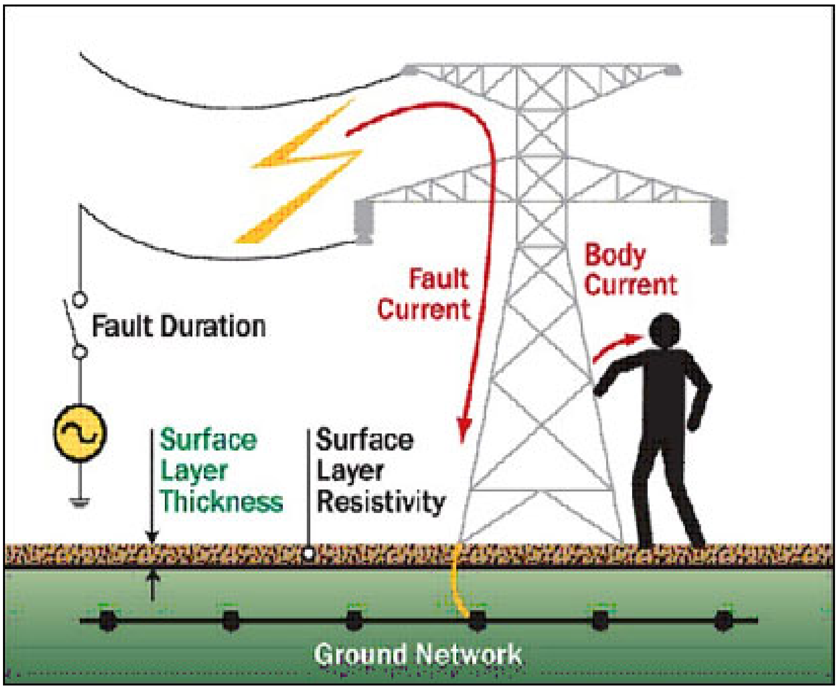

Figure 3.8: Touch voltage during a line-to-earth short-circuit

3.5 Procedures for step and touch voltage reduction

Mitigating step and touch voltage hazards are usually accomplished through one or more of the following three main techniques:

- Reduction in the resistance to ground of the grounding system
- Proper placement of ground conductors
- The addition of resistive surface layers

Understanding the proper application of these techniques is the key to reduce and eliminate any earth potential rise hazards; only through the use of highly sophisticated 3-dimensional electrical simulation software that can model soil structures with multiple layers and finite volumes of different materials, the engineer can accurately model and design a grounding system that will safely handle high-voltage electrical faults.
Although personal safety is of primary concern, effect of electric current, resistance of human body and tolerable voltage criteria considerations are also essential in the design system to ensure the protection of personal equipment. The design for substation grounding system is considered for worker's safety in normal state and in case of fault with an high current flow to substation grounding or approached area. Several methods may be used to protect employees from hazardous ground-potential gradients, including equipotential zones, insulating equipment, and restricted work areas:

- The creation of an equipotential zone will protect a worker standing within it from hazardous step and touch potentials. Such a zone can be produced through the use of a metal mat connected to grounded object; in some cases, a grounding grid can be used to equalize the voltage within the grid. Equipotential zones will not, however, protect employees who are either wholly or partially outside the protected area.
- Use insulating equipment, such as rubber gloves, can protect employees handling grounded equipment and conductors from hazardous touch potential. The insulating equipment must be rated for the highest voltage that can be impressed on the grounded objects under fault conditions (rather than the full system voltage).

The purpose of grounding system at a substation includes:

- Provide the ground connection for the grounded neutral transformer reactors and capacitors
- Ensure safety to operating personal by limiting potential differences that can exist in a substation
- Provide a means of discharging and de-energizing equipment to proceed with maintenance on the equipment
- Provide a sufficiently low resistance paths to ground to minimize the rise in ground potential with respect to remote ground.

Chapter 4

IEC 60909-0 short-circuit current calculation

4.1 Introduction

Most of the softwares used for electrical networks design or power flows calculation, conductors section sizing and electrical risk analysis use more than one standard specially for the short circuit current calculation. In this chapter it's explained a particular standard type for the short-circuit current calculation during a particular type of fault; this explanation allows to understand the method with which NEPLAN software calculates the short-circuit currents in a determinate point of the network using the theory of the symmetrical components.
This standard, is explained in the IEC 60909-0; IEC, International Electrotechnical commision is a worlwide organization wich promote international co-operation on all question concerning standardization in the electrical and electronic field.
This particular standard calculation is applicable to the analysis of short-circuit currents:

- Low-voltage three-phase systems
- High-voltage three-phase systems

operating at a nominal frequency of 50 Hz or 60 Hz. For this calculation, an equivalent voltage source is introduced and it is possible the calculation of short-circuit currents in case of balanced or unbalanced short-circuits like those shown in fig. 4.1 except the case of a single line-to earth fault, occurring in an isolated neutral earthed system or a resonant earthed neutral system because this fault is beyond the scope of this standard.
The calculation of the short-circuit impedances is in general based on the rated data of the electrical equipment and the topological arrangement of the system; it has the advantage of being possible either for existing systems and for systems at the planning stage.
In general, two short-circuit currents, with different magnitude, can be calculated:

- Maximum short-circuit current which determines the capacity or rating of electrical equipment
- Minimum short-circuit current which can be, for example, for the selection of fuses, for the setting of protective devices, and for checking the run-up motors

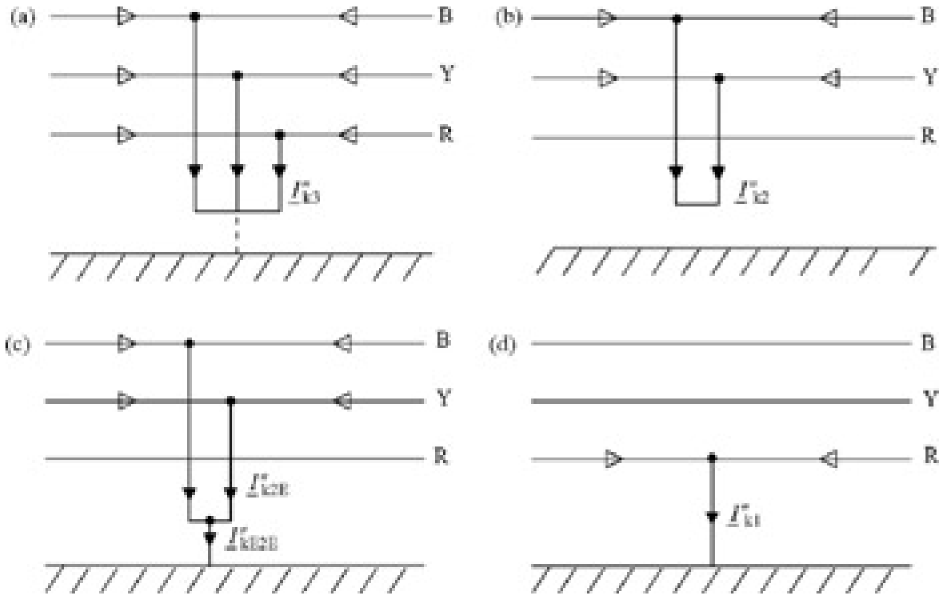

Figure 4.1: Characterization of the short-circuits

4.2 Definitions and short circuit types

Short circuit
Accidental or intentional conductive path between two or more conductive parts forcing the electric potential differences between these conductive parts to be equal or close to zero.
Short circuits are also divided in:

- Balanced short-circuit (only three-phase short-circuits)
- Unbalanced short-circuit

4.2.1 Symmetrical components theory

For unbalance conditions the calculation of the fault current si more complex; one method of dealing that is by the use of symmetrical components. In the symmetrical components theory, the unbalance system is broken down into three separate symmetrical systems, each of which is easily solved. The theory of symmetrical component says that any set of three vectors (currents for example) can be decomposed in three set of three vectors called the three symmetrical component systems as shown in fig. 4.2 and they are:

- Positive-sequence current $I_{(1)}$ that consists of three vectors which rotate in anticlockwise direction
- Negative-sequence current $I_{(2)}$ that consists of three vectors which rotate in clockwise direction
- Zero-sequence current $I_{(0)}$ that consists of three vectors in the same phase position

Considering the line conductor L1 as reference, the currents $I1$, $I2$ and $I3$ are given by:

$$I1 = I1_{(1)} + I1_{(2)} + I1(0)$$

$$I2 = a^2 I2_{(1)} + aI2_{(2)} + I2(0)$$

$$I3 = aI3_{(1)} + a^2 I3_{(2)} + I3(0)$$

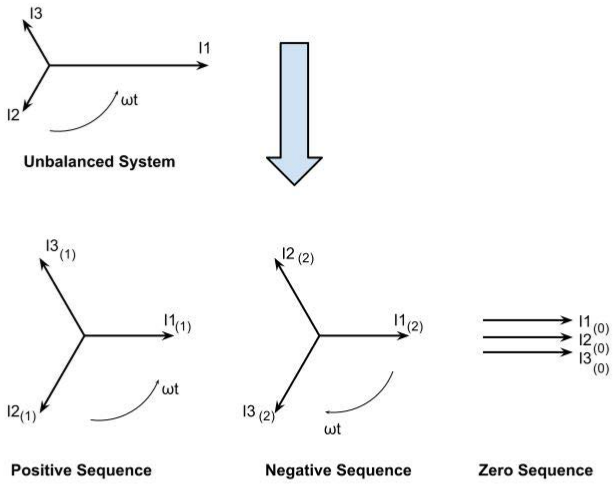

Figure 4.2: Decomposition of a 3-phase unbalanced current vectors

where the operator a is defined as :

$$a = e^{\frac{2}{3}\pi i}$$

The type of short circuit which leads to highest short-circuit current depends on the value of the positive-sequence, negative-sequence, and zero-sequence short circuit impedances of the system components, which are calculated considering the ratio between the voltage and the current values assummed when to those components are applied positive sequence, negative sequence and zero sequence voltage sources.
For the calculation of the initial symmetrical short-circuit current $I_k^{"}$,I_b and I_k at the short circuit location, the system may be converted by network reduction into an equivalent short-circuit impedance Z_k at the short circuit location that is made up of the impedances (zero, positive-sequence, negative-sequence depending on which kind of short-circuit current has to be calculated) of the lines, sources, devices (power systems), electrical equipments, loads or generators.
Calculations are simplest for balanced short-circuits on radial systems due to the contribution of the short-circuit current which can be evaluated separately for each source; when the network is meshed, the sources are distributed or if there is an unbalanced short circuit, it is necessary to calculate short-circuit impedances $Z_1 = Z_2$ and Z_0 at the short circuit location.

4.2.2 Short circuit types

Line-to-line short-circuit current
Accidental or intentional conductive path between two or more line conductors with or without earth connection:

- Three-phase short-circuit fig. 4.1-a
- Two-phase short-circuit fig. 4.1-b

Line-to-earth short-circuit current
Accidental or intentional conductive path in a solidly earthed neutral system or an impedance earthed neutral system between a line conductor and the local earth.

- Two-phase-to-earth short-circuit fig 4.1-c
- Phase-to-earth short circuit fig 4.1-d

Far-from generator short-circuit fig. 4.4
Short-circuit during which the magnitude of the symmetrical a.c. component of the prospective short-circuit current remains essentially constant.

Near-to-generator short-circuit fig. 4.3
Short circuit to which at least one synchronous machine contributes to the initial symmetrical short-circuit current which is more than twice the machine's rated current, or a short circuit whose asynchronous motors contribute more than 5% of the initial symmetrical short circuit-current $I_k^{"}$ without motors.

Initial symmetrical short-circuit current $I_k{}^{"}$
R.m.s. value of the a.c. symmetrical component of a prospective short-circuit current, applicable at the instant of short-circuit if the impedance remains at zero-time value.

Decaying (aperiodic) component $i_{d.c.}$ of short-circuit current
Mean value between the top and the bottom envelope of a short-circuit current decaying from an initial value to zero.

Peak short-circuit current i_p
Maximum possible instantaneous value of the prospective short-circuit current.

Symmetrical short-circuit breaking current I_b
R.m.s. value of an integral cycle of the symmetrical a.c. component of the prospective short-circuit current at the instant of the contact separation of the first pole to open of a switching device.

Steady-state short-circuit current I_k
R.m.s. value of the short-current which remains after the decay of transient phenomena.

Nominal system voltage U_n
Voltage(line-to-line) by which a system is designated, and to which certain operating characteristics are referred.

Equivalent voltage source $cU_n/\sqrt{3}$
Voltage of an ideal source applied at the short-circuit location in the positive-sequence system for calculating the short-circuit current; this is the only active voltage of the network.
All the current types can be read in the fig. 4.3 and the factor c for equivalent voltage source can be chosen knowing the network nominal voltage and characteristics; in our case, since this study is focused on transmission networks which normally have a nominal voltage of 275 kV or 400 kV the c factor values are:

- c=1.0 for minimum short-circuit current calculations
- c=1.1 for maximum short-circuit current calculations

4.3 Calculation method

General

A complete calculation of short-circuit currents should give the currents as a function of time at the fault location from the beginning of the short-circuit up to its end. Depending on the type of short-circuit there are two cases which can be studied:

- Far-from-generator short-circuit fig. 4.4
- Near-to-generator short-circuit fig. 4.3

Depending on the application of the results, it is of interest to know the r.m.s. value of the symmetrical a.c component and peak value i_p of the short-circuit current following the occurrence of a short circuit. The highest value i_p depends on the time constant of the decaying aperiodic component and the frequency f, that is on the ratio R/X or X/R of the short-circuit impedance $\underline{Z_k}$, and it is reached if the short circuit starts at zero voltage; i_p also depends on the decay of the symmetrical a.c. component of the short-circuit current.

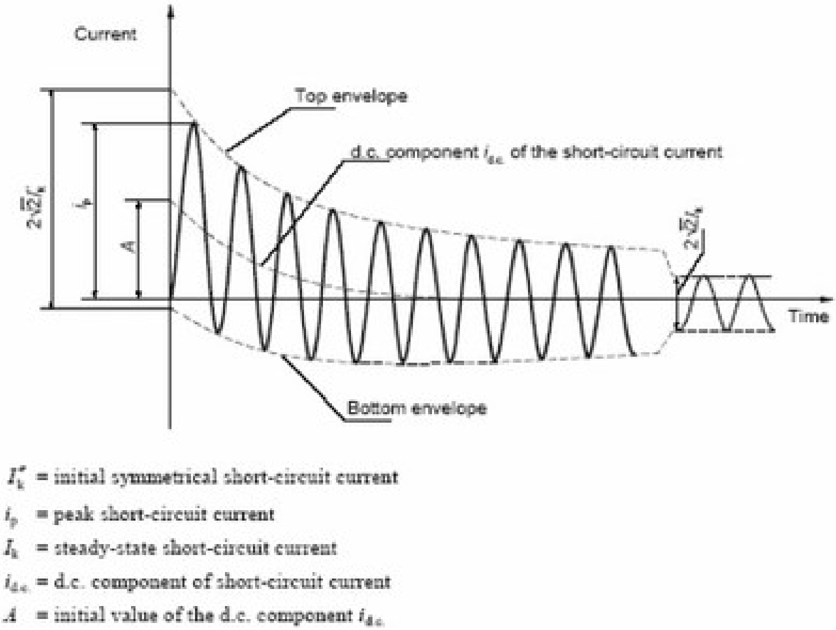

Figure 4.3: Current of a near-to-generator short-circuit with decaying a.c. component

4.3.1 Short-circuit currents calculation

In case of a far-from generator short-circuit, the short-circuit current can be considered as sum of the following two components:

- The a.c. component with constant amplitude during the whole short-circuit
- The aperiodic d.c. component beginning with an initial value and decaying to zero.

Figure gives schematically the general course of the short-circuit current in the case of a far-from-generator short circuit. The symmetrical a.c. currents $I_k^{"}$ and I_k are r.m.s values and are nearly equal in magnitude. In case of a near-to-generator short circuit, the short-circuit current can be considered as the sum of the following components:

- The a.c. component with decaying amplitude during the short-circuit,
- The aperiodic d.c. component beginning with an initial value and decaying to zero. In the calculation of the short-circuit currents in a systems supplied by generators, power stations units and motors, it is of interest not only to know the initial symmetrical short circuit current $I_k^{"}$ and the peak short-circuit current i_p, but also the symmetrical short-circuit breaking current I_b and the steady-state short-circuit current I_k. In this case, the symmetrical short-circuit breaking current I_b is smaller than the initial symmetrical short-circuit current $I_k^{"}$ and the steady-state short-circuit current I_k is smaller than the symmetrical short-circuit breaking current Ib.

4.3.2 Calculation assumptions

The calculation of the maximum and minimum short-circuit currents is based on the following simplification:

a) For the duration of the short circuit there is no change in the type of the short-circuit involved, that is, a three-phase short-circuit remains three-phase and a line-to-earth short circuit remains during the time a line-to-earth short-circuit.

b) For the duration of the short-circuit, there is no change in the network involved.

c) The impedance of the transformer is referred to the tap-changer in main position.

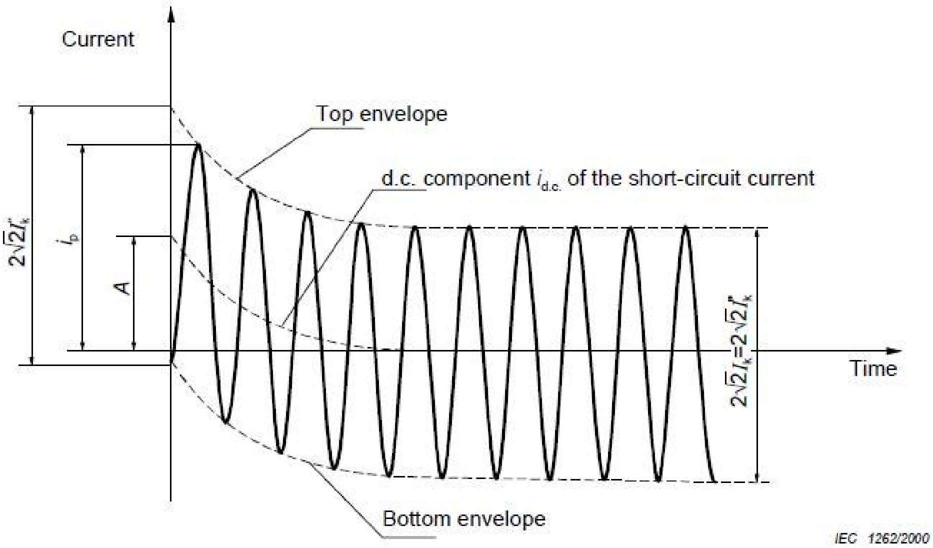

Figure 4.4: Current of a far-from-generator short-circuit with constant a.c. component

d) Arc resistances are not taken into account.

e) All line capacitances, shunt admittances and no-rotating loads, except those of the zero-sequence system, are neglected.

4.3.3 Equivalent voltage source at the short-circuit location

The method used for calculation is based on the introduction of an equivalent voltage source at short-circuit location as shown in fig. 4.5. The equivalent voltage source is the only active voltage of the system, all the network feeders, synchronous machines are replaced by their internal impedances.
In all cases it is possible to determine the short-circuit current at the short circuit location with the help of an equivalent voltage source; additional calculations about all the different possible load flows at the short circuit time are superfluous.

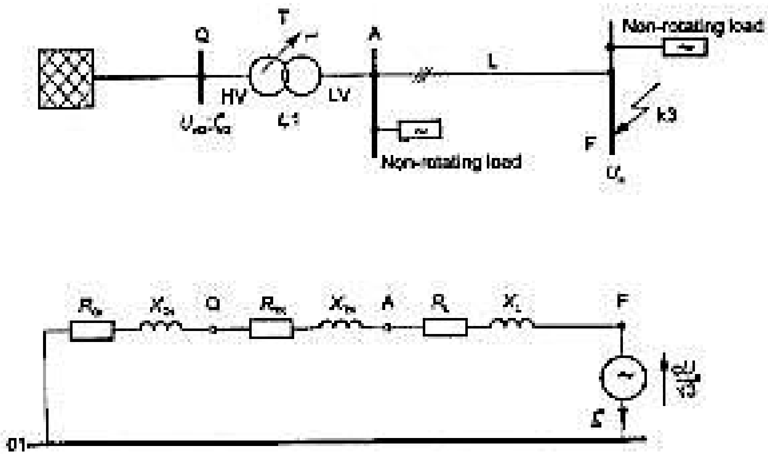

Figure 4.5: Illustration of initial symmetrical short-circuit current $I_k^{''}$ calculation in compliance with the procedure for the equivalent voltage source

4.3.4 Maximum and minimum short-circuit currents

Maximum short circuit currents

To calculate the maximum short-circuit currents, it is necessary to introduce the following conditions:

- Voltage factor c_{max} shall be applied for the calculation of maximum short-circuit current in the absence of a national standard
- Choose the system configuration and the maximum contribution from power plants and network feeders which lead to maximum value of short-circuit current at the short-circuit location, or for accepted sectioning of the network to control the short-circuit current
- When equivalent impedences Z_Q are used to represent the external network, the minimum equivalent short-circuit impedance which corresponds to the maximum short-circuit current contribution from the network feeders shall be used
- Motors shall be included
- Resistance R_L of lines (overhead lines and cables) has to be introduced at a temperature of 20 °C.

Minimum short-circuit currents

To calculate the minimum short-circuit currents, it is necessary to introduce the following conditions:

- Voltage factor c_{min} for the calculation of minimum short circuit currents shall be applied
- Choose the system configuration and the minimum contribution from power stations and network feeders which lead to a minimum value of short-circuit current at the short-circuit location
- Motors shall be neglected
- Resistances R_L of lines (overhead lines and cables, line conductors and neutral conductors) shall be introduced at a higher temperature

$$R_L = [1 + \alpha(\theta_e - 20)] * R_{L20}$$

where:

- R_{L20} is the resistance at a temperature of 20 °C
- θ_e is the conductor temperature in Celsius degrees at the end of the shor-circuit duration;
- α is a factor equal to 0,004/K, valid with sufficient accuracy for most practical purposes for copper, aluminium and aluminium alloy.

4.4 Comments

As explained in this chapter, NEPLAN software calculates, according with IEC standard and taking into account all the standard hypothesis, different short-circuit currents at a given fault point in case of three-phase and line-to-earth short-circuit. For this thesis, since it was done a steady state study of the current distribution and not a transient study, only the steady state short circuit current I_K and also the peak short circuit current I_p have been calculated to have and idea about the maximum magnitude values that can be assumed by the fault currents.
In this chapter what has been treated are the hypothesis which are used on the software calculations; the formulas for the short-circuit currents are different and they change in function of the type of the network, short-circuit, fault current type, network characteristics and components. All of them are function of zero, positive and negative-sequence impedances or their combination. All of them are reported on the IEC standard 60909-0 "*Short-circuit currents in three-phase a.c. systems*" document for each type of fault and current.

Chapter 5

NEPLAN short-circuit analysis

5.1 Introduction

NEPLAN is a high-end power system analysis tool for applications in transmission, distribution, generation, industrial application and it's used in more than 90 countries. NEPLAN is not only available for electrical networks, but offers state-of-the-art analysis method for gas, water and district heating as well. The most user-friendly graphical user interface allows the user to perform study cases very efficiently and it suits best for:

- Power flow studies in meshed networks
- Renewable energy system
- Smart Grid application

Besides steady state calculations, power quality, optimization aspects and protection design, the NEPLAN simulator allows also the controls for dynamic simulations and to integrate Matlab/Simulink models.

5.2 Network analysis

This chapter faces the short-circuit current calculation at different substation busbars. The system model was already available for NEPLAN software and it is represented in fig. 5.1; this model has been built in these years by students step by step knowing the different characteristics of the grid as number of lines ,their geometrical and electrical datas, transformers, substations and generators. The construction of this model was possible thank also to the data-base values present on-line on the NATIONAL GRID web-site which is obliged to provide all the data relative to the network configuration in the Electrical Ten Year Statement ETYS, document which is produced by National Grid in its role as National Electricity Transmission System Operator (NETSO) and aims to provide clarity and transparency on the potential development of the GB transmission system for a range of scenarios.
The document considers the developments through strategic network modelling and design capability, while trying to capture future uncertainty with regards to the generation mix, operation of the network and technology development.
NEPLAN file was relative only to the part of the grid owned by the NATIONAL GRID and not to all the UK network as can be deduced from the lines real disposition an substation connections shown in fig. 5.2 compared to the NEPLAN network model represented in fig. 5.1.

As we know, the power flows in a transmission network are not the same during the day, season or year because of the different loads profile and energy curve demand requested by the customers.
During the whole year, the network, is set as the best configuration to face the changing of the loads and the increment or decrement of the energy demand; day-by-day the Great Britain electricity transmission system operator has to follow in the realtime the continuous matching demand and generation output, ensuring the stability and security of the power system and the maintenance of satisfactory voltage and frequency as explained previously in chapter 1.

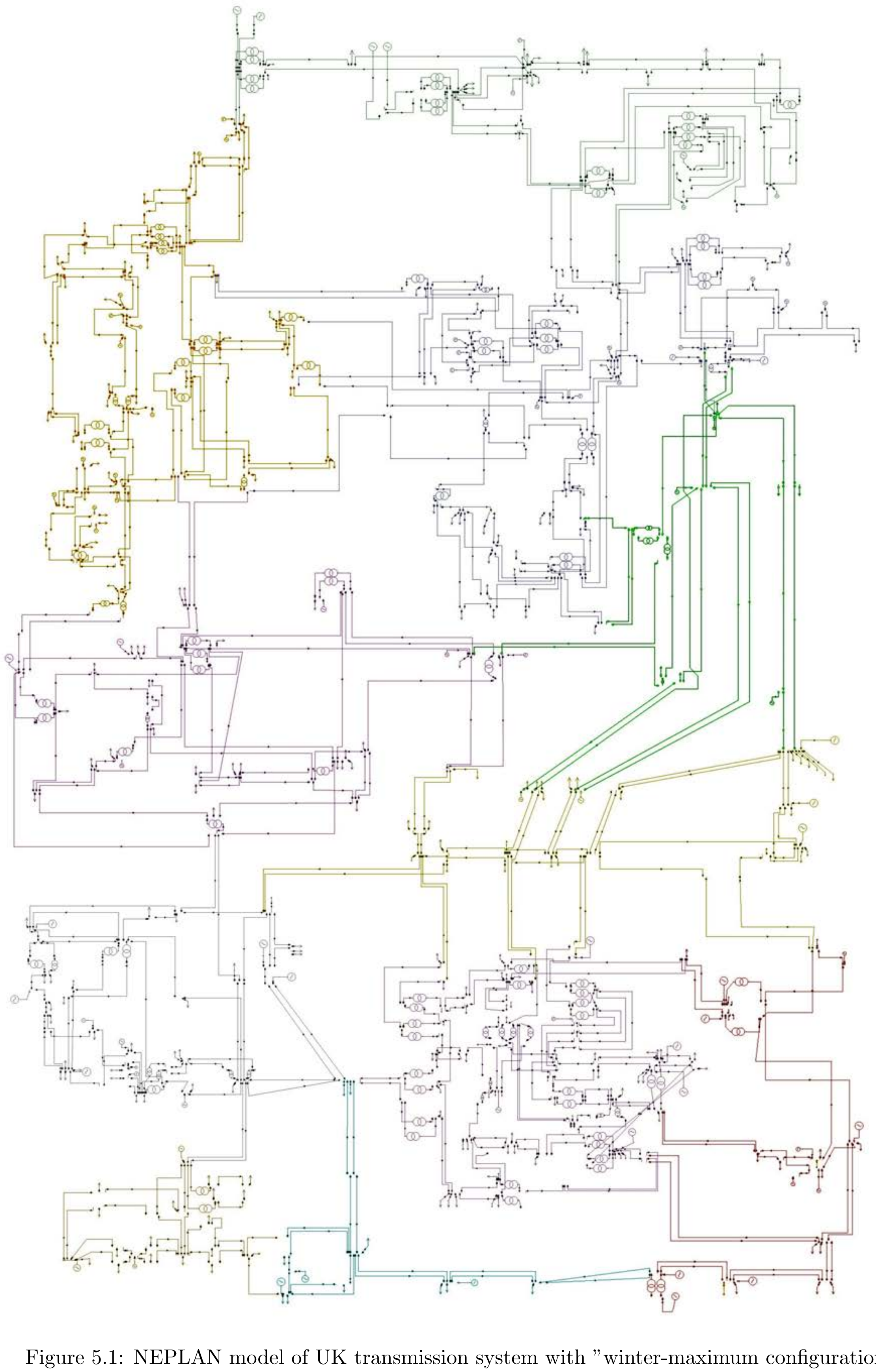

Figure 5.1: NEPLAN model of UK transmission system with "winter-maximum configuration"

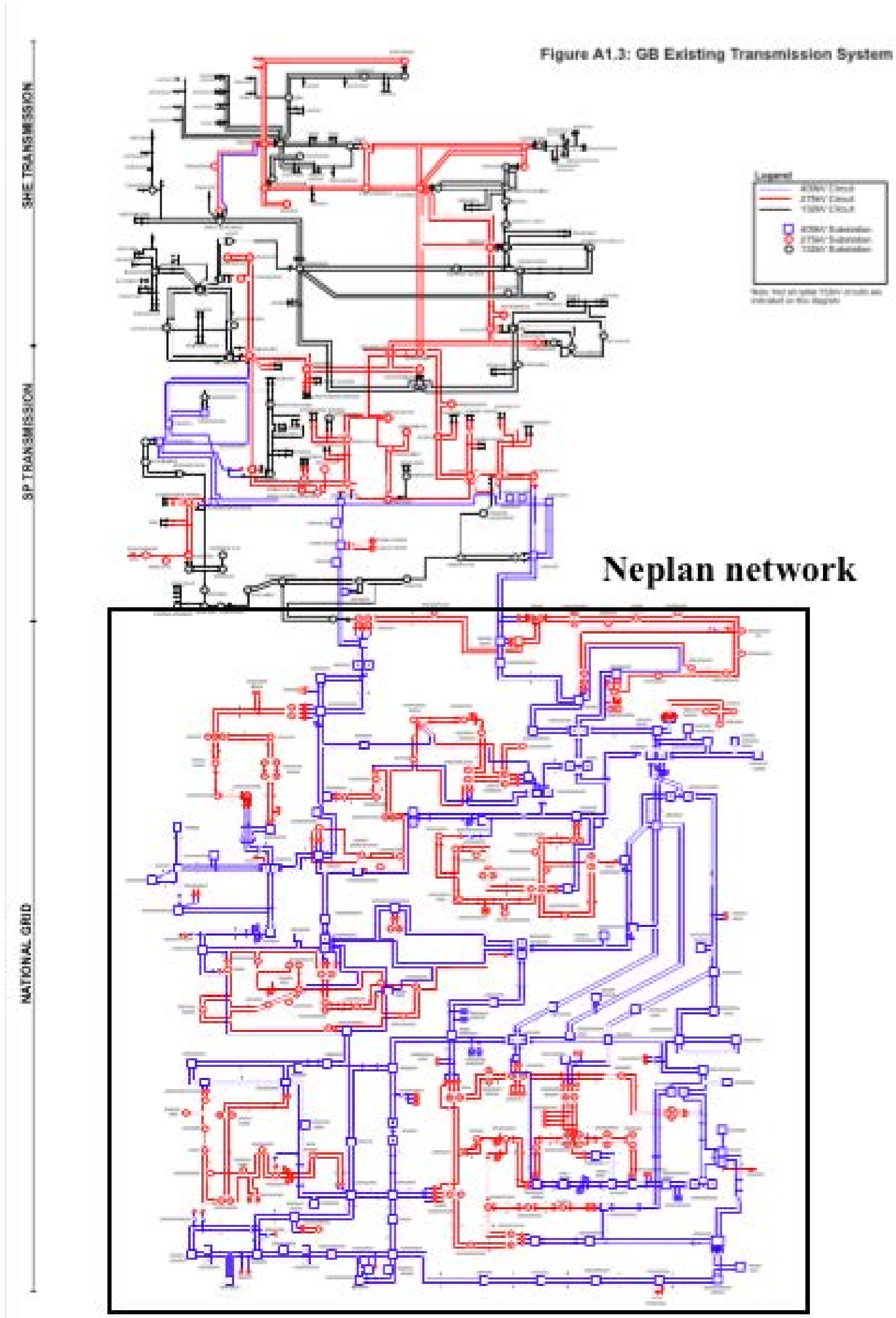

Figure 5.2: Lines distribution, RED: 275 kV substations and lines, BLUE: 400 kV substations and lines; BLACK: 132 kV substations and lines

Considering that the network structure changes during a period, the system file was available in three different configurations:

- Summer minimum
- Winter maximum
- Half min-max

These configurations are different in connection to the number of generators employed, which are used to supply the energy demand variation during the considered period and the value of the loads therefore the power flows are addicted to the chosen set-up configuration.
For this analysis the *winter maximum configuration* was chosen, due to the higher loads and power flow levels, which gives the highest values of the short-circuit currents magnitude useful for the study of the worst case scenario and the statistical approach of the ERP evaluation in the following chapters.
The power transmission network presents 2 different types of high voltages, 275 kV, 400 kV and few lines with 132 Kv as shown in fig 5.2; for this project, only the short circuit at 10 different substation was analysed; all of the substations are placed in the same area and connected each other, with a nominal voltage of 275 kV and they are here reported below:

- **ALDWARKE**
- **NEEPSEND**
- **PITSMOOR**
- **WINCOBANK**
- **TEMPLEBOROUGH**
- **SHEFFIELD CITY**
- **BRINSWORTH**
- **WEST MELTON**
- **THURCROFT**
- **THORPE MARSH**

The NEPLAN disposition of the chosen substations is represented in fig. 5.3; The figure shows all the nominal voltages, characteristics as the length of the lines connected, loads and transformers.

In the NEPLAN model all of the HV substations are identified by a code (tab. 5.1) and all of their data are shown from tab. 5.2 to tab. 5.11; for each substation are written the connected lines, with their length and descriptions, the loads with their apparent power **S**[MVA], reactive power **Q**[MVar], true power **P** [W] and if there are present, transformers with their apparent power **S**[MVA].

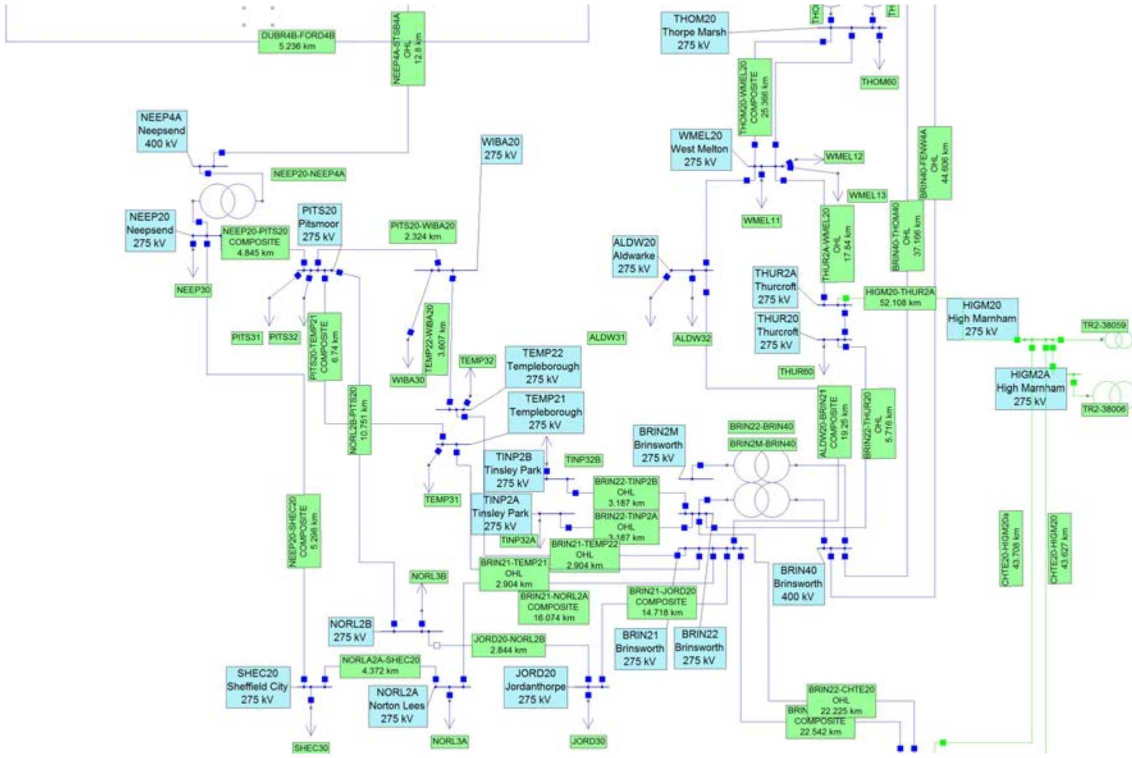

Figure 5.3: Substations disposition in the NEPLAN model

SUBSTATION	**CODE**
ALDWARKE	ALDW20
NEEPSEND	NEEP20
PITSMOOR	PIT20
WINCOBANK	WIBA20
TEMPLEBOROUGH	TEMP22
SHEFFIELD CITY	SHEC20
BRINSWORTH	BRIN21
WEST MELTON	WMEL20
THURCROFT	THUR20
THORPE MARSH	THOM20

Table 5.1: Substation code identifications

LINE	**DESCRIPTION**	**LENGTH** [km]
ALDW20-WMEL20	overhead line	9.08
ALDW20-BRIN21	composite	19.25

TYPE	**S** [MVA]	**P** [MW]	**Q** [MVar]
LOAD	48	36	31.749
LOAD	107.317	88	61.424

Table 5.2: ALDWARKE substation loads and connected lines

LINE	**DESCRIPTION**	**LENGTH** [km]
NEEP20-SHEC20	composite	5.298
NEEP20-PITS20	composite	4,845

TYPE	**S** [MVA]	**P** [MW]	**Q** [MVar]
LOAD	91,579	87	28,596
TRANSF.	750	/	/

Table 5.3: NEEPSEND substation loads and connected lines

LINE	**DESCRIPTION**	**LENGTH** [km]
PITS20-NEEP20	composite	4.845
PITS20-WIBA20	overhead line	2,324
PITS20-TEM21	composite	6,74
PITS20-NORL2B	overhead line	10,751

TYPE	**S** [MVA]	**P** [MW]	**Q** [MVar]
LOAD	55,914	52	20.552
LOAD	7,407	6	4.344

Table 5.4: PITSMOOR substation loads and connected lines

LINE	**DESCRIPTION**	**LENGTH** [km]
WIBA20-PIT20	overhead line	2,342
WIBA20-TEMP22	overhead line	3,607

TYPE	**S** [MVA]	**P** [MW]	**Q** [MVar]
LOAD	36,364	32	17,272

Table 5.5: WINCOBANK substation loads and connected lines

LINE	**DESCRIPTION**	**LENGTH** [km]
TEMP22-WIBA20	overhead line	3,607
TEMP22-BRIN21	overhead line	2,904

TYPE	**S** [MVA]	**P** [MW]	**Q** [MVar]
LOAD	4,667	3,5	3,087

Table 5.6: TEMPLEBOROUGHT substation loads and connected lines

LINE	**DESCRIPTION**	**LENGTH** [km]
NEEP20-SHEC20	composite	5.298
NORLA2A	overhead line	4,372

TYPE	**S** [MVA]	**P** [MW]	**Q** [MVar]
LOAD	86,458	83	24.208

Table 5.7: NEEPSEND substation loads and connected lines

LINE	**DESCRIPTION**	**LEGTH** [km]
BRIN21-TEMP22	overhead line	2.904
BRIN21-NORL2A	composite	16,074
BRIN21-JORD20	composite	14,718
BRIN21-CHTE20	composite	22,542
BRIN21-ALDW20	composite	19,25

Table 5.8: BRINSWORTH substation loads and connected lines

LINE	**DESCRIPTION**	**LENGTH** [km]
WMEL20-THOM20	composite	25.366
WMEL20-ALDW20	overhead line	9.08
WMEL20-THUR2A	overhead line	17.84

LINE	**S** [MVA]	**P** [MW]	**Q** [MVar]
LOAD	145,789	138.5	45.523
LOAD	145,789	138.5	45.523
LOAD	1360	360	0

Table 5.9: WEST MELTON substation loads and connected lines

LINE	**DESCRIPTION**	**LENGTH** [km]
THUR20-BRIN22	overhead line	5.716
THUR20-WMEL20	overhead line	17.84

TYPE	**S** [MVA]	**P** [MW]	**Q** [MVar]
LOAD	190,625	183	53,375

Table 5.10: THURCROFT substation loads and connected lines

LINE	**DESCRIPTION**	**LENGTH** [km]
THOM20-WMEL20	composite	25,473

TYPE	**S** [MVA]	**P** [MW]	**Q** [Mvar]
LOAD	145.789	130.5	45.523
TRANSF.	750	/	/

Table 5.11: THORPE MARSH substation loads and connected lines

Considering these ten substations, the next step was the calculation of two different types of short-circuit using the short-circuit analysis according with the hypothesis of IEC 60909-0 standard explained in the previous chapter. After that, using another standard known as "*SUPERPOSITION WITH LOAD FLOW*" the magnitude of voltages at the busbars and their distribution in the surrounding area were calculated, focusing at the voltages underneath the 95 % of the nominal voltage.
Considering a line-to-earth short-circuit in each substation busbar, the voltage increment distribution will be almost the same because all the substation are connected each other and placed in the same area. This analysis is really important to understand the behaviour of the network during a fault at a substation, how the voltage increases at the fault time and how it spreads geographically. We can draw a parametric configuration of the distributions considering the substations which assume the voltages from 0% to 95 % of Vn during the fault, consequently it gives an idea of how the potential rises from the fault point to the surrounded areas and where the short-circuit current influences the network normal operation.

5.3 Short-circuit currents calculation

NEPLAN allows to calculate short-circuit currents with different standards and for different types of fault like those shown in the fig. 4.1. Using the IEC standard and according with its hypothesis, the NEPLAN equivalent voltage source parameters are set as:

- c factor 1.1 for the maximum short-circuit currents calculation
- c factor 1.0 for the minimum short-circuit currents calculation

Table 5.12 shows all the currents calculated with the short-circuit analysis in each substation considering maximum and minimum short-circuit current values, steady state I_k and I_p short-circuit currents.

Looking at table 5.12 the highest current values are at THORPE MARSH substation and minimum values are at SHEFFIELD CITY substation; considering globally all the calculated values, they are quite in accord with the known maximum short-current current levels given by the NATIONAL GRID wich gives a maximum short circuit current value for the UK transmission system of ≈ 60 kA.
These values were used for the analysis in the final chapter of a meshed network built considering these substation and their real connections to study the earth fault current distribution on the substation earthing systems.

SUBSTATION	THREE-PHASE SHORT-CIRCUIT				LINE-TO-EARTH SHORT-CIRCUIT			
	MAXIMUM		MINIMUM		MAXIMUM		MINIMUM	
	I_k [A]	I_p [A]	I_k [A]	I_p [A]	I_k [A]	I_p [A]	I_k [A]	I_p [A]
NEEPSEND	23174	59810	21067	54373	18268	47149	16607	42863
PITSMOOR	23556	60715	16473	42381	18438	47523	16762	43203
WINCOBANK	23243	59796	21130	54360	18120	46619	16473	42381
TEMPLEBOROUGH	23368	60184	21243	54713	18185	46837	16532	42579
SHEFFIELD CITY	21453	54939	19503	49945	16449	42123	14953	38293
BRINSWORTH	27176	70507	24706	64098	22346	57974	20314	52704
ALDWARKE	23654	58475	21504	53159	18229	46150	16572	41955
WEST MELTON	27672	70769	25156	64335	21535	56098	19941	50998
THURCROFT	25931	65325	23574	59387	20604	51905	18731	47186
THORPE MARSH	29060	76359	26419	69417	25276	66415	23574	59387

Table 5.12: Maximum and minimum steady state currents I_k, peak currents I_p in each substation busbars in case of three-phase or line-to-earth short-circuit

5.4 Voltages on the healthy phases

Since the IEC standard uses an equivalent voltage source at the fault location, it's not possible to calculate the voltages on the surrounding busbar nodes with the same standard calculation used at the substation faults; NEPLAN gives the voltage magnitude during the short-circuit and this is exactly the equivalent voltage source value used in the IEC 60909-0 standard. To obtain the real voltages in each phases and in any busbars of the network the "*Superposition with load flow*" method has to be used.
It is difficult to know the voltages before short-circuit, specially in a planning state, where the load flow can only be approximated, NEPLAN provides a simplified superposition method where the internal voltage sources are set to 110% for maximum short-circuit calculation or 100% for the minimum short-circuit calculation of the nominal system voltage of the feeding elements and also, for an exact superposition method, a load flow has to be calculated before starting the short circuit calculation.
During the line-to-earth short-circuit only the fault phase has a potential of 0 V but on the healthy phases it might assume not negligible values as those reported in tab. 5.13; as expected at SHEFFIELD CITY substation which has the minimum values of short-circuit currents, the voltages on the healthy phases are highest and at THORPE MARSH substation which has the highest values of short-circuit currents the voltages on the healthy phases are the lowest. Considering the gap between maximum and minimum values we can say that the L2 and L3 phases voltages don't exceed the 80 % of the nominal voltage; this means that the HV transmission system operates in good condition even in case of substation fault because of the high level of short-circuit power *Pcc* which limits the spread of the short-circuit effects in all the network.

SUBSTATION	**L2 VOLTAGE** [kV]	**L3 VOLTAGE** [kV]
NEEPSEND	162,79	147,74
PITSMOOR	163,39	147,84
WINCOBANK	163,54	148,11
TEMPLEBOROUGH	163,62	148,24
SHEFFIELD CITY	164,24	149,61
BRINSWORTH	159,78	145,14
ALDWARKE	164,21	149,54
WEST MELTON	160,46	141,96
THURCROFT	161,96	146,47
THORPE MARSH	150	137,25

Table 5.13: Substation voltage magnitudes in the working phases during a line-to-earth short-circuit

5.5 Voltage distribution

Taking into account the busbar voltages during each short-circuit fault and considering only the line-to-earth short-circuit type, a geographic disposition of the potential rise and parametric distribution have been made. This representation shows the points where the busbar potentials belongs to a voltage range from 0 to 95% of the nominal voltage during a line-to-earth short-circuit placed at the ten considered substations; this study allows to understand how a fault in a particular point of the network within the considered area influences the current and voltage values on the transmission system . All the considered substations are located in the same area called " FAULT AREA" represented in fig. 5.4. The voltage rise distribution was drawn checking the potential values in the whole network at substation busbars and comparing them with the nominal voltage either of 275 kV and 400 kV substations; the curve which includes the voltage values underneath 95% of the nominal voltage was designed overlaying the

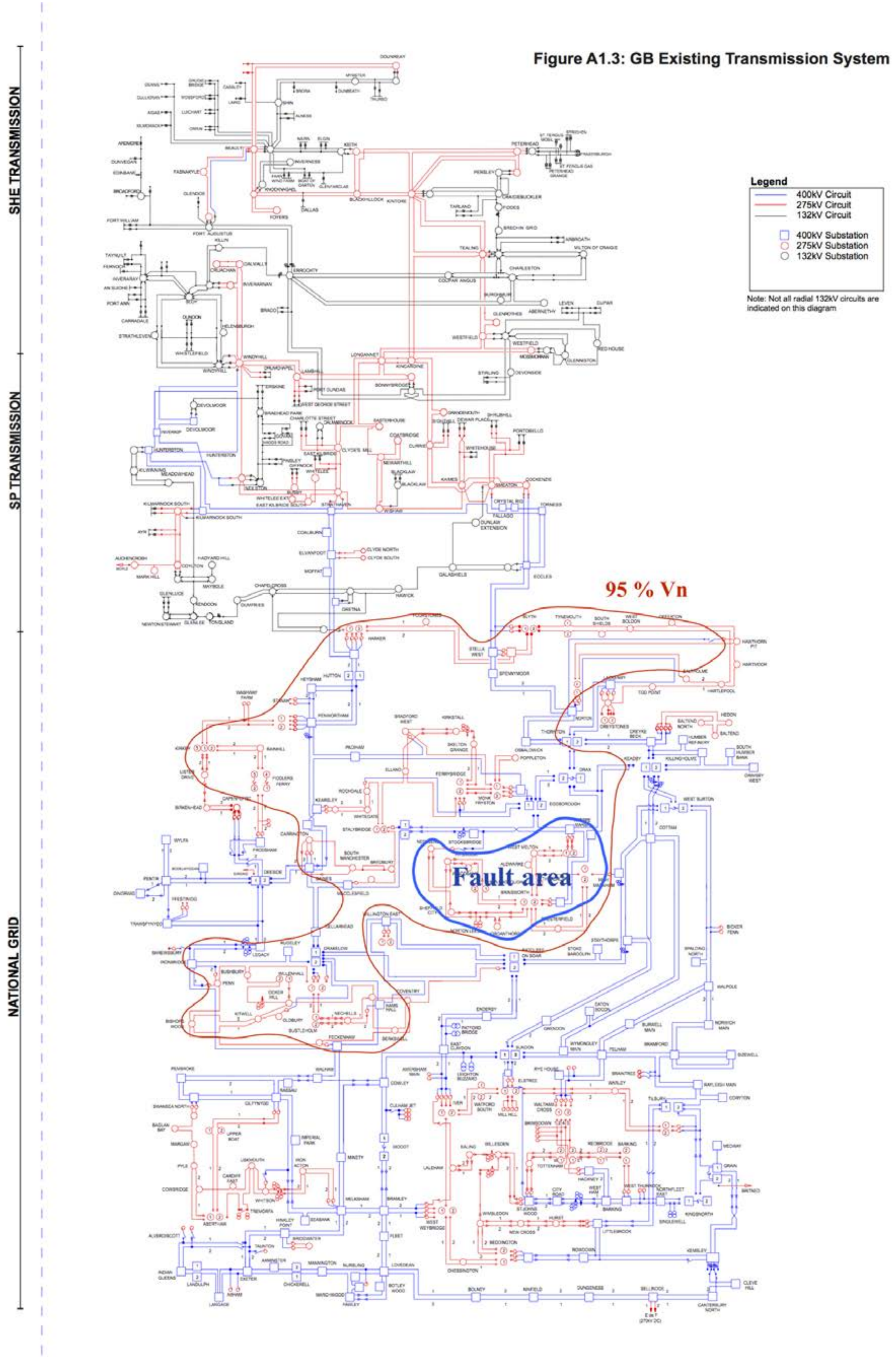

Figure 5.4: Voltage distribution during line-to-earth short-circuits placed within the "FAULTED AREA"

ten distribution curves given by the voltage data obtained during the short-circuit analysis one by one in each substation, making a single representation.
Looking at fig. 5.4 it can be notice that the voltage distribution on the transmission network is not equally balanced related to the position of the "FAULT AREA"; the line-to-earth short circuit affects mainly the network's area above the fault point and not the area below it, this because that part of grid has less short-circuit power Pcc then the area below.
This study can be used to know which part of network has to be considered for an earth potential rise and earth fault current distribution study evaluation during the shor-circuit; knowing how the fault affects the network operation and which are the more weak nodes in terms of voltage reduction, allowed us to choose the right system section which can represent the model excluding the part which is not influenced by the fault and therefore negligible for a more accurate analysis.

Chapter 6

ATPDraw current distribution analysis

6.1 Introduction

ATP is a universal program system for digital simulation of transient or electromagnetic phenomena; with this digital program, complex networks and control systems of arbitrary structure can be simulated. ATPDraw is a graphical, mouse-driven preprocessor to the ATP version of the Electromagnetic Transients Program (EMTP) on the MS-Windows platform; in ATPDraw the user can construct an electrical circuit using the mouse and selecting components from menu, then ATPDraw generates the ATP input file in the appropriate format based on "what you see is what you get". Using this software, it was possible to study the current distribution in different circuit configurations, changing number of substations, fault position, connected lines and their length or number of generators, analysing the earth fault current flows, earth potential rise and how they are influenced by the different electrical parameters. The magnitude of a phase-to-ground short-circuit current and its distribution among the various return paths depends on a number of factors, the most important of which are:

- Generating sources and transformer impedances
- Self and mutual impedances of phase and neutral conductors
- Grounding grid impedances of terminal stations and intermediate substations
- Transmission tower footing impedances
- Fault locations

6.2 Set-up parameters

The UK high voltage power system is basically composed by long overhead lines which connect the high voltage substations each other; all the substations have an earthing system composed by an impedance Ze directed grounded with values around 0,1 Ω and, the overhead lines, are composed by: tower pylons, which carry the phase conductors of the three phase power system and the earth wire with the functions explained in the section 2.2.

In this chapter were faced different types of network configurations with the same nominal voltage of 275 kV feeded by one or more three-phases sinusoidal generators with one or more substations represented with their earth impedance Ze connected to the overhead earth wires and the ground, placing the short-circuit point at a substation within the network or along an overhead line.

To construct the desired network configuration with ATPDraw it's necessary to know all the elements, electric and geometrical parameters and connections which will be inserted on the software interface and, after that, used for the system steady state simulation. The software allows to construct an overhead line model easily; as we know, on transmission systems with a nominal voltage of 275 kV or 400 kV, an overhead line which connects one or more substation is composed by a high number of spans with a mean

length of 360 meters. With this software it was possible to construct a single overhead line span model, only knowing all the geometrical data of tower pylon, the distance between the phases, the earth wire and soil, and the electrical data of the conductors.
Knowing these parameters they can be easily insert on the right software settings as shown in fig. 6.1 and ATPDraw constructs automatically the span model for the system like that shown in fig. 6.4.

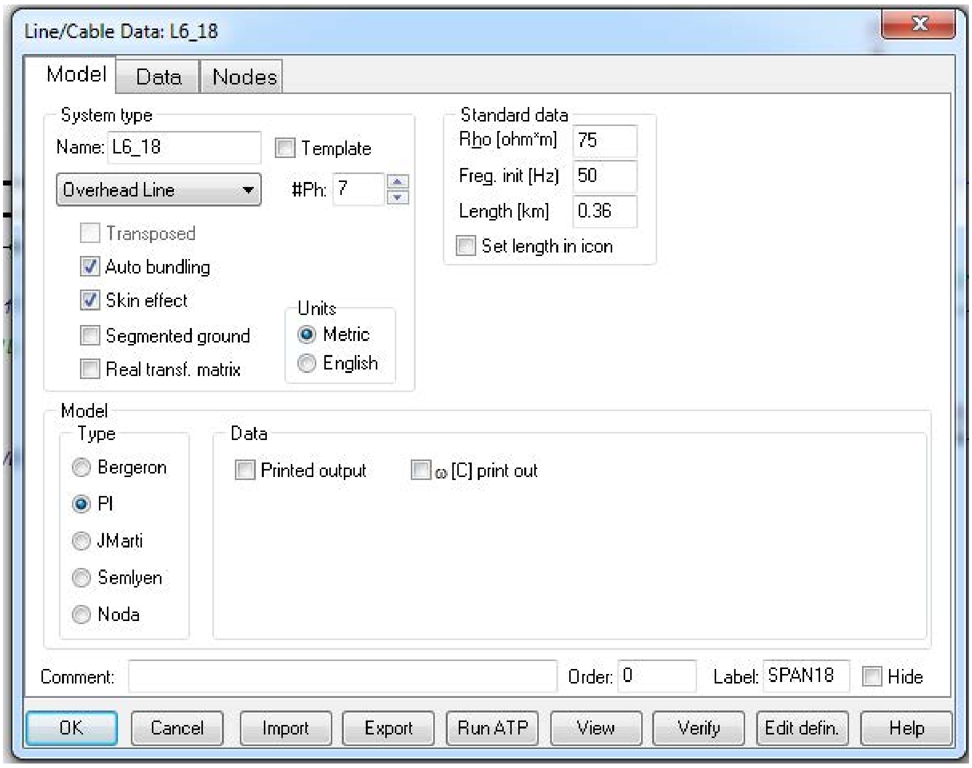

Figure 6.1: ATPDraw line data settings

Once set the line parameters, the span model was represented by a single block and, to build the desired overhead line we can repeat it for all the length in function of the number of spans that we need; for example, if we want a 5 km long line we will need, more or less, 14 spans therefore 14 span blocks as that represented in the picture 6.4.
If all the spans, which compose the line, have the same characteristics, ATPDraw allows to build a single TEMPLATE where it's possible to modify the length, the frequency or soil resistance along the line only in the TEMPLATE block and the software sets automatically the new selected parameters in all the associated spans. Between each span in the overhead lines, there are also two tower pylons with a structural function of carrying the conductors, which can be represented by a simple resistance connected either to the earth-wire and to the ground; the tower pylons have a tower footing resistance RT which assumes values between 10-20 Ω.
In the case of study, for the overhead lines representation, it has been used a LCC SECTION rather than a LCC TEMPLATE for each span because, if we needed, was possible to change a single span length or one of the single span parameters without modifying all the span which composed the line (using the TEMPLATE configuration it has been noticed that the software presents an error of working: when we tried to change a single line length, on TEMPLATE associated spans the single span lengths don't change, so it was preferable using the LCC SECTION model). Using the SECTION configuration, the data and parameters which had to be set, are those shown in table. 6.1; in this case, for all the circuit and all the network configurations a single type of overhead line with the same tower pylon design has been used and it is represented in fig. 6.5.

The conductors present on the overhead lines are: two three-phase systems connected in parallel at each substation and, on the top of the pylon one earth-wire connected at both sides to the substation earthing systems.

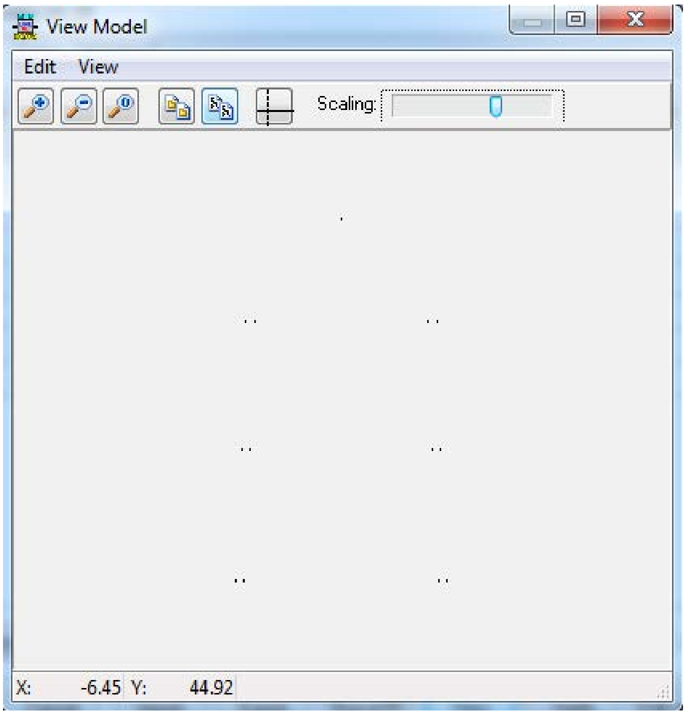

Figure 6.2: ATPDraw geometrical conductor bundles disposition

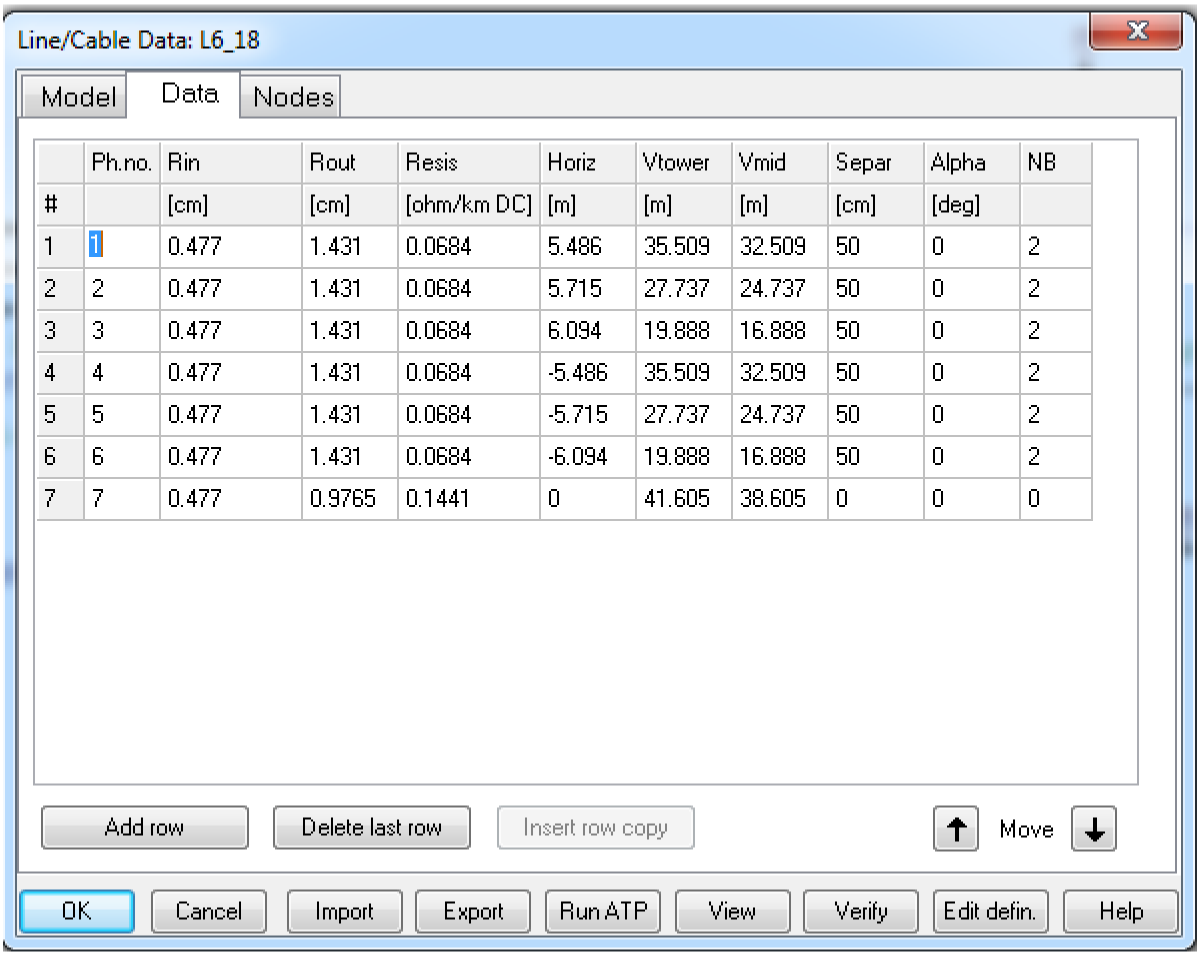

	Ph.no.	Rin	Rout	Resis	Horiz	Vtower	Vmid	Separ	Alpha	NB
#		[cm]	[cm]	[ohm/km DC]	[m]	[m]	[m]	[cm]	[deg]	
1	1	0.477	1.431	0.0684	5.486	35.509	32.509	50	0	2
2	2	0.477	1.431	0.0684	5.715	27.737	24.737	50	0	2
3	3	0.477	1.431	0.0684	6.094	19.888	16.888	50	0	2
4	4	0.477	1.431	0.0684	-5.486	35.509	32.509	50	0	2
5	5	0.477	1.431	0.0684	-5.715	27.737	24.737	50	0	2
6	6	0.477	1.431	0.0684	-6.094	19.888	16.888	50	0	2
7	7	0.477	0.9765	0.1441	0	41.605	38.605	0	0	0

Figure 6.3: ATPDraw geometrical and electrical conductors data

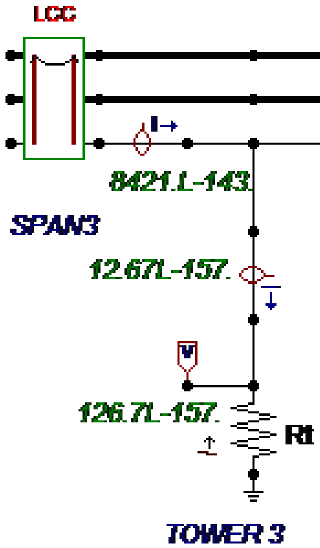

Figure 6.4: ATPDraw span model

The conductors used are the following:

- ZEBRA type for phase conductors
- LYNX type for the earth wire

All of them are ACSR (Aluminum Conductors Steel Reinforced) conductors with internal structure shown in fig. 6.6; these are concentrically stranded conductors and they comprise one or more layers of EC grade aluminum wires high-strenght electrolytic grade zinc coated steel core with the specifications shown in tab. 6.1.

To simplify the case of study, the short-circuit at the substations or in any chosen point is represented by a time switch on the phase C which closes it to earth impedance Ze, in case of substation fault shown in fig 6.7, or directly to the ground in case of fault along the overehead line; the fault time is set from 0 to 0.08 seconds and, after that, it returns to the steady state open circuit.
The line-to-earth short-circuit simulation is shown in fig. 6.8 and, as can be seen, one phase is connected to earth by the switch, therefore its voltage is almost zero and the other two phases assume a lower value then the nominal voltage until the re-open of the switch at 0.08 seconds.

Relating to the different network configurations, for the substation earthing systems an impedance Ze with values between 0.1 Ω and 0.3 Ω was used and for soil resistance ρ, values between 50 and 100 Ωm, in one case 1000 Ωm. In ATPDraw short-circuit simulation PI mode has been used as transmission line representation; usually this model is used for the steady state studies and not for short-circuit studies which are transients but, since the aim of this analysis is the knowledge of magnitude and current distribuition during the worst case scenario, it can be possible to use the PI model to simplify the case of study.The employed sources are represented by an ideal three-phase sinusoidal generator with 275 kV RMS line-to-line voltage value and its short-circuit impedance Zcc connected in series; the three phases of the generator are star connected and the neutral point is grounded to the substation earth impedance as shown in fig 6.9.

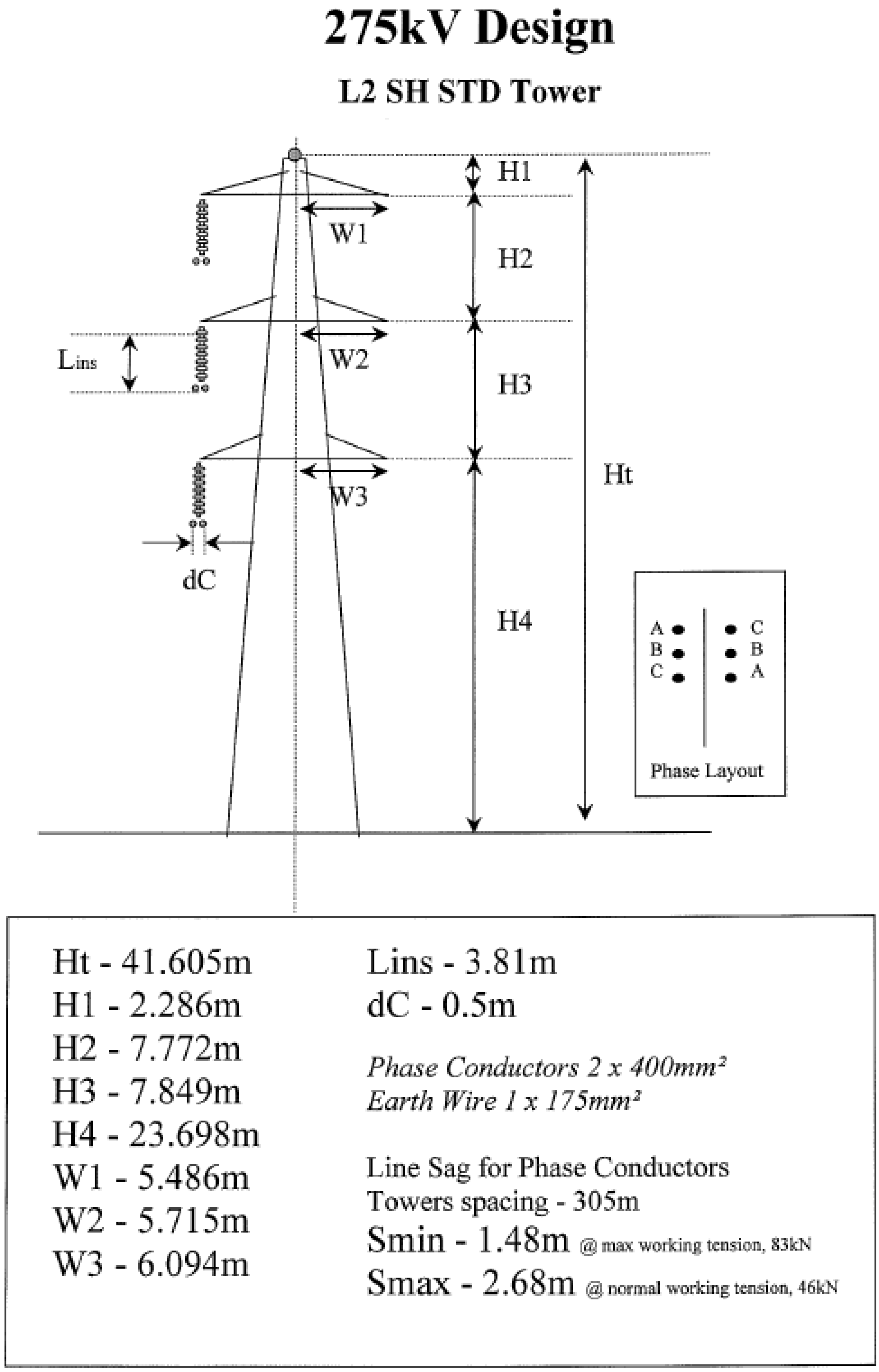

Figure 6.5: Geometrical data and pylon configuration of L2 type overhead line used for high voltage transmission systems

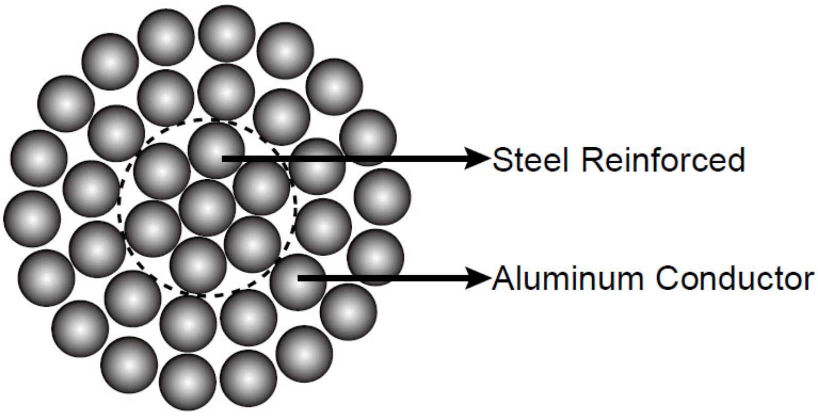

Figure 6.6: ACSR (Aluminum Conductor Steel Reinforced)

NAME	ZEBRA	LYNX
DIAMETER [mm]	28,52	19,53
EQUIVALENT AREA [mm^2]	400	175
FIRST ELEMENT	ALUMINUM	ALUMINUM
CONDUCTORS [$n°$]	54	30
DIAMETER [mm]	3,18	2,79
SECOND ELEMENT	STEEL	STEEL
CONDUCTORS [$n°$]	7	7
DIAMETER [mm]	3,18	2,79
KILOMETRIC RESISTANCE [Ω/km]	0,0684	0,1441
CONSTRUCTION	(54 x 3,18)+(7 x 3,18)	(30 x 3,18)+(7 x 3,18)

Table 6.1: Phase conductors and earth wire geometrical and electrical characteristics

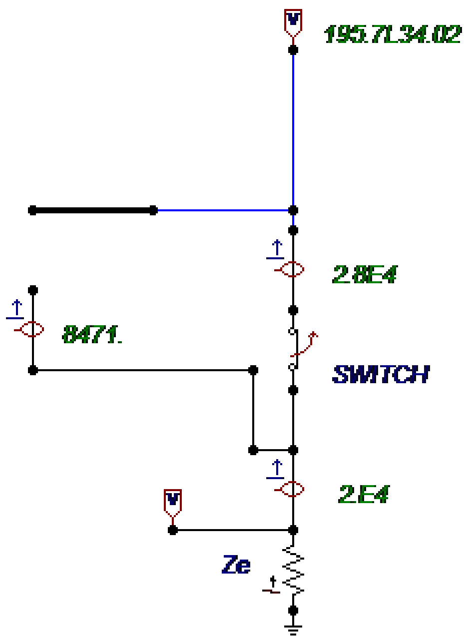

Figure 6.7: Short-circuit model

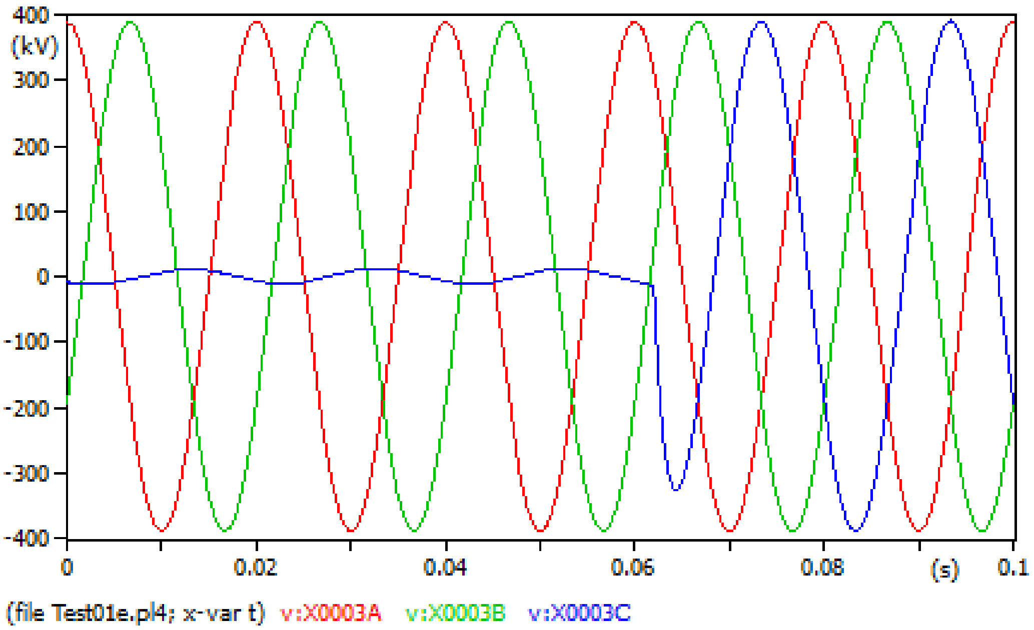

Figure 6.8: Line-to-earth short-circuit simulation

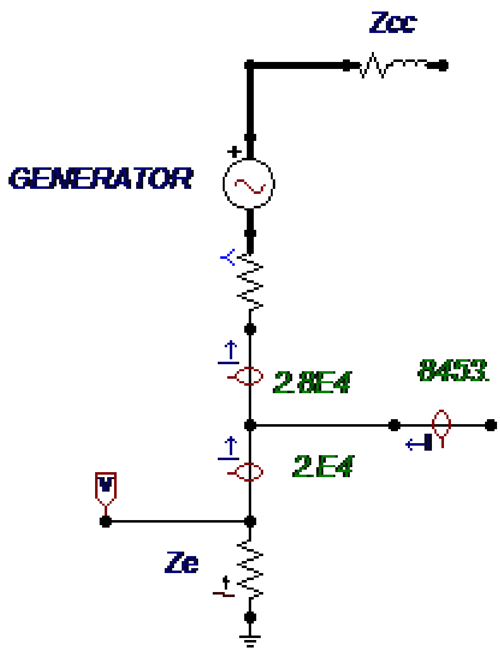

Figure 6.9: ATPDraw source model

All the considered network configurations are different each other, in addition to changing the electrical parameters as Z_e or R_T, to study the effects of them variations on the current distribution, line length, short circuit impedances Zcc of the sources, feeding type and fault locations were changed; the cases of study are the following:

- **CASE 1-Substation fault, simple radial network model**
- **CASE 2-Middle substation fault, 3 substations, 2 generators,** $Zcc1 = Zcc2$ **and** $L1 = L2$
- **CASE 3-Middle substation fault, 3 substations, 2 generators,** $Zcc1 > Zcc2$ **and** $L1 = L2$
- **CASE 4-Middle substation fault, 3 substations, 2 generators,** $Zcc1 = Zcc2$ **and** $L1 < L2$
- **CASE 5-Middle substation fault, 5 substations, 4 generators,** $Zcc1 = Zcc2 = Zcc3 = Zcc4$
- **CASE 6-Span fault, 5 substations, 2 generators,** $Zcc1 = Zcc2$

6.3 CASE 1

Once chosen all the blocks which rappresent the spans and the generators and placed the short circuit position, the first analysed network was a simple radial network shown in fig. 6.11 composed by a source model which feeds a short-circuit placed at the end of an overhead line 7.2 Km long whith 20 spans.
To evaluate the magnitude of the currents and voltages, current and voltage probes in each span along the earth wire and in each tower footing resistance were used; the analysis was done changing tower footing resistance RT, soil resistance ρ or substation earth impedance Ze values to evaluate the network behaviour and its sensitivity to the variation of th parameters.
One of the most important value to calculate is the magnitude of the fault current I_f and its distribution through the earth system impedance I_{gr} and through the connected earth wire I_w; The following results show the earth fault current partion through the earthing system and the earth wire changing the electrical parameters:

- $\frac{I_{gr}}{I_f}=\frac{5774}{8658}=66\%$ $[RT=20\ \Omega,\ \rho=100\ \Omega\text{m},\ Ze=0.1\ \Omega]$
- $\frac{I_{gr}}{I_f}=\frac{5882}{8692}=67\%$ $[RT=10\ \Omega,\ \rho=50\ \Omega\text{m},\ Ze=0.1\ \Omega]$
- $\frac{I_{gr}}{I_f}=\frac{5823}{8672}=67\%$ $[RT=15\ \Omega,\ \rho=75\ \Omega\text{m},\ Ze=0.1\ \Omega]$
- $\frac{I_{gr}}{I_f}=\frac{5493}{8658}=63\%$ $[RT=15\ \Omega,\ \rho=75\ \Omega\text{m},\ Ze=0.3\ \Omega]$

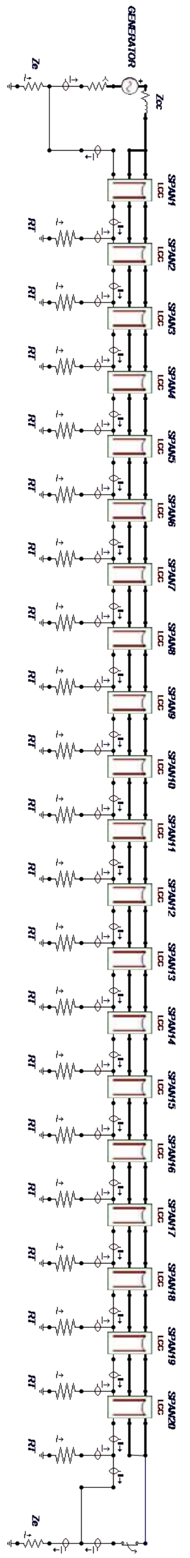

Figure 6.10: SIMPLE NETWORK, short-circuit at the end of the line feeded by a generator with an overhead line (7,2 Km, 20 spans, 360 m/span

6.3.1 Results

Here below there are reported all the charts relative to the tower footing current distribution along the line, the current phase angle distribution on the towers and the span current distribution along the earth wire.

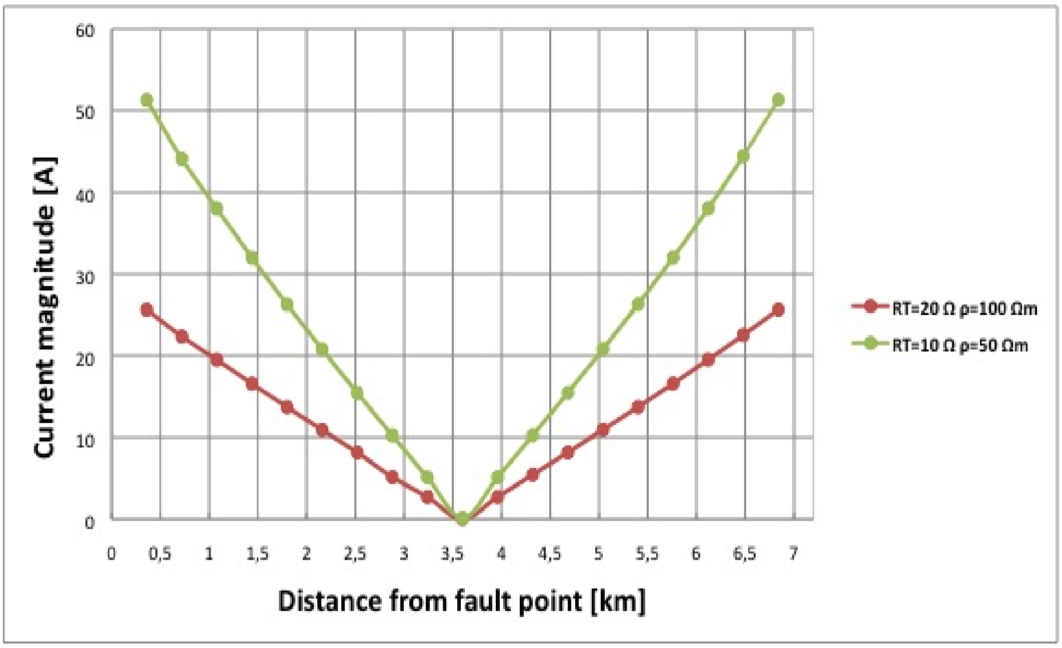

Figure 6.11: Tower footing current distribution with a substation fault placed at the end of the line changing soil and tower footing resistance

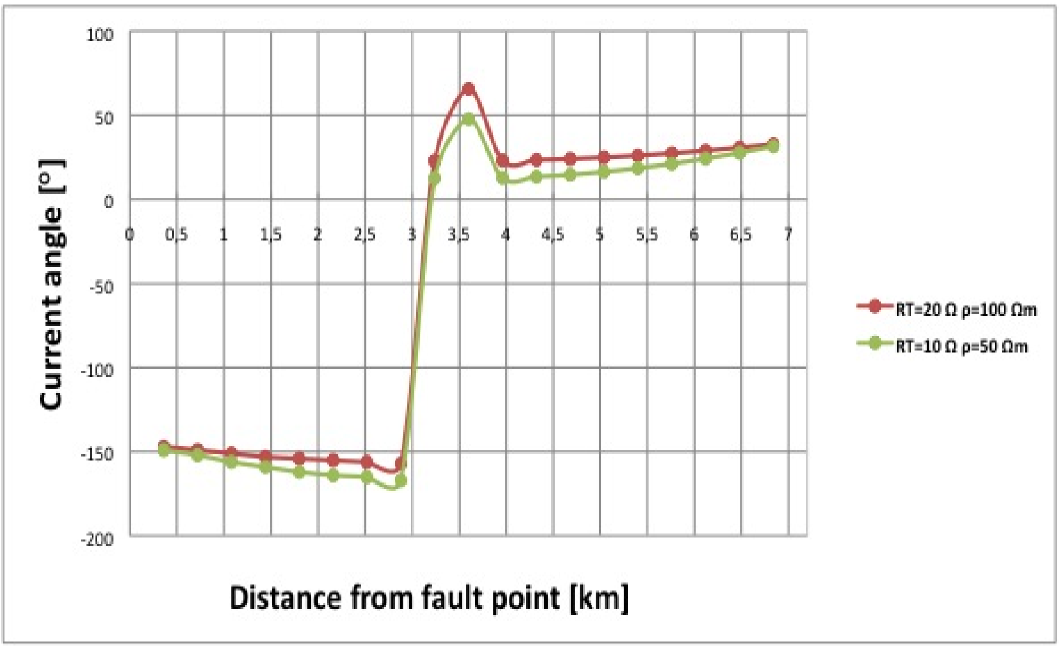

Figure 6.12: Tower footing current phase angle distribution with a substation fault placed at the end of the line changing soil and tower footing resistance

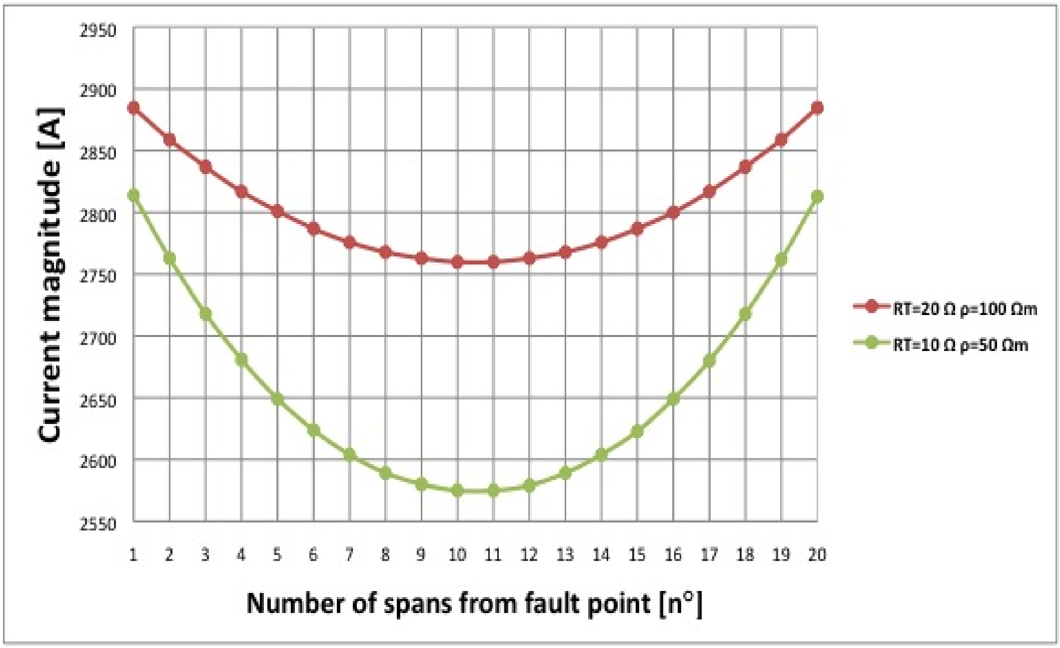

Figure 6.13: Span current distribution along the earth wire with a substation fault placed at the end of the line changing soil and tower footing resistance

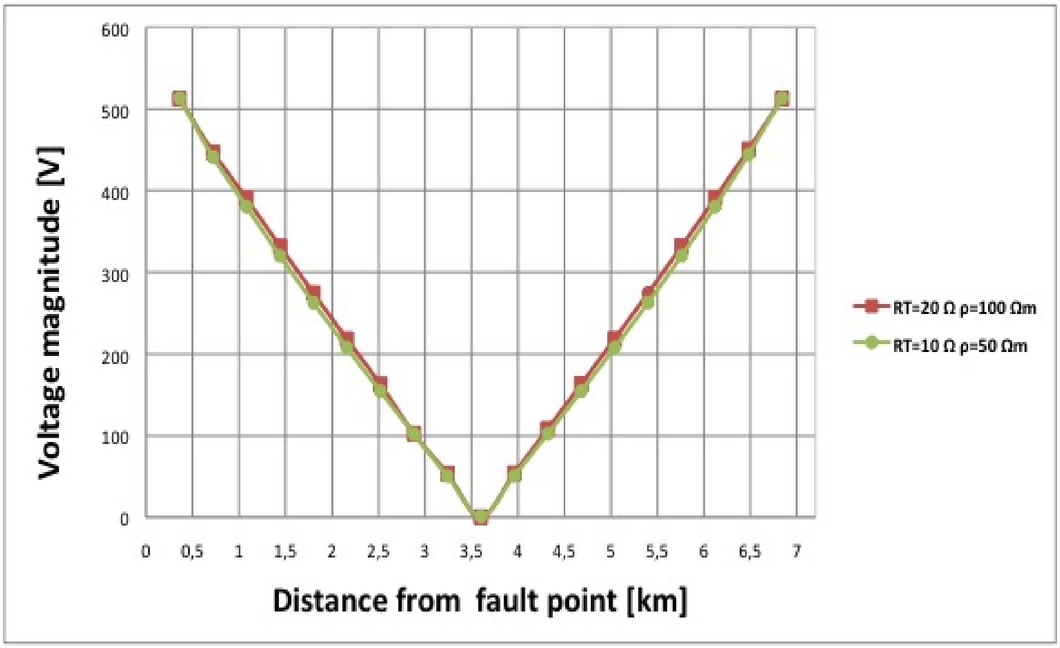

Figure 6.14: Tower footing voltage distribution with substation fault placed at the end of the line changing soil and tower footing resistance

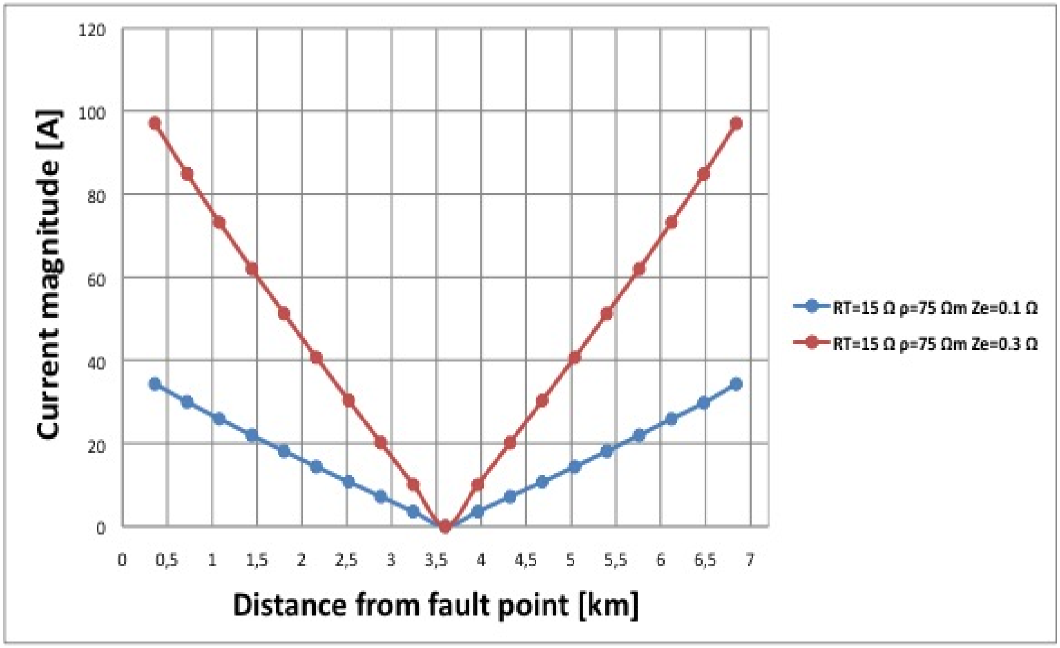

Figure 6.15: Tower footing current distribution with substation fault placed at the end of the line changing earth substation impedances; soil resistance and tower footing resistance values are fixed

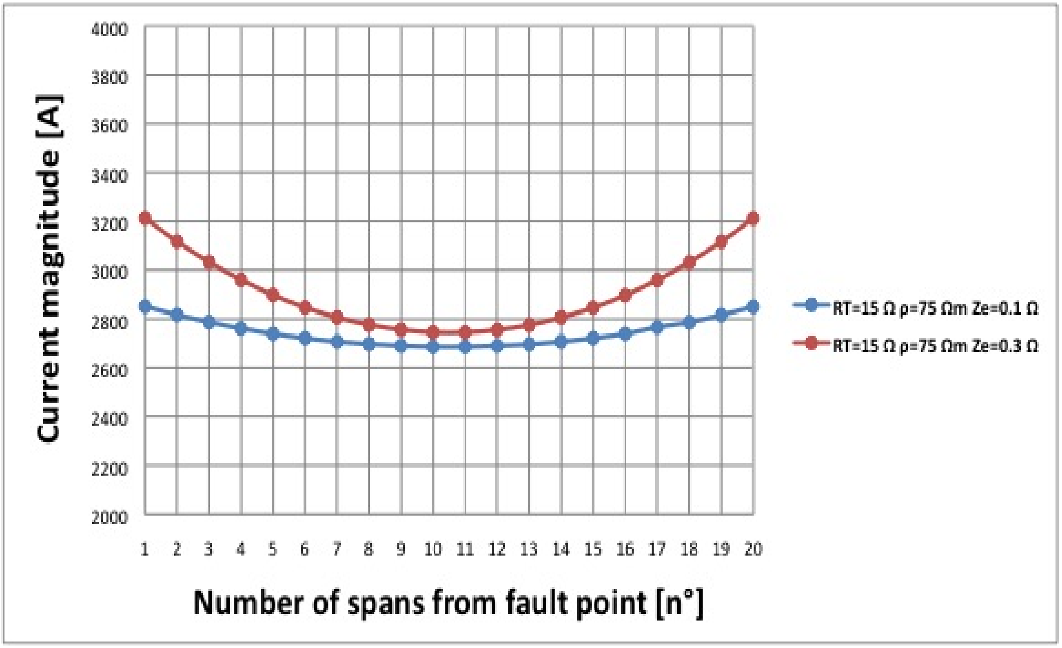

Figure 6.16: Span current distribution along the earth wire with a substation fault placed at the end of the line changing earth substation impedances,; soil resistance and tower footing resistance value are fixed

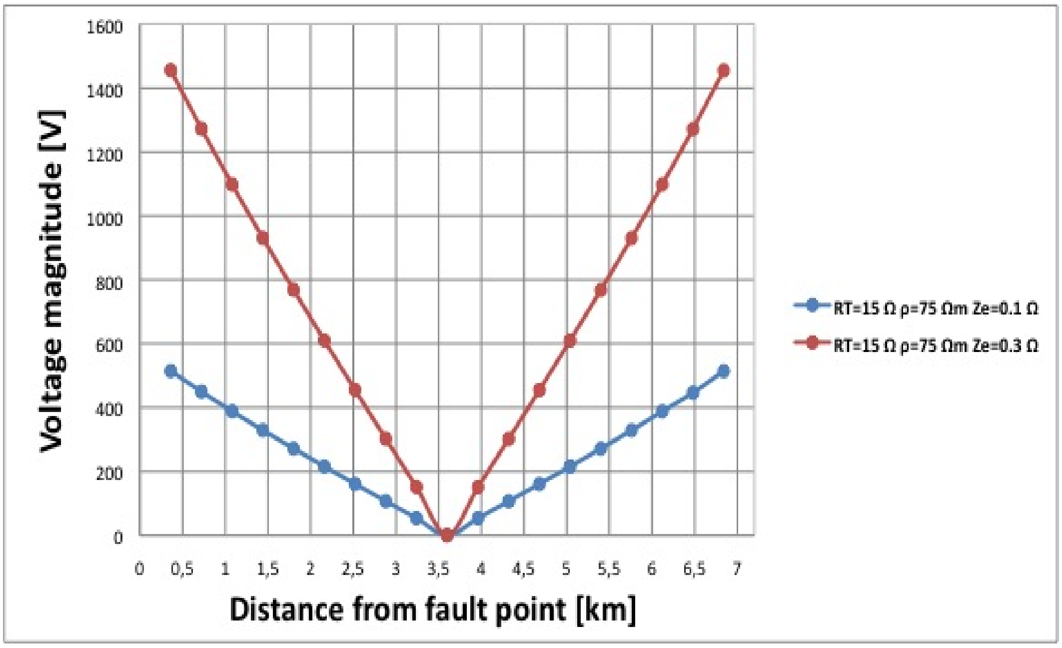

Figure 6.17: Tower footing voltage magnitude distribution with substation fault placed at the end of the line changing earth substation impedances; soil resistance and tower footing resistance values fixed

6.3.2 Comments

Looking at fig. 6.11 it can be noticed that the trend of the tower footing current magnitude is symmetrical respect the middle point of the line at 3,6 km; at the end, where the fault is placed and at the beginning, where there is the generator the current magnitude is maximum and has the same value of 51,34 A instead, at the middle of the line, there is the minimum magnitude which has a value 0,113 A. Fig. 6.11 shows that there is no difference between red and green chart trends but only a magnitude reduction; in the red one at side points the current magnitude is reduced by half magnitude respect to the green chart, indeed the maximum values are respectively of 25,64 A and 51,34 A. This aspect is quite interesting because it seems that the values at the side points are strictly dependent on the value of tower footing resistance or soil resistance which changes from a RT=10 Ω and ρ=50 Ωm to double values causing the maximum current magnitude reduction.

Looking at figure 6.12 which represent the tower footing current phase angle, both charts have almost the same values and trends except for a small downward translation of the green chart decreasing the soil and tower footing resistance; from the fault point, the phase angle has a value of -147 degrees, after that it starts decreesing slowly untill a fast rise at the third km, where there is a phase reverse from -157 to 65,69 degrees; after the peak point on the middle line tower, the phase angle decreases on the next tower and then it increases slowly until a value of 32,82 degrees at the end of the line. This trend yields that, considering opposite flows for current which have a phase angle from 0 to 180 and currents from 0 to -180, on the first half of the towers from the generator to the middle tower, the current flow is from the soil, through the tower footing resistance to the earth wire and, for the second half, from the middle tower to the fault point the current flow is from the earth wire to the ground through the tower pylons.

The span current magnitude distribution which is represented in fig. 6.13 presents, as seen for the tower footing current, a symmetrical trend respect the middle line point with maximum values at side points and a minimum value at the middle; in this case, differently from the tower footing current magnitude charts, changing the soil resistance or tower footing resistance parameters don't influence only the side values at the spans close to the generator and the substation but also the minimum value indeed, as can be seen in figure , the minimum value passes from 2760 A to 2575 A lowering RT and ρ parameters. Figure 6.14 which represents the tower footing current voltage distribution shows that there is no difference between the two charts changing the electrical parameters because, when there is RT= 20 Ω the current values are lower than when there is RT= 10 Ω indeed to obtained the voltage on the tower we have to multiply the tower footing resistance by the current which flows through it so the values for the voltage

are almost the same for both cases with a maximum values at fault and generator points of ≅ 513 V and ≅ 0 V at the middle line tower. Analysing figures 6.15, 6.16 and 6.17, the difference between the red and blue case of study is only the changing of earth substation impedance from 0,1 Ω to 0,3 Ω; as shown in fig 6.15, the tower footing current magnitude is higher when the earth substation impedance is 0,3 Ω and this yields that increasing the substation impedance we can reduce the tower current flow as said previously for the effect of soil or tower footing resistance. Figure 6.16 shows that the changing of earth substation impedance doesn't affect that much the span current magnitude; the trend and the values along the line are quite similar except for the side values where there is a difference of 362 A between the two cases.
The tower footing voltage represented in fig. 6.17 needs some more considerations; the picture shows that increasing only the earth substation impedance by 0,2 Ω influences a lot the voltage distribution along the line on the tower pylons; at the beginning and at the end of the overhead line when the earth impedance changes, the voltage magnitude passes from 514,35 V to 1456 V value which is almost three times higher as the increment of earth substation impedance; at the middle of the line the voltage is still $\cong 0V$ as we saw in the previous cases therefore we can say that the middle value of voltage or tower current magnitude is always almost equal to zero regardless of soil resistance ρ tower footing resistance RT and earth substation impedance Ze values.
In conclusion we can say that the fault current distribution is directly connected to the complex impedance of the line which includes mutual impedance between phases and earth wire but it also depends on soil and tower footing resistance parameters; when the soil resistance is higher, the current flows more through the earth wire than through the soil as can be seen passing from the green trend to the red trend looking at figures 6.13 and it is more distributed on the spans along the overhead earth wire. The most effect of parameter RT, Ze and ρ is on the voltage and on the tower footing current distribution with a particular attention at the values present at the end and at the beginning of the overhead line which connects the power source to the fault substation.

6.4 CASE 2

After the simple radial network model, trying to reach step by step a final configuration of a meshed network model to simulate a real network, a more complex circuit composed by 3 substation with the same earth impedance has been analysed. The line-to-earth short-circuit has been placed at the middle substation and two generators are at side substation feeding the fault point with two overhead lines with the same length and characteristics as the line seen previously in the simple model; the circuit is shown in fig. 6.19 and, as can be seen from the figure this kind of network is symmetrical considering the short-circuit point. Once you get all the components of the overhead lines, ATPDraw allows to compress all of them as tower pylons, spans and line sections in a single block called GROUP (fig. 6.18) which schematises the whole line in a single software block making clearer the system representation; its terminals are respectively the terminals of the beginning and of the end of the overhead line taken into account as can be seen in the ATPDraw circuit model.

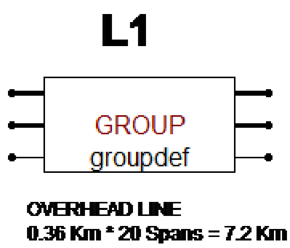

Figure 6.18: GROUP ATPDraw line model

In this case and in the simple network as well, the generators were connected in series with their short-circuit impedance Zcc which now has been set to the same value for both power sources as though the two upstream networks have got the same short-circuit real power Pcc; this means the same contribution

to the short-circuit current.
The ratio between the current which flows through the substation earthing system I_{gr} and the short-circuit current I_f is:

- $\frac{I_{gr}}{I_f} = \frac{17000}{26000} = 65\%$

As seen for the simple model, even if the network configuration is changed, the ratio between I_{gr} and I_f remains the same, this means that this value basically does not depend on number of generators or number of lines which connect the faulted substation to the power source. In this configuration both lines have the same characteristics either for the length and for the electrical parameters as soil and tower footing resistance, therefore in both earth wires at the fault connection the same current magnitude flows and it's equal to:

- I_{w1}=I_{w2}=4671 A

Analysing the flows, the current quote that flows up through the earthing system at side substations is:

- I_{Ze1}=I_{Ze3}=8996 A

As expected since there are two equal generators which feed the fault, the part of the current which flows up through the earthing systems have the same value and the ratio between the ground current which flows up through the earth impedance and the generator current I_g (which is exactly half of the short-circuit current magnitude) is:

- $\frac{I_{gr}}{I_g}=\frac{8996}{13000}=65\%$ [RT=10 Ω, ρ=50 Ωm]

This kind of network configuration is symmetrical because the two sections which feed the fault have exactly the same characteristics, indeed the charts results show that the distribution of the current on the spans and on the tower footing resistances is the same for both lines, therefore it's necessary representing only one section distribution.

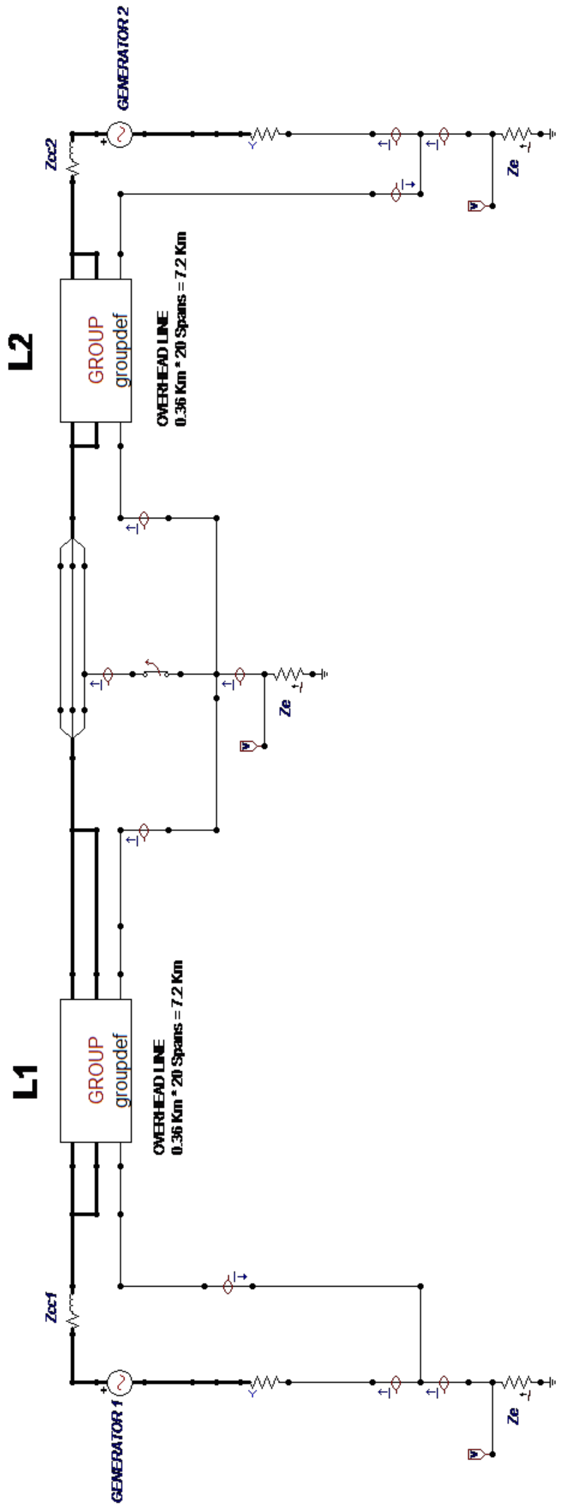

Figure 6.19: Middle substation fault feeded by two generators at side substations with two overhead lines 7,2 km long

6.4.1 Results

The chart results are reported below:

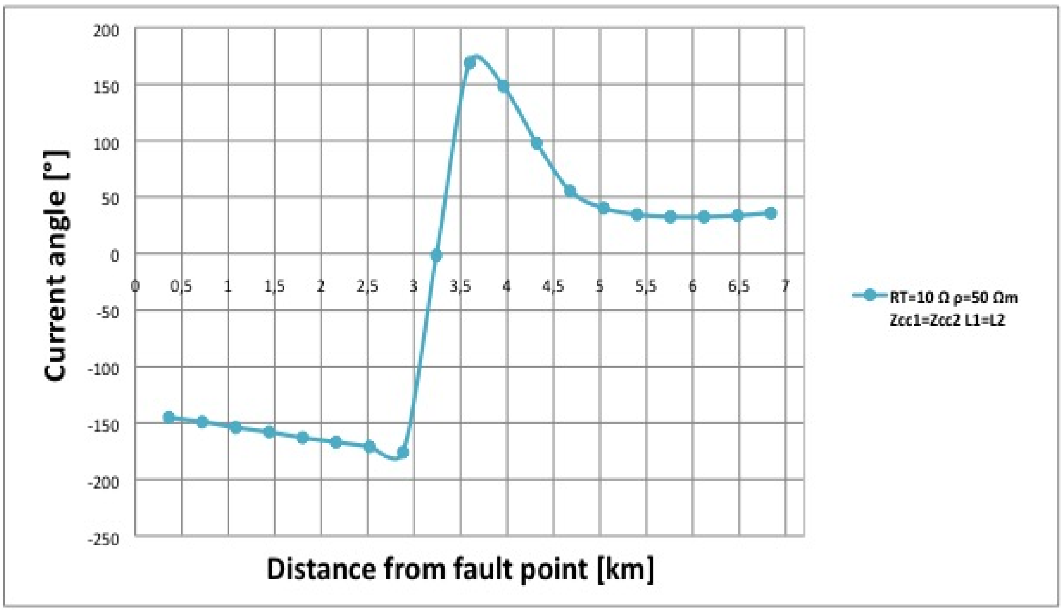

Figure 6.20: Tower footing current phase angle distribution along line L1 with middle substation fault and fixed values of soil and tower footing resistance

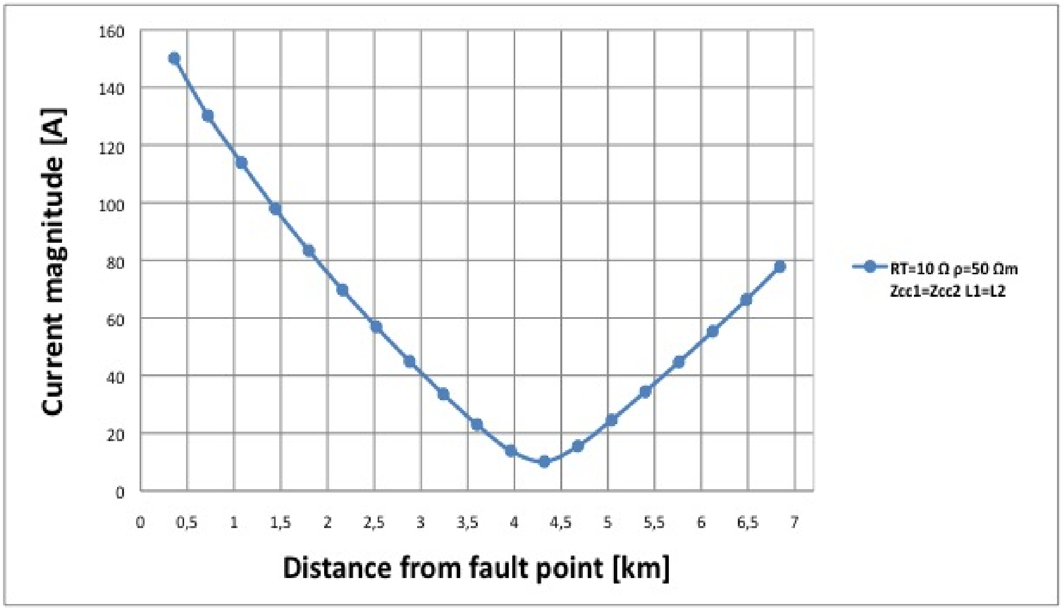

Figure 6.21: Tower footing current distribution along line L1 with middle substation fault and fixed values of soil and tower footing resistance

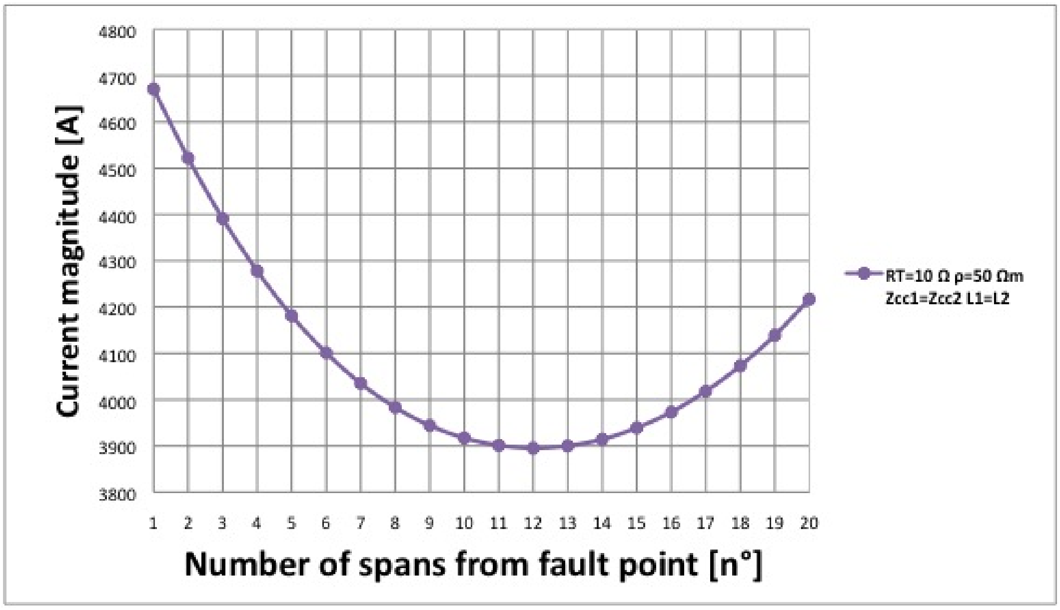

Figure 6.22: Span current distribution along L1 earth wire with middle substation fault and fixed values of soil and tower footing resistance

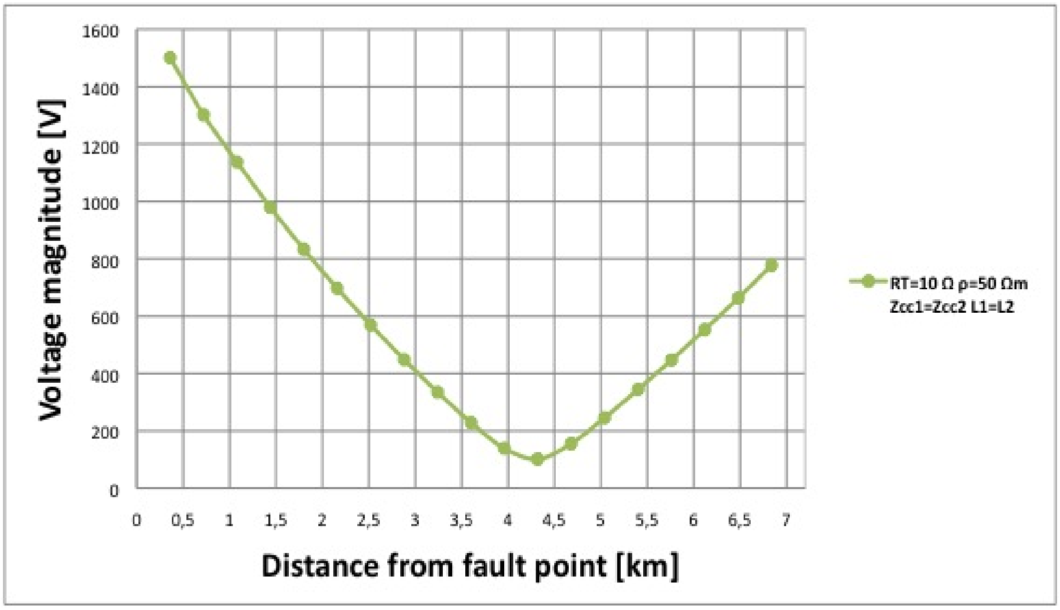

Figure 6.23: Tower footing voltage distribution along line L1 with middle substation fault and fixed values of soil and tower footing resistance

6.4.2 Comments

In this case all the obtained results are relative to electrical parameter values fixed: RT=10 Ω and ρ=50 Ωm. As can be seen from fig 6.21, at the beginning of the line the tower current magnitude is not the same seen at the final tower of the simple network; the reason is because the fault now is feeded by two generators which contribution is exactly half part of the short-circuit current; this current once it flows through the earth substation impedance splits in two parts with the same magnitude beacause of two equal line sections at both sides, it flows through the soil and up through the generators earth-systems. Looking at fig. 6.20, which represent the tower footing current phase angle, it has exactly the same trend seen for the simple network along the line, this means that even if the short circuit is feeded by two power sources the flow current direction, doesn't dipend on the different configuration, in each overhead line the phase angle still has a reverse at the middle tower.
Fig 6.21 and fig 6.23 which represent tower footing current and voltage distribution have the same trend because the voltage magnitude are current values multiply by the tower footing resistance RT which doesn't change; looking at tower current distribution in fig. 6.21 we can notice that, differently from the simple network, the trend is not symmetrical any more even if the fault is connected by the same overhead line to the generator.
Since the short-circuit current is given by two generator contributions, it flows with the same distribution in both lines, split in earth wire, soil and towers; its minimum value is not at the middle of the line anymore but at 4,32 km from fault point with a magnitude of 10,17 ampere, the maximum value now is close to the fault position with a magnitude of 150,1 A.
In this case of study the most part of current flows through the earth wire as can be seen in fig. 6.22 which shows its span current distribution; the trend is quite similar to the tower footing current distribution but the magnitude, for example on the first span close to the fault point, is very high with a value of 4671 A and the minimum point, in this case at 4,32 km again, is 3895 A.

6.5 CASE 3

In this case, the network is the same reported in fig. 6.19, the only thing that changes is the different values of short-circuit impedance between the generators $Zcc_1 = 1 + j30\Omega$ and $Zcc_2 = 1 + j10\Omega$; since they have different modulus, the distribuition of the current along the line will be different between L1 and L2 beaucse of the different contribution of the power sources to the short-circuit therefore we need to analyse both line distributions.
The ratio between the ground currentI_{gr} and the fault current I_f magnitude at the middle substation is :

- $\frac{I_{gr}}{I_f}=\frac{26266}{40504}$=64,8% [$RT$=10 Ω, ρ=50 Ωm]

As for the simple network and the second case of study, even if the fault current is higher beacuse of the contribuition of 2 generators, the partition with the ground current I_{gr} remains around 65%.
The current partition between the two substations earthing systems is:

- I_{Ze1}= 9394 A I_{Ze3}= 6956 A

As expected the highest current value passes through the first substation earth impedance beacause of the highest short-circuit power, caused by the lower short-circuit impedance of the generator 1 which contributes to the fault current.

6.5.1 Results

Here below are reported the charts of the distributions either for line L1 and line L2 because they are very different.

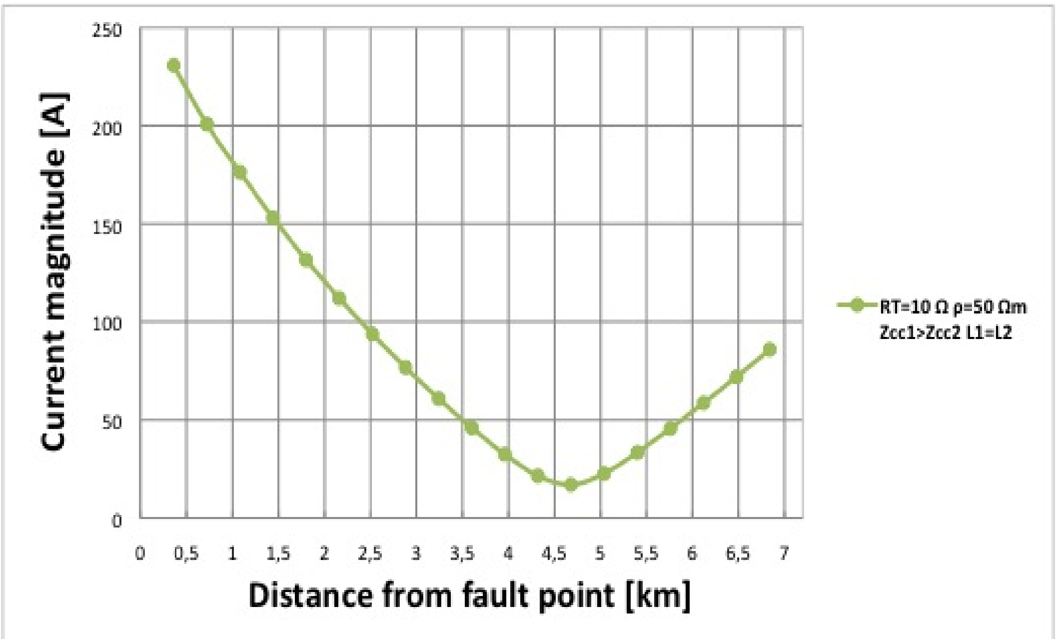

Figure 6.24: Tower footing current ditribution along the line L1 with middle substation fault and fixed soil and tower footing resistance parameters

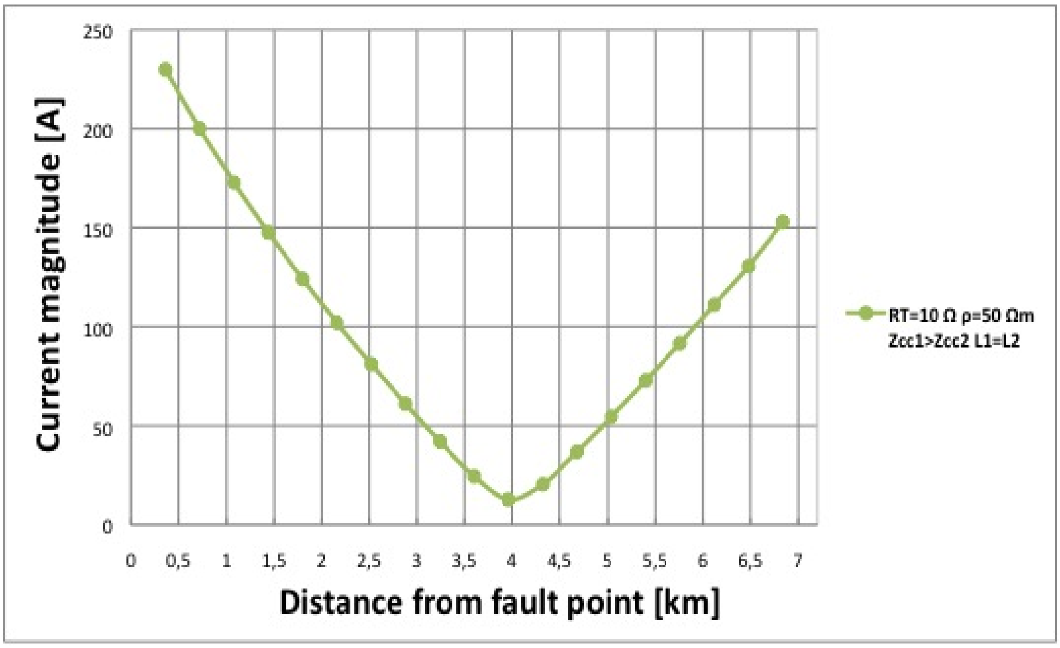

Figure 6.25: Tower footing current distribution along the line L2 with middle substation fault and fixed soil and tower footing resistance parameters

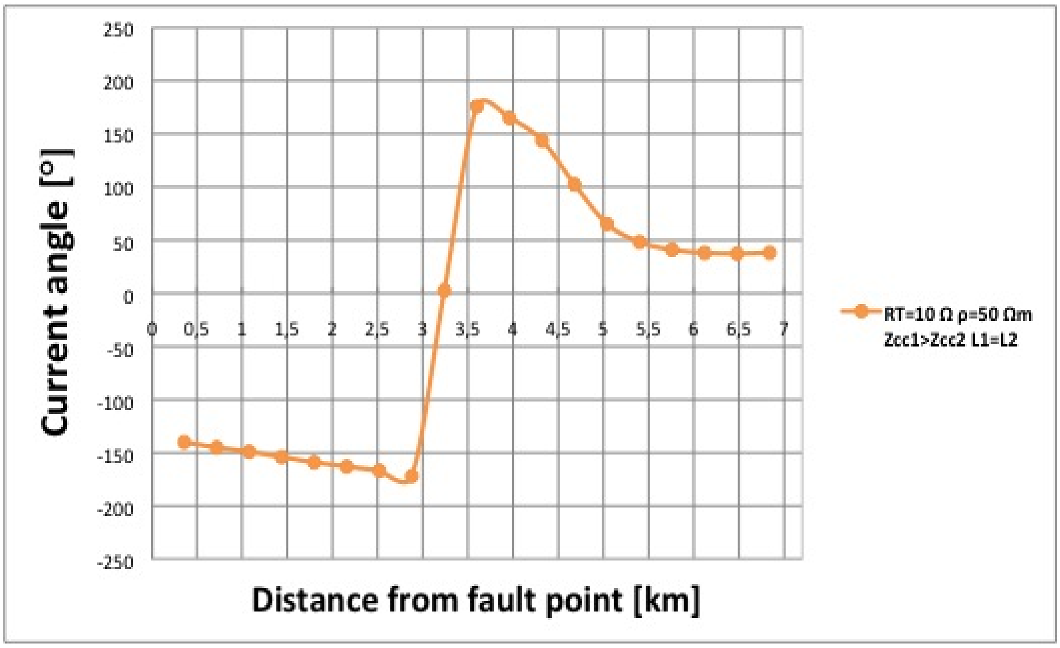

Figure 6.26: Tower footing current phase angle distribution along the line L1 with middle substation fault and fixed soil and tower footing resistance parameters

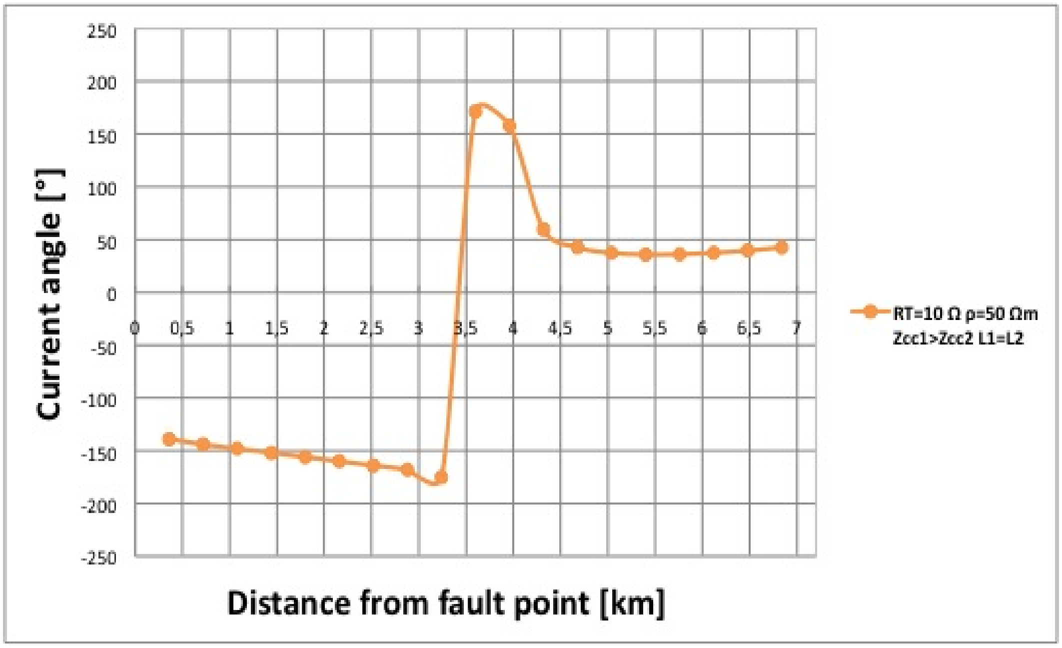

Figure 6.27: Tower footing current phase angle distribution along the line L2 with middle substation fault and fixed soil and tower footing resistance parameters

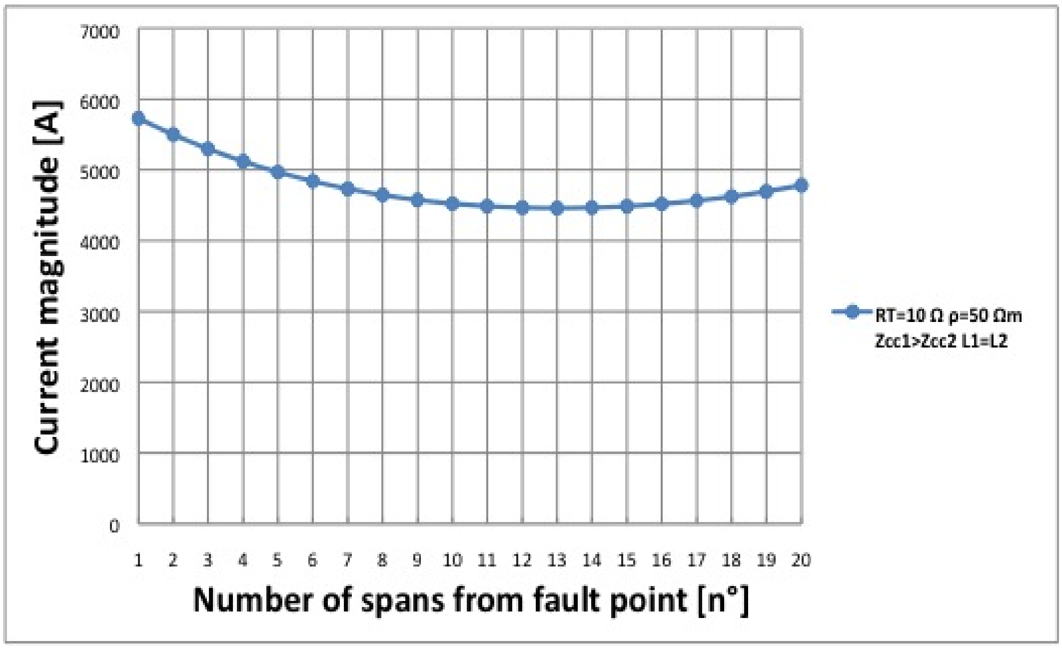

Figure 6.28: Span current distribution along earth wire of line L1 with a middle substation fault and fixed soil and tower footing resistance parameters

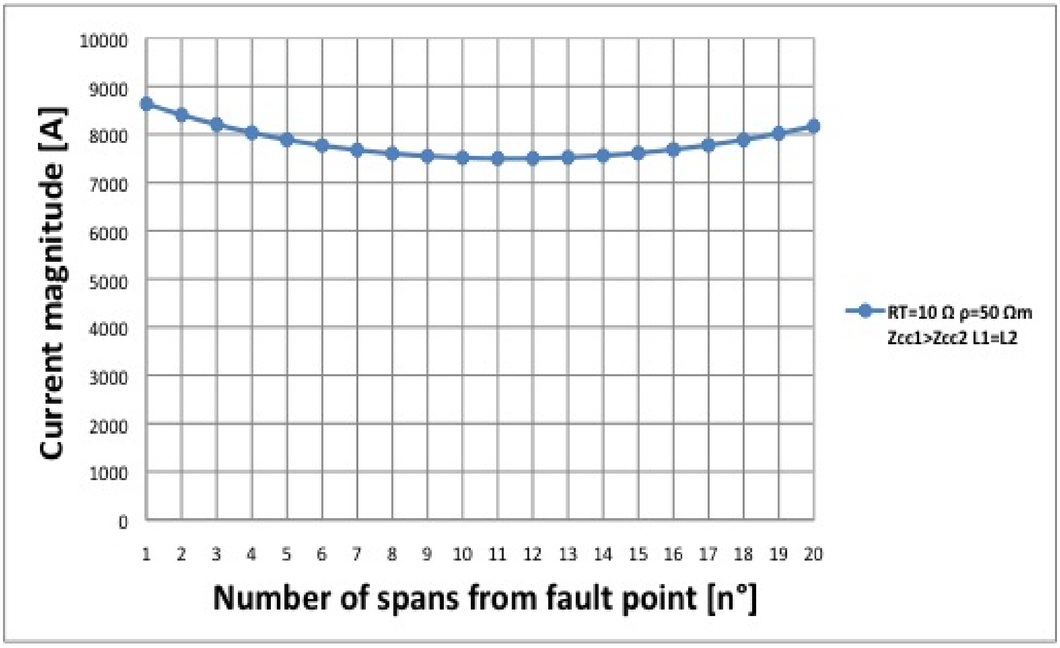

Figure 6.29: Span current distribution along earth wire of line L2 with middle substation fault and fixed soil and tower footing resistance parameters

6.5.2 Comments

In this case both line distributions are shown because the network is not symmetrical respect the fault anymore; since the short-circuit impedances of the generators are different, a lower Zcc means that the grid with that short circuit impedance is more powerful in terms of short-circuit real power Pcc, this influences the current distribution on the towers and on the earth-wire.
Figures 6.24 and 6.25 show the tower footing current distribution along the line L1 and L2, the trend is quite similar but with different magnitude values, indeed, where the line has a lower short-circuit impedance the current magnitude at the beginning of the line on the tower close to the generator is higher than the other line, 152 A on line L1 against 85,9 A on line L2. The minimum value is still at 4,2 km from the fault point, either for line L2 and line L1, as the case with $Zcc1 = Zcc2$ and it's value is $\approx$ 0 A. The short-circuit impedance change doesn't affect that much che tower footing current magnitude trend, the minimum point remains at the same distance from the fault point and the maximum values have a difference of $\approx$ 66 A. Looking at the tower footing current angle distribution shown in fig. 6.26 and 6.27, the trends remain the same with just a faster decrease after the peak of the phase angle on the line L2, this means that a difference in terms of short-circuit power of the feeding sections doesn't affect the tower footing phase angle and therefore, the current flow directions.
Fig 6.28 and 6.29 which represent the span current distribution along the earth wire, it can be notice that, the distribution along both lines is quite uniform but, on the overhead line L2 where the generator presents a lower short-circuit impedance the magnitude of the current values is higher; the maximum current on the line L2 is 8634 A respect to the maximum value on the line L1 of 5728 A. This variation means that the short-circuit power influences mostly the earth-current magnitude rise where the power source has a less short-circuit impedance Zcc.

6.6 CASE 4

For this study, the network is composed as the previous case but with the line L2 longer than L1 with exactly a double lentgh but with same tower pylon structure configuration, conductors characteristics and electrical parameters. Line L2 has 40 spans for a total lenght of 14.4 km composed by two equal line blocks as can be seen in the circuit represented in fig 6.30; the values of soil and tower footing resistance are the same set in the previous case $\rho = 50\Omega$m and RT=10 Ω, the generators short circuit impedances Zcc have the same value and the fault is still placed at the middle substation.
Since L2 is longer than L1, the magnitude of the earth-wire current L1 overehead line will be higher than the magnitude along the spans of the earth wire of the line L2; along the spans connected to the fault point the current values are:

- I_{w1}= 4837 A $\qquad I_{w2}$= 3761 A

  The ratio between the ground current I_{gr} and the short-circuit current at the fault point $I_f$is:

- $\frac{I_{gr}}{I_f}=\frac{16000}{24000}=66\%$ $\qquad [RT=10\ \Omega,\ \rho=50\ \Omega\text{m}]$

at the generator points the ratio between the groud currents $I_{gr1}I_{gr2}$ and the generator currents I_{g1}, I_{g2} is :

- $\frac{I_{gr1}}{I_{g1}}=\frac{9394}{14000}=67\%$ $\qquad [RT=10\ \Omega,\ \rho=50\ \Omega\text{m}]$
- $\frac{I_{gr2}}{I_{g2}}=\frac{6956}{10000}=69\%$ $\qquad [RT=10\ \Omega,\ \rho=50\ \Omega\text{m}]$

As can be notice, one more time, the current ratio I_{gr}/I_f at the fault point remains around the 65% as seen for the previous cases; in all them, changing line lenghts or short-circuit impedance or even making a not symmetrical feeding sections does not affect the earth fault current partition at theshort-circuit point.
The current which flows through the earth wire is lower along both lines respect to the case with different generators short-circuit impedances and equal line lengths but the highest current value on the span connected to the earthing substation system is along line L1; this line is shorter than L2 so it has a lower total self impedance as thought it has a less short-circuit impedance seen from the power source to the

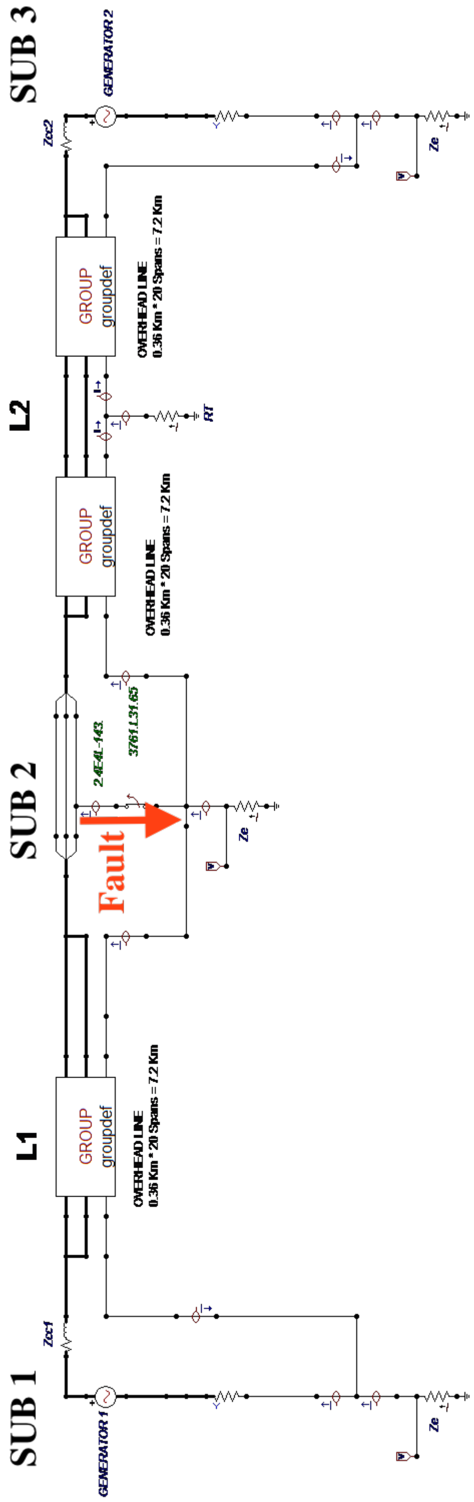

Figure 6.30: Middle substation fault feeded by two generators at side substations with two overhead lines with different length

fault point. In this case the fault impedance of the left section is lower as the case where line L2 had a lower short circuit impedance of power source. As the previous cases, the chart results are different for the two lines because the un-symmetrical configuration respect to the middle substation yields a different distribution along the two section which compose the network.

6.6.1 Results

Here below are reported the obtained results.

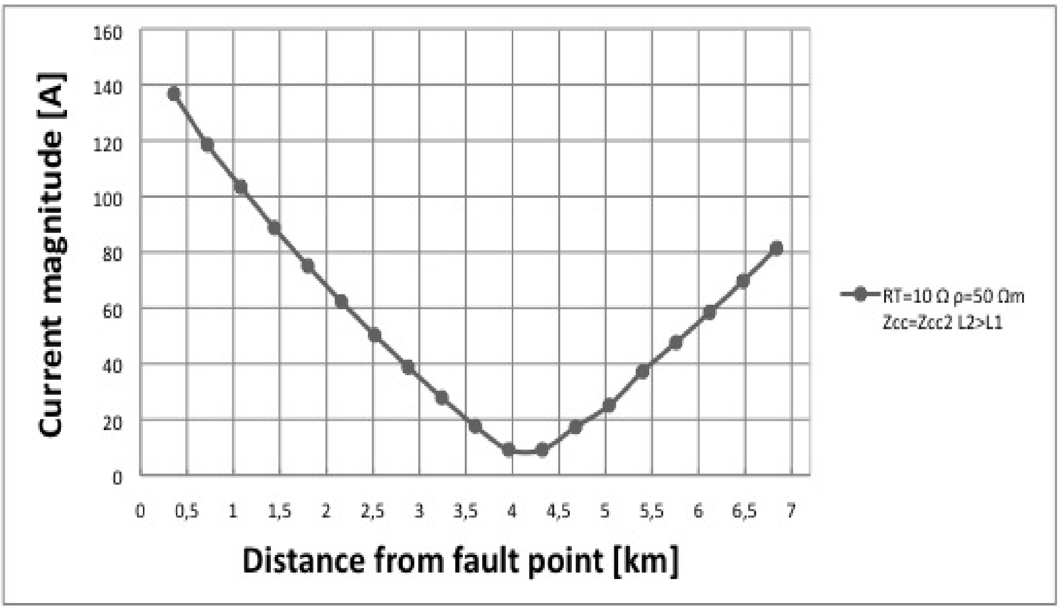

Figure 6.31: Tower footing current distribution along the line L1 with middle substation fault; soil and tower footing resistance values fixed

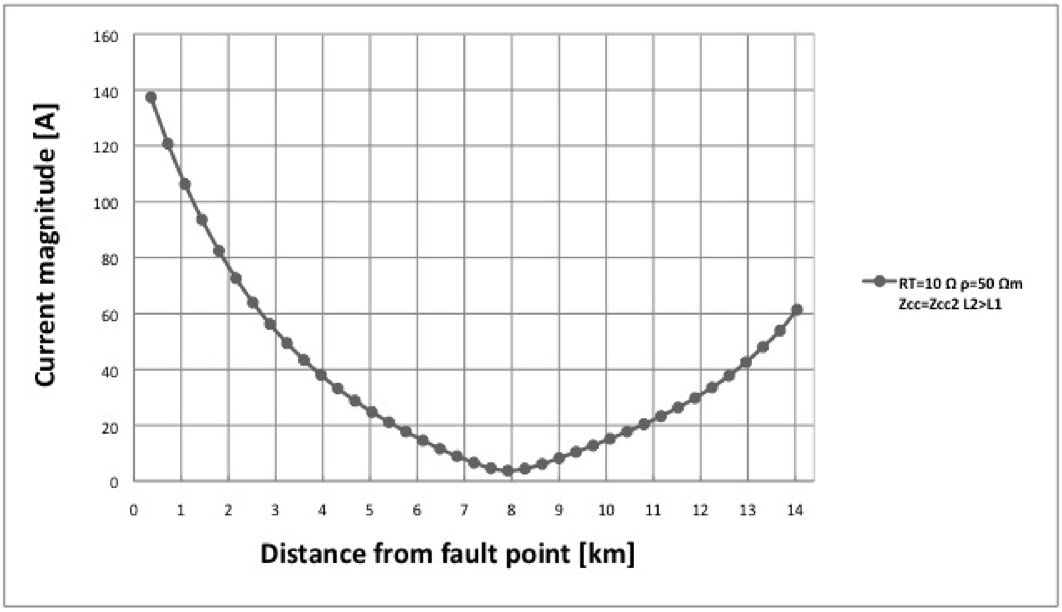

Figure 6.32: Tower footing current distribution along the line L2 with middle substation fault; soil and tower footing resistance values fixed

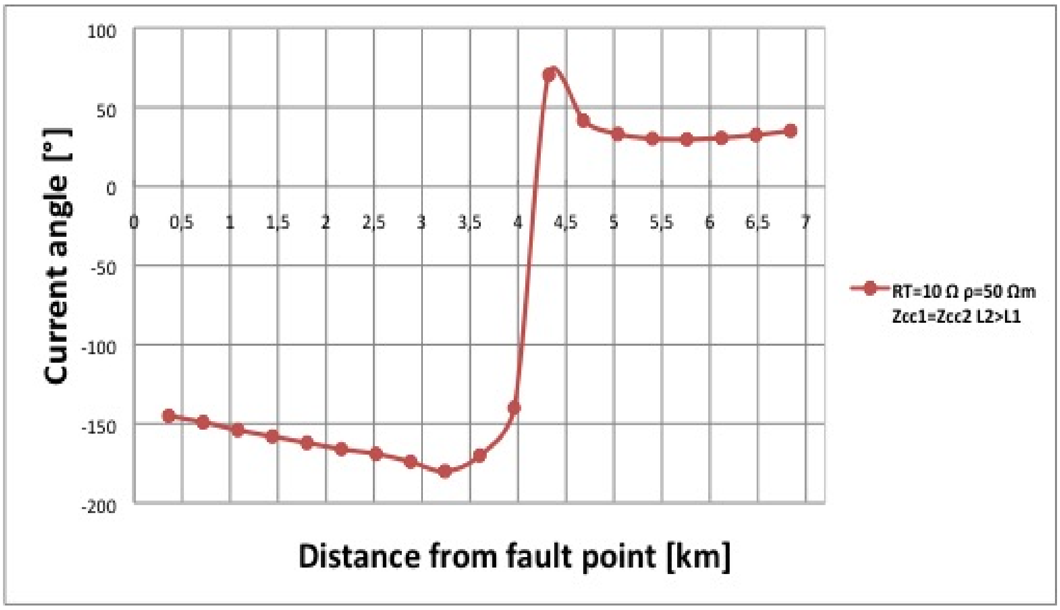

Figure 6.33: Tower footing current phase angle distribution along line L1 with middle substation fault; soil and tower footing resistance values fixed

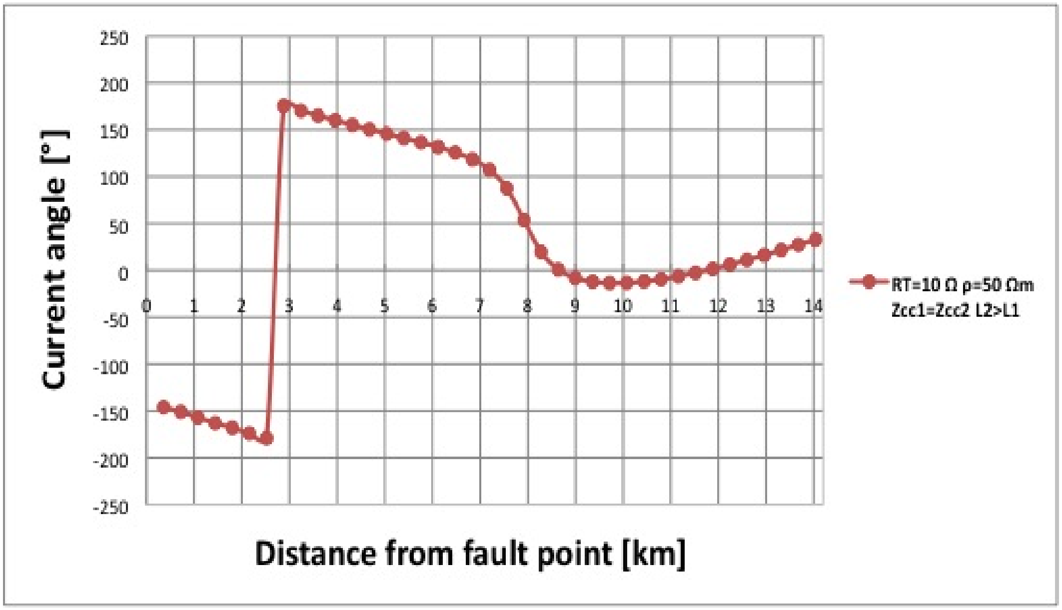

Figure 6.34: Tower footing current phase angle distribution along line L2 with middle substation fault; soil and tower footing resistance values fixed

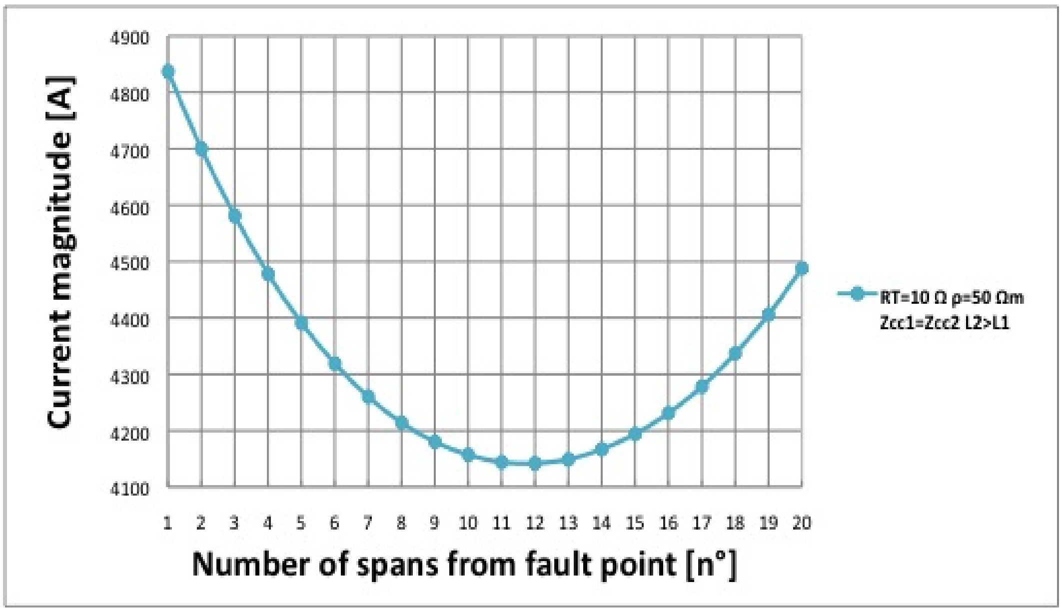

Figure 6.35: Span current magnitude distribution along earth wire of line L1 with middle substation fault; soil and tower footing resistance values fixed

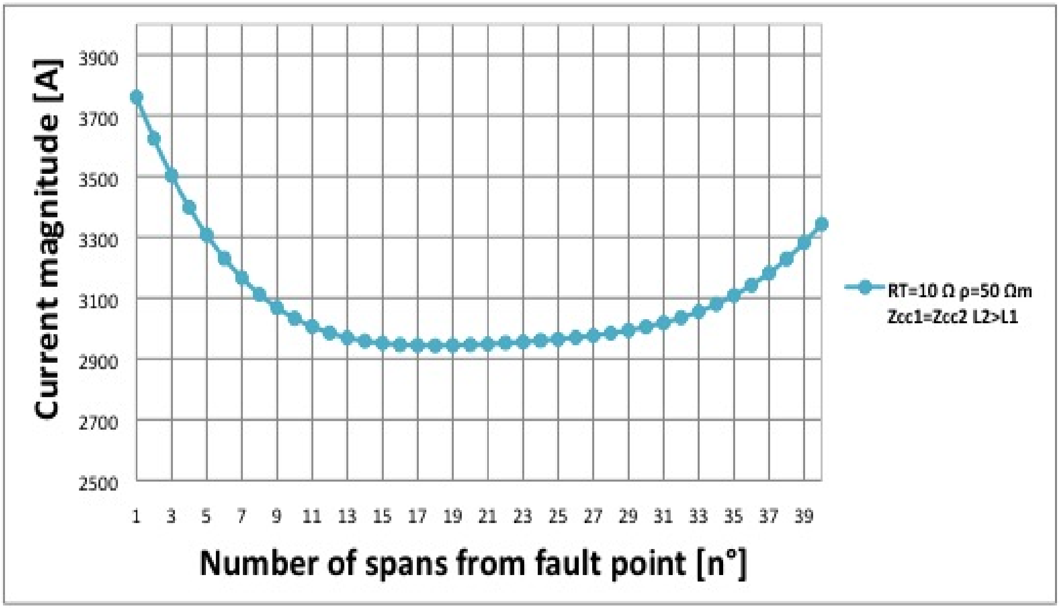

Figure 6.36: Span current magnitude distribution along earth wire of the line L2 with middle substation fault; soil and tower footing resistance values fixed

6.6.2 Comments

The tower footing current distribution looking at fig. 6.31 and 6.32 presents the same trend with the minimum value approximately at the middle point for both overhead lines and with the same magnitude even if L2 is longer than L1. The tower footing angle distribution represented in fig 6.33 and 6.34 between L2 and L1 is quite different; the phase reverse is not at the same point, for L1 is at the middle of the line but for L2 we have to reverses either at the beginning and at the middle.
As shown in fig. 6.35 and fig. 6.36 the current magnitude values which mostly change between the two different line sections are the earth-wire span current distributions; the shape of distribution basically is the same along the two earth wires with minimum value at the middle, but there are higher values of current magnitude at the beginning and at the end of the shorter line. Looking at the charts, the most interesting trend is present in fig 6.34 which shows the tower footing current angle distribution along line L2; the trend is quite similar to those seen previously for simple model and the cases with $Zcc1 = Zcc2$ or $Zcc1 < Zcc2$ only at the begging of the line going from the fault point to the generator untill 7,2 km which is the part of the line represented by the first ATPDraw block; after this point the angle decreases its value until a minimum point at 10 km and then it raises towards the power source substation.
This trend yields that even if the overhead line L2 is longer, for the first half until 7,2 km as long as the other line L1, the phase angle trend is quite similar, but, analysing the global length of the right overhead-line section the phase angle trend is completely different; the angle reverse is not at 4,2 km anymore as seen for line L2 but is at 2,88 km from the fault point afterwards there are two new reverses at 9 km and 11,16 km until reaching $\approx$ 50 degrees at the side substation 3.
Related to fig. 6.31 and 6.32 the tower footing current distribution mainteins the same trend in both lines but with different current values on the towers close to the generator; 81,39 A for line L1 and 61,41 A for line L2, in this case the difference is not so high and the minimum value which is almost equal to 0 A for both lines is at different points, 4,2 km for line L1 and 6,12 km from fault point for line L2; this means that a different line lentgh influences the shifting of the current distribuition along the different sections.
Comparing fig. 6.35 and fig. 6.36 we can say that the span current distribuition on the longest line is more uniform, indeed as can be seen, the value of the span current at the middle of the line from the 13th span to 27th span is quite steady as opposite to line L1, this yelds that longer is an overehad line more uniform is the distribution of the current along its earth wire with a more flat current concentration on the spans in the middle.

6.7 CASE 5

The network showed in fig. 6.38 consists in 5 substations with the same earth impedance Ze=0,1 Ω; the fault is placed at middle substation 3 and in the other 4 substations there are four equal generators with the same electrical parameters, 275 kV line-to-line RMS value, zero degrees phase angle with their short-circuit impedances Zcc connected in series. The connection between the substations is provided by 4 overhead lines 7,2 km long with the same geometrical and electrical data and L2 tower pylon configuration; the only thing that changes is the soil resistance which is increased from 50 Ωm to 100 Ωm respect the previous cases.
The short-circuit current magnitude will be given by the contribution of four equal sources from the right and left sections of the network; considering the fault location, the system is symmetrical, feeded by two equal section. The right section characteristics are the same of the left section therefore, as said for the second case studied, only the current distribution along one of these section for example on the left section can be analysed because they have the same characteristics; the current distribution along the lines between substation 1 and the faulted substation 3 will be the same along the line between faulted substation 3 and substation 5.
The earth fault current partition at the fault point, considering the ratio between the ground current I_{gr} and the fault current I_f, is:

- $\frac{I_{gr}}{I_f}=\frac{17000}{26000}=65\%$ $[RT=10\ \Omega,\ \rho=50\ \Omega\text{m}]$

The percentage of earth fault current which flows in the ground remains still the same but both values are higher due to the contribution of four generators to the short-circuit event. If the fault is feeded at both sides by two overhead lines with the same characteristics and also the generators have got the same electrical parameters, the current partition on the earth-wire at fault point will be exactly the same :

- I_{w1}=4896 A I_{w2}=4896 A

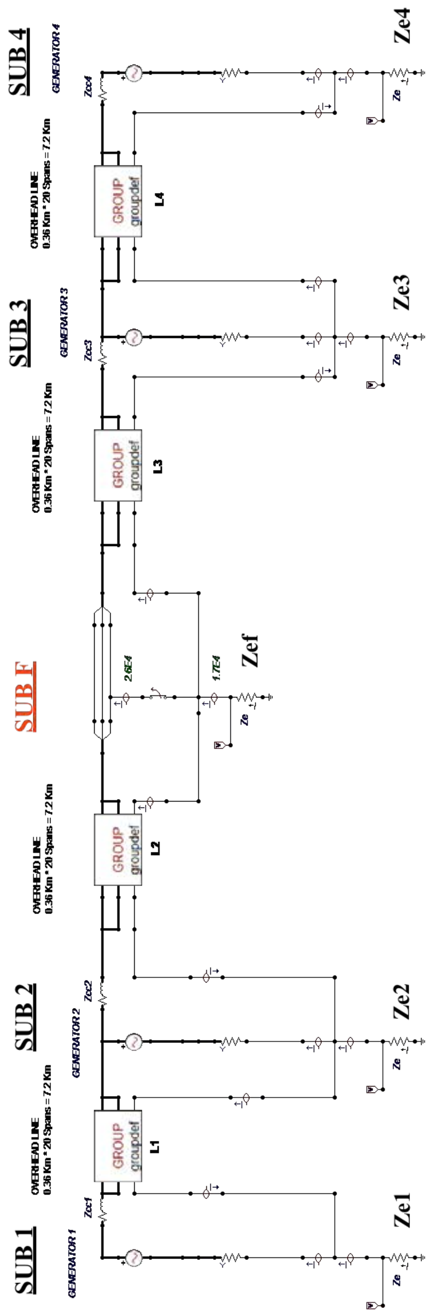

Figure 6.37: Middle fault substation feeded by 2 sections composed each by 2 generators at 2 substation connected by 7,2 km overhead line with L2 pylon configuration

6.7.1 Results

Here below are reported the graphic distributions of the tower footing current magnitude and phase angle, tower footing voltage and the span current along the left section.

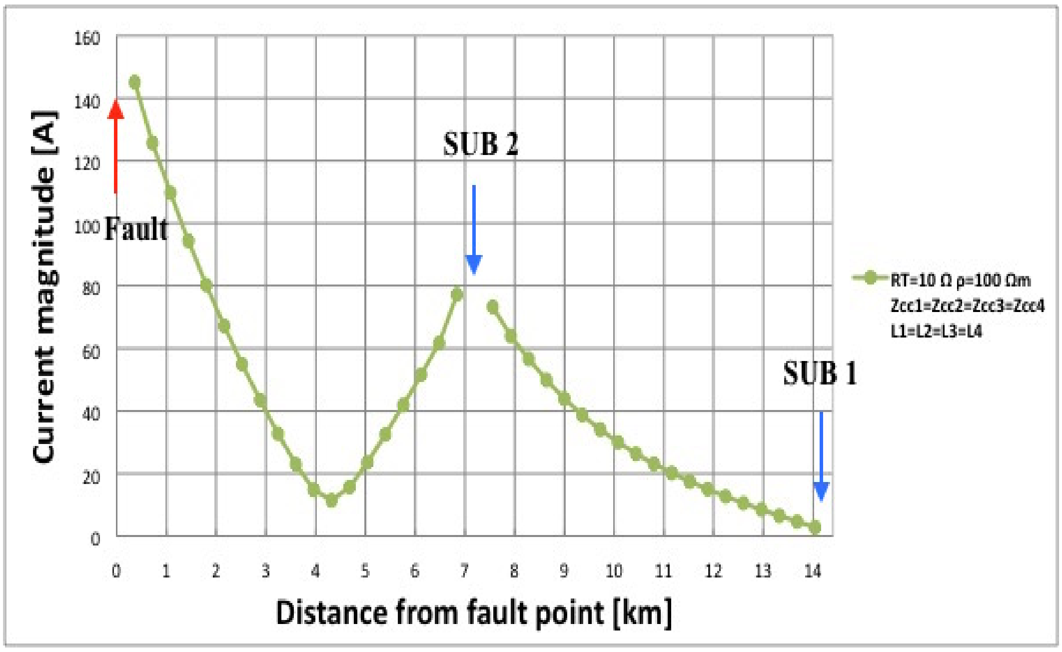

Figure 6.38: Tower footing current distribution along the network left section with fixed parameters of soil and tower footing resistance

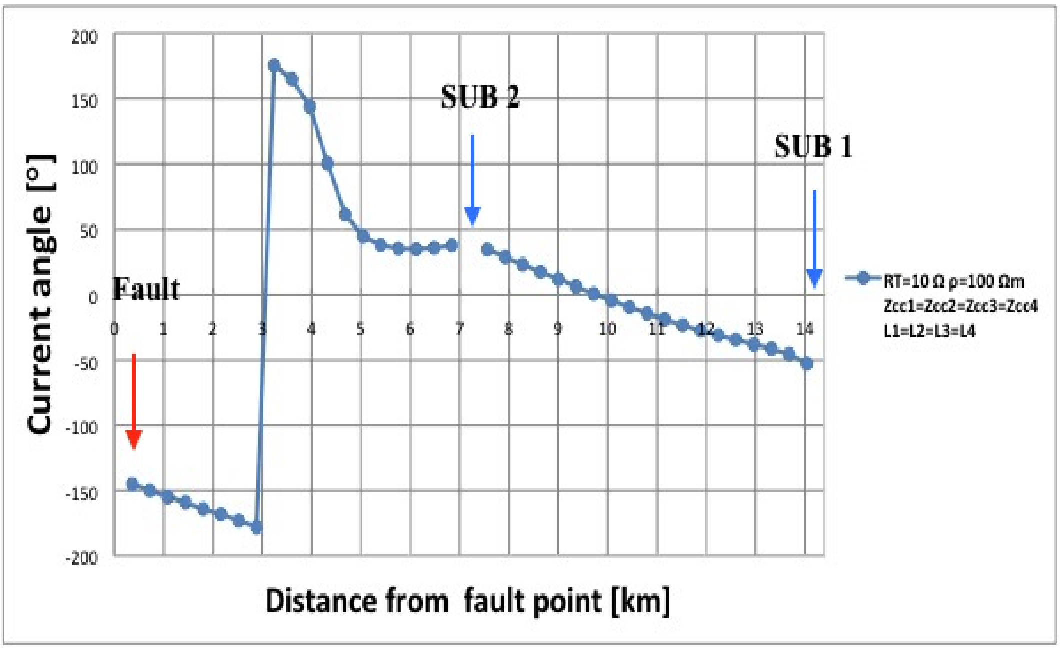

Figure 6.39: Tower footing current phase angle distribution along the network left section with fixed parameters of soil and tower footing resistance

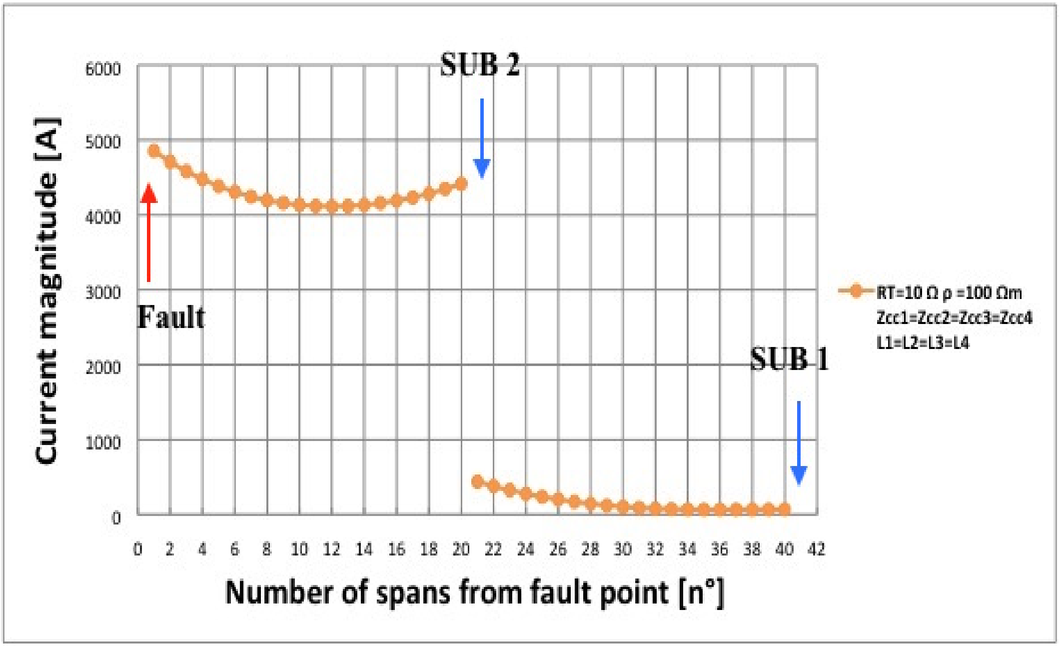

Figure 6.40: Span current magnitude distribution along the earth wire of network left section with fixed parameters of soil and tower footing resistance

6.7.2 Comments

In the charts, all the discontinuity points represent the position of the generators or substations. In this case, analysing only network section on left of the fault, the discontinuity point at the middle represents the substation 2 identified by the generator 2.
The current distribution shown in fig 6.38 for the first half represents the tower footing current magnitude along the line L2 and it has the same un-symmetrical distribution shape seen in the previous networks with the minimum value at 4,2 km but, along the line L1 the distribution is completely different; the magnitude of the current decreases and reaches the 0 value close to the substation 1. We can say that the tower footing current is distributed mostly along the line which connect the second substation to the fault substation; the short-circuit current contribution is given by all the network generators but the return current paths along the system are limited to the area wich includes the closest power source system.
The span current distribution along the two sections has the same trend but looking at fig. 6.40, at the substation point where there is generator 2 the value passes instantly to approximately 4550 A to 500 A, this current gap can be explained taking into account the amount of current that flows up through the substation earthing system 2, indeed a large amount of current flows back through the earth-wire and from the soil, than flows up through the generator 2; only a small current keep flowing through the earth wire along line L1 towards the substation 1, indeed along the line L1 the span current magnitude has a value between 439,5 A at the beginning after substation 2 and 67,31 A along the last span close to the generator 1.
Looking at fig. 6.39 which shows the tower footing current phase angle, the distribution along the line L2 has the same trend seen in the previous cases, after substation 2 along line L1 the trend is very different, the phase angle starts from 34,55 degrees and it decreases constantly reaching the zero value at 9,32 km from the fault, then it becomes negative until the substation 1 where it has a value of -52,7 degrees; this trend is quite similar to the 4th case studied where the fault was feeded by line of different lengths. Along line L2 which was the double length line the phase angle distribution was different only at the final part where the angle after a decrement rises again; this difference could be explained by the presence of the generator at the middle of the section which affects the angle assumed by the tower current as can be seen comparing fig. 6.39 and 6.34; the first part of the section behaves like a simple network with generator that feeds the fault, it doesn't matter if there is another generator connected upstream after the substation 2, the current distribution trend along line L2 is independent from it, the presence of one or more generators connected after the first closest substation to the fault point influences only

the distribution along the lines which connect the generators each other and not along the lines which connect the power sources to the fault point.

6.8 CASE 6

For this last example, the network configuration is composed by 5 substations with the same earth impedance value Ze=0,1 Ω, 2 three-phase sinusoidal generators direct grounded at sides substations 1 and 5, five line blocks with same geometrical characteristics used previously with L2 pylon configuration, each of them 7,2 km long for a total length of 36 Km from generator 1 to generator , soil resistance of 100Ωm and tower footing resistance of 10 Ω. As can be seen in the network reported on fig. 6.42 the section between the third and the fourth substation is made of two blocks, therefore the line L3+L4 which connects substation 3 and substation 4 is longer respect line L1, L2 and L5 exactly a double length with the consequence of an unsymmetrical network respect the short-circuit position.
In this case the fault wasn't placed at a substation anymore but between tower 5 and 6 along the line block L3 to simulate a short-circuit on the span between the two tower pylons as shown in fig. 6.41, for this reason we will not have a middle fault point but an unbalanced fault point relating to the network whole length; this choice is a further study to understand the effects of a span fault along the line of the network and what can produce on the substation earthing systems.
To represent the current and voltage trend on the towers and along the earth wire spans, this time all the charts are relating to the total length from generator 1 to generator 2, in this way it is easier to understand the current distribution and to do an accurate analysis; this kind of approach gives a clearer evaluation about the current which flows through the earth substation impedances even if the fault is not close to them or is directly on an overhead line which connects two or more substations.
Setting the fault at the chosen point, the value of the short-circuit current is

$$I_f = 19.139KA$$

; the magnitudes of the currents which flow through the substation earth impedances are:

- $I_{Ze1} = 6507 < 37,7°A$ SUBSTATION 1
- $I_{Ze2} = 75.95 < -119°A$ SUBSTATION 2
- $I_{Ze3} = 2908 < 9,88°A$ SUBSTATION 3
- $I_{Ze4} = 98.36 < -126°A$ SUBSTATION 4
- $I_{Ze5} = 5945 < 37,9°A$ SUBSTATION 5

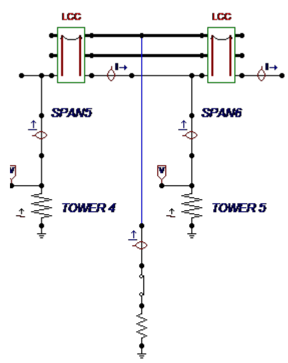

Figure 6.41: Span fault model

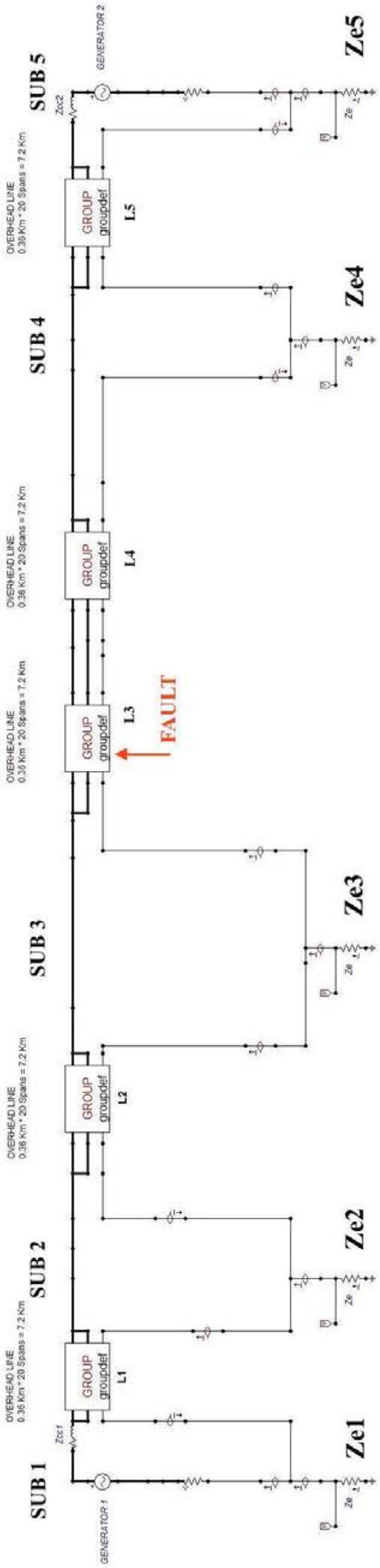

Figure 6.42: 5 substation network, 2 side generators with fault between tower 5 and 6 along line L3

6.8.1 Results

Here below are reported the current and voltage distribution along the network from generator 1 to generator 2.

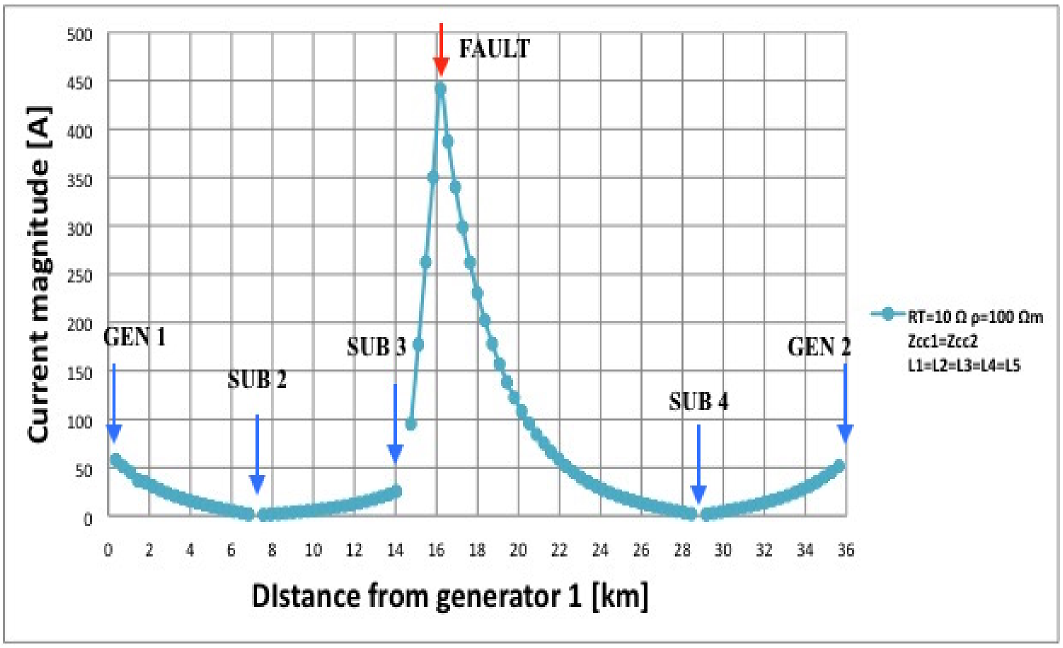

Figure 6.43: Tower footing current distribution along the network from substation 1 to substation 5 with span fault between tower 5 and 6 of line L3 and fixed parameters of soil and tower footing resistance

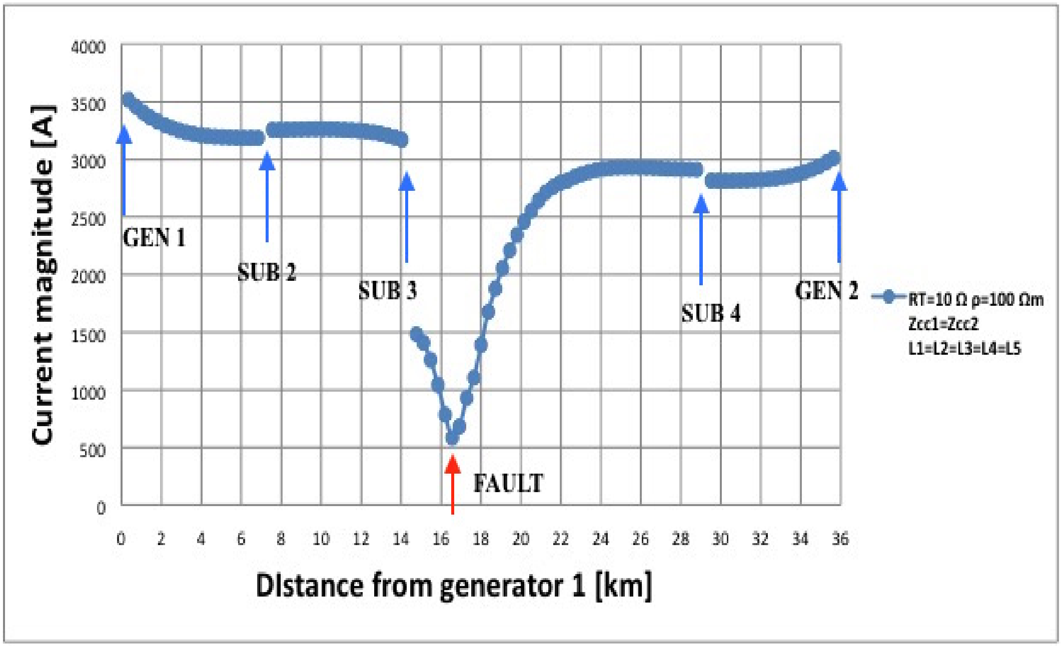

Figure 6.44: Span current distribution along the earth wire of the network from substation 1 to substation 5 with span fault between tower 5 and 6 of line L3 and fixed parameters of soil and tower footing resistance

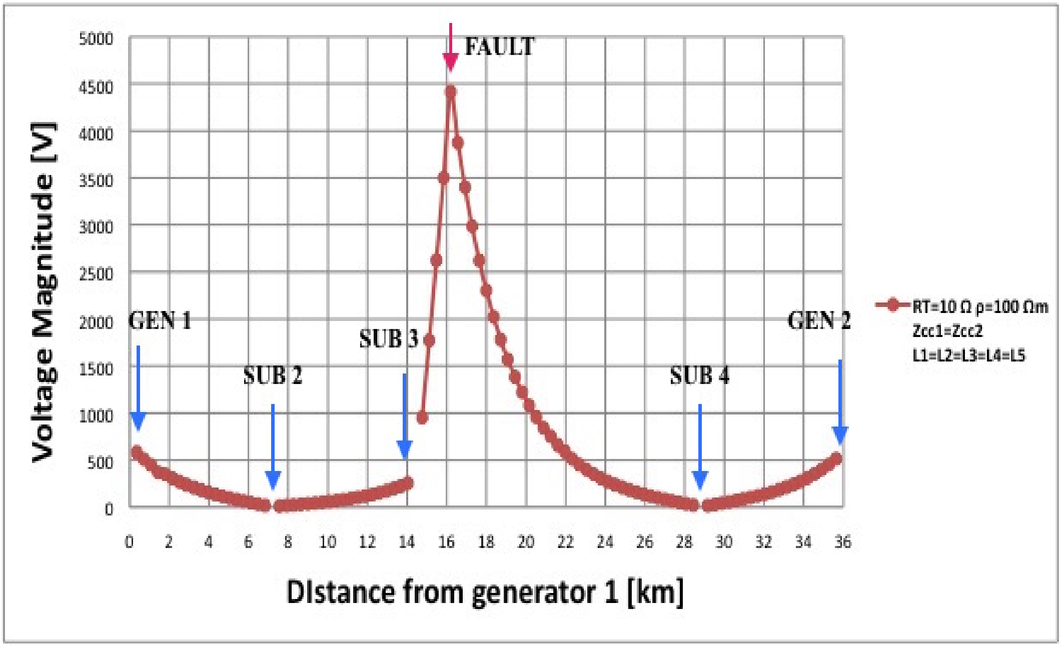

Figure 6.45: Tower footing voltage distribution along the network from substation 1 to substation 5 with span fault between tower 5 and 6 of line L3 and fixed parameters of soil and tower footing resistance

6.8.2 Comments

Fig. 6.43 shows the tower footing current magnitude distribution; on the chart there are some discontinuity points where the substations are placed; even if there are these points, the distribution is quite continuous with small gaps at the towers immediately before and after the substations.
Since the fault in this case is set at a span between two towers we can see that the maximum value of tower footing current is exactly on the tower close to the fault point at 16,2 km; starting from this point and going on towards the generators the current decreases until the next substations and then it rises again until the side substations reaching a value of current magnitude equal to 50 A on the towers close to the generators. The interesting thing that we can notice on fig. 6.43 is that even if the fault is not at the middle of the system the current distribution along this network is almost symmetrical respect to the fault point; between the fault and the next substation on the left there are only 4 towers while 14 towers between the fault and the next substation on the right but the current distribution has the same trend; this means that even if the fault is at the beginning, at the middle or at the end of an overhead-line the tower footing current distribution will be almost symmetrical respect to the fault point where there will be present the maximum value.
Related to fig. 6.44 which shows the span current distribution along the earth wire, the trend is opposite respect to fig. 6.43, on the spans beside the fault point, in this case there are the minimum current values and proceeding from the fault towards the generators the magnitude rises until 3517 A along the span close to generator 1 and until 3109 A close to generator 2 so the distribution along the line is not symmetrical specially looking at the distance of 14,4 km where there is a significant discontinuity point with a magnitude gap of 1687 A due to a high current quote which flows up through the substation 3 earthing system. The last chart represented in fig. 6.45 shows the tower footing voltage distribution along the network; as can be notice, it has the same trend of fig. 6.43 changing the scale value.
The voltage is obtained multiplying the tower current for the tower footing resistance RT which is, in this network, set to 10Ω obtaining the earth potential values; the maximum voltage as seen for the tower footing current, is on the pylon close to the fault point with a magnitude equal to 4414 V.

Chapter 7

Statistic study of Earth Potential Rise distribution

7.1 Introduction

The Earth Potential Rise (EPR) is defined as the voltage between a grounding system to remote earth. As previously said, when a current flows through the tower pylons or the earth substation impedances during a line-to-earth short-circuit, their potential to remote earth increases, and it can be calculated with the following forumla:

$$U_E = R_E * I_E$$

where:

- R_E is the resistance to earth, calculated or measured [Ω]
- I_E is the earth fault current [A]

The EPR statistic distribution study is useful to understand how much the potential magnitude rises nearby the fault and along the transmission line to prevent any damage to the people who are directly in contact with tower pylons, electric equipment or any other metallic part connected to earth within the substations during a line-to-earth short-circuit or people who are only standing close to flow current paths.
In this chapter, a particular analysis has been faced using a network composed by 4 substations, 3 overhead lines which connect them with the same length and characteristics of previous cases, represented in fig. 7.1 with two different configurations changing tower footing resistance ρ and tower footing resistance RT maintaining the same value of earth substation impedances Ze=0,1 Ω; the variation of these parameters allows a better evaluation of the earth potential rise and how they influence its distribution.
The different configurations are:

- RT=10 Ω ρ=50 Ωm **FIRST CONFIGURATION**
- RT=20 Ω ρ=1000 Ωm **SECOND CONFIGURATION**

To do a statistic type of study, the fault point has been placed in each span along the line from first span after SUB 1 to the last span before SUB 4 and in each substation earth impedance Ze; the short-circuit connects one phase of the system, in this case phase C, to the soil or to the earth substation impedance with a negligible resistance value as shown in fig. 7.2 .

Changing the fault position, point by point, the value of potential rise and what it produces on the others tower pylons and substation impedances has been analysed; since there are 63 possible positions for the EPR study and for each of them there are 63 voltages values due to the number of possible fault points, only the following points were considered for the statistic analysis:

- EARTH IMPEDANCE, Ze2
- TOWER 1, L1

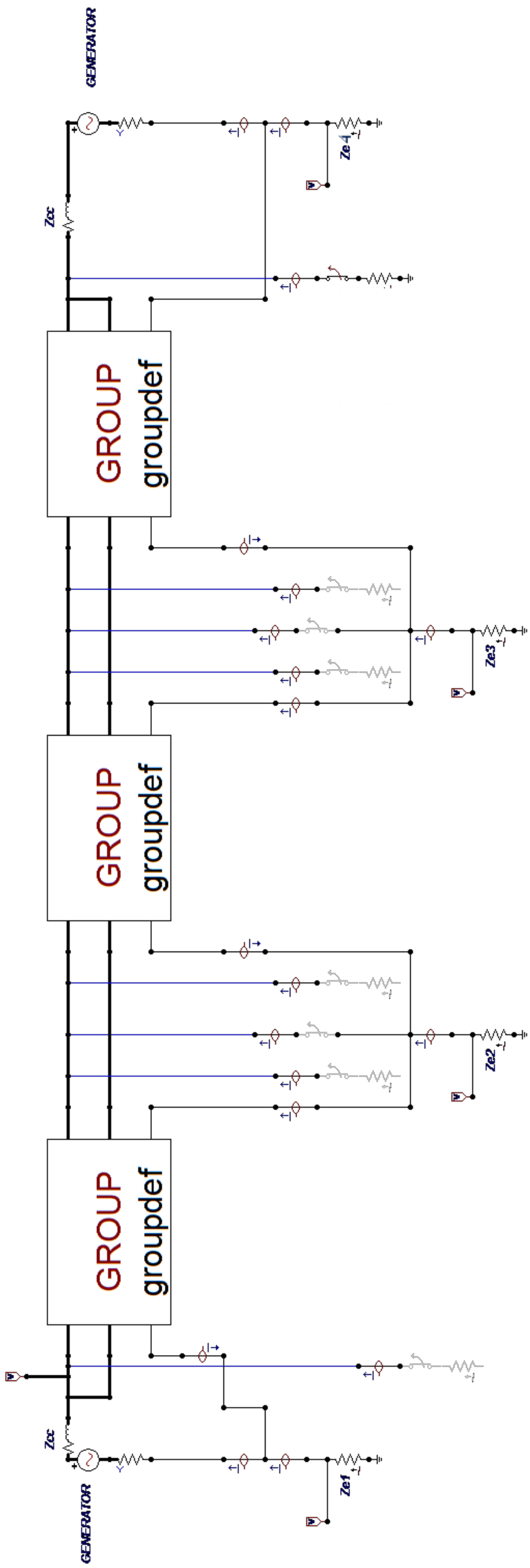

Figure 7.1: 4 substations network for the earth potential rise statistic study changing the fault position along the system

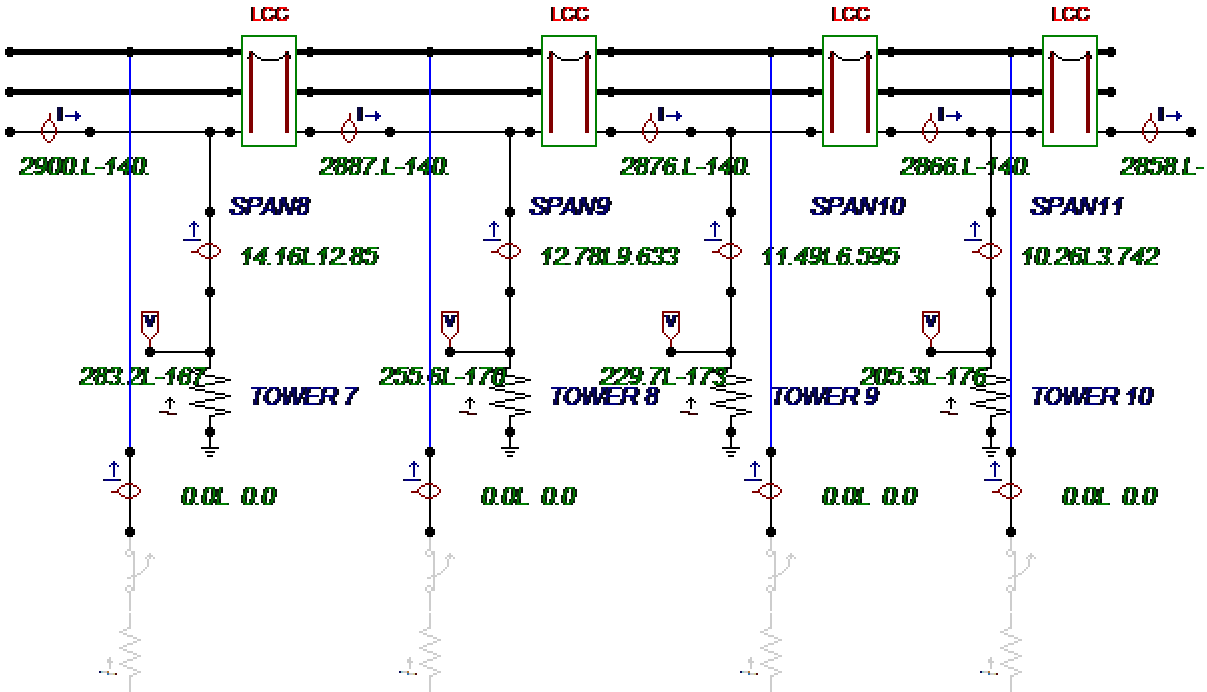

Figure 7.2: Example of span fault placed along the line which connects the phase C to the soil with a negligible value of fault resistance

- TOWER 3, L1
- TOWER 8, L1
- TOWER 15, L1
- TOWER 19, L1
- TOWER 10, L2

For the study a single short-circuit type as been used; as we know changing the fault location along the line causes a variation of the short-circuit current which can not have the same magnitude.
If the fault is close to the generator, the short-circuit current will be the highest and if the fault point is at the middle of the network, the current will be the lowest. This is due to the impedance of the line between the power source and the fault point, seen by the generator.
Placing the short-circuit along the first span after substation 1, the impedance will be higher than the total impedance seen from the generator if the fault is placed at the middle of the network between substation 2 and 3 therefore we will not have a single value of short-circuit current but a range from the maximum value to the minimum for both circuit configurations set as can be seen here below:

- 14854-17085 A **FIRST CONFIGURATION**
- 31230-56651 A **SECOND CONFIGURATION**

Once obtained the values, measuring in each considered position the EPR and changing the fault point along the network, it was possible drawing a histogram for each considered tower RT or earth impedance Ze with the distribution of the potential values ranges, allowing to know the peak concentration and the relative EPR value. The shape of the distribution gives knowledge of the potentially danger for people relatively close to towers and substation or directly contact with electric equipment during the fault time and the probability of a possible electrocution risk.

For both configurations the charts of the distribution and the associated table of magnitudes have been reported; in these tables the values are relatively to the voltage magnitude calculated when the fault position changes moving along the line from the first generator on substation 1 to the second generator on substation 4.

7.2 FIRST CONFIGURATION

7.2.1 Maximum and minimum values

In each point, considering the obtained data, there are a minimum and a maximum value of EPR and they are:

- Vmax=1713 [V] Vmin=347.9 [V] **TOWER 1, L1**
- Vmax=2819 [V] Vmin=270.1 [V] **TOWER 3, L1**
- Vmax=3583 [V] Vimn=210 [V] **TOWER 5, L1**
- Vmax=3980 [V] Vmin=53.79 [V] **TOWER 8, L1**
- Vmax=3274 [V] Vmin=49.39 [V] **TOWER 15, L1**
- Vmax=1166 [V] Vmin=10.64 [V] **TOWER 19, L1**
- Vmax=3796 [V] Vmin=3.83 [V] **TOWER 10, L2**
- Vmax=1543 [V] Vmin=3.258 [V] **EARTH IMPEDANCE Ze2**

7.2.2 Results

Below there is a report of the charts and the tables relative to the EPR distribution and obteined values with soil resistance ρ=50 Ωm and tower footing current RT=10 Ω; on the tables, the results have to be read from top to bottom and they are relative to the fault which changes the position from substation 1 to substation 4.

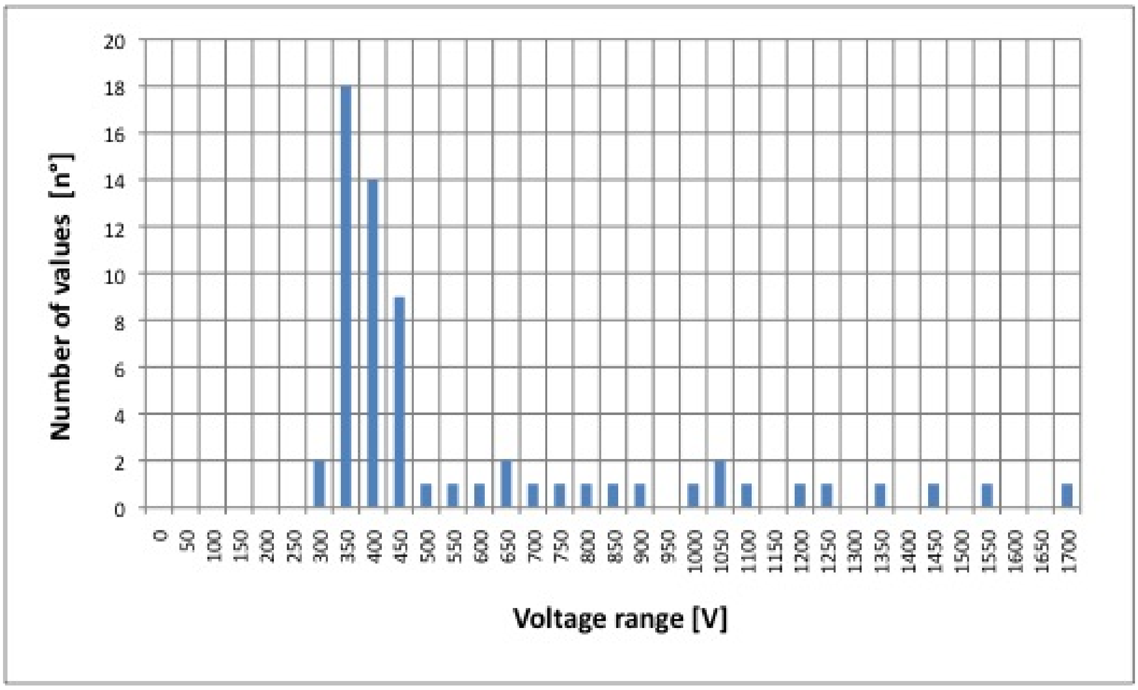

Figure 7.3: EPR statistic distribution on tower 1 of line L1

FAULT POSITION	EPR MAGNITUDE [V]						
L1	1093	1713	1587	1486	1378	1289	1209
L1	1135	1067	1003	944	888	835,4	785,6
L1	738	693,6	651	610,2	571,1	533,5	496,9
Ze2	492,7						
L2	488,8	481,4	474,5	468,2	462,3	456,8	451,5
L2	446,5	441,8	437,2	432,8	428,6	424,6	420,7
L2	417	413,4	410,1	406,9	404,1	401,5	
Ze3	401,5						
L3	397,3	393,4	389,7	386,2	383	379,8	376,8
L3	373,9	371,1	368,4	365,8	363,3	360,8	358,5
L3	356,3	354,2	352,3	350,6	349,1	347,9	

Table 7.1: EPR values, obtained on tower 1 of line L1 changing the fault point along the network

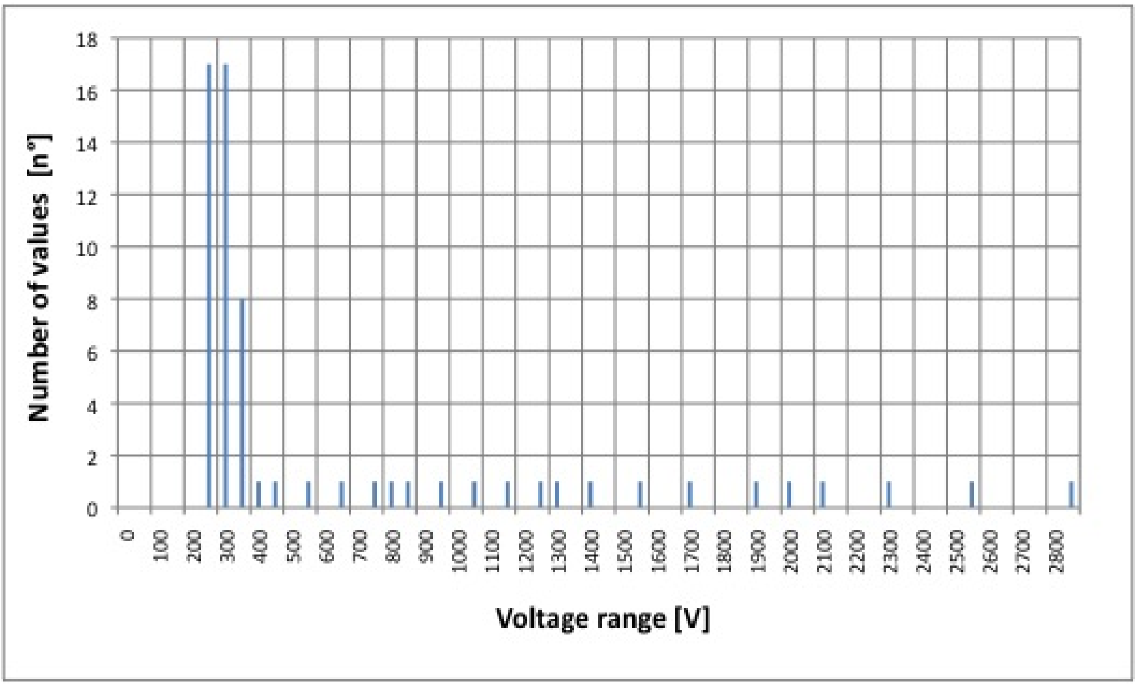

Figure 7.4: EPR statistic distribution on tower 3 of line L1

FAULT POSITION	EPR MAGNITUDE [V]						
L1	848,6	1330	2078	2891	2590	2330	2104
L1	1905	1730	1572	1430	1299	1178	1065
L1	958,7	857,2	760	666,3	575,6	487,7	402,6
Ze2	352,6						
L2	392,7	383,9	376	368,9	362,5	356,8	351,6
L2	346,8	342,5	338,4	334,7	331,3	328,1	325,1
L2	322	319	317,3	315,2	313,2	311,5	
Ze3	312,2						
L3	308,5	305,2	302,4	299,7	297,2	294,8	292,5
L3	290,2	288,1	286	284	282	280,1	278,3
L3	276,6	275	273,5	272,2	271	270,1	

Table 7.2: EPR values, obtained on tower 3 of line L1 changing the fault point along the network

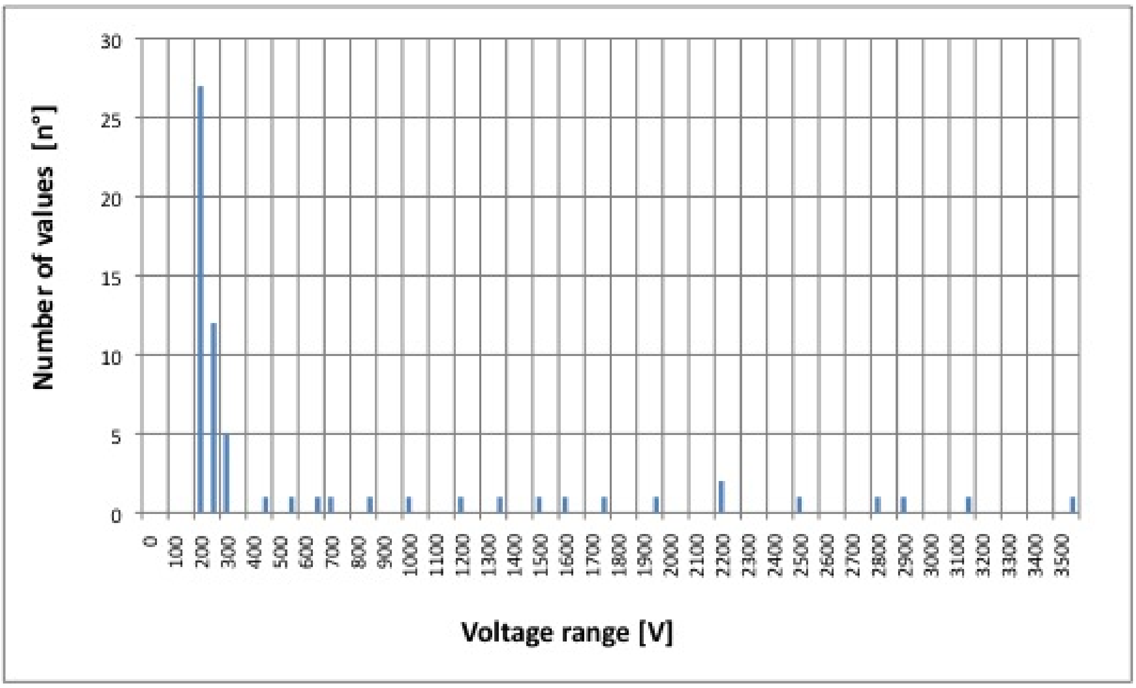

Figure 7.5: EPR statistic distribution on tower 5 of line L1

FAULT POSITION	EPR MAGNITUDE [V]						
L1	659,9	1034	1616	2248	2905	3583	3179
L1	2826	2516	2243	1998	1776	1574	1387
L1	1213	1048	891,4	741,9	598,9	463,7	341,4
Ze2	223,2						
L2	329,2	318,4	308,7	300	292	285	279
L2	274	269	265	261,6	258,3	255	252,7
L2	250,3	248,2	246,3	244,7	243,2	242,2	
Ze3	243,4						
L3	239,5	237,2	235	233	231	229,2	227
L3	225,6	224	222,4	220,8	219,3	217,8	216,4
L3	215,1	213,8	212,7	211,7	210,8	210	

Table 7.3: EPR values, obtained on tower 5 of line L1 changing the fault point along the network

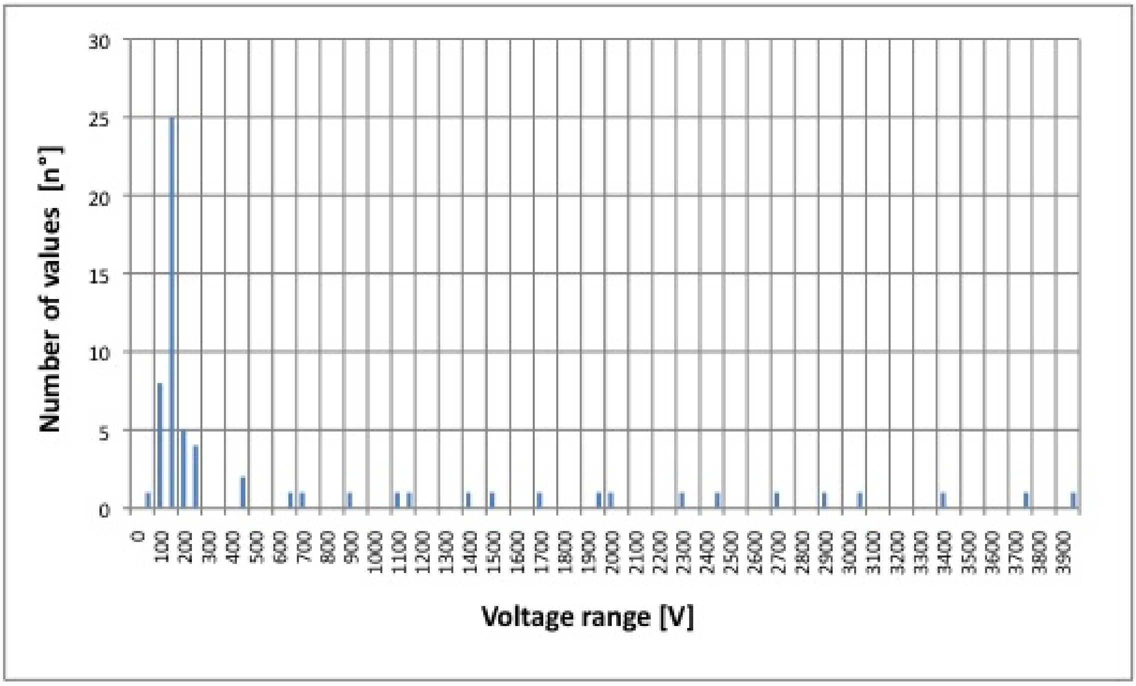

Figure 7.6: EPR statistic distribution on tower 8 of line L1

FAULT POSITION	EPR MAGNITUDE [V]						
L1	452,1	708,7	1107	1540	1990	2455	2937
L1	3443	3980	3497	3066	2680	2329	2006
L1	1707	1427	1161	909,7	671,6	454,1	291,3
Ze2	53,79						
L2	276,4	262,8	250,4	239,3	229,2	220,2	212,2
L2	205	198,7	193,2	188,3	184	180,3	177,1
L2	174,4	172	170	168,2	166,7	165,4	
Ze3	167,7						
L3	163,7	162,1	160,7	159,3	158	156,8	155,6
L3	154,4	153,3	152,2	151,1	150	149,1	148,2
L3	147,3	146,4	147,7	145	144,4	143,9	

Table 7.4: EPR values, obtained on tower 8 of line L1 changing the fault point along the network

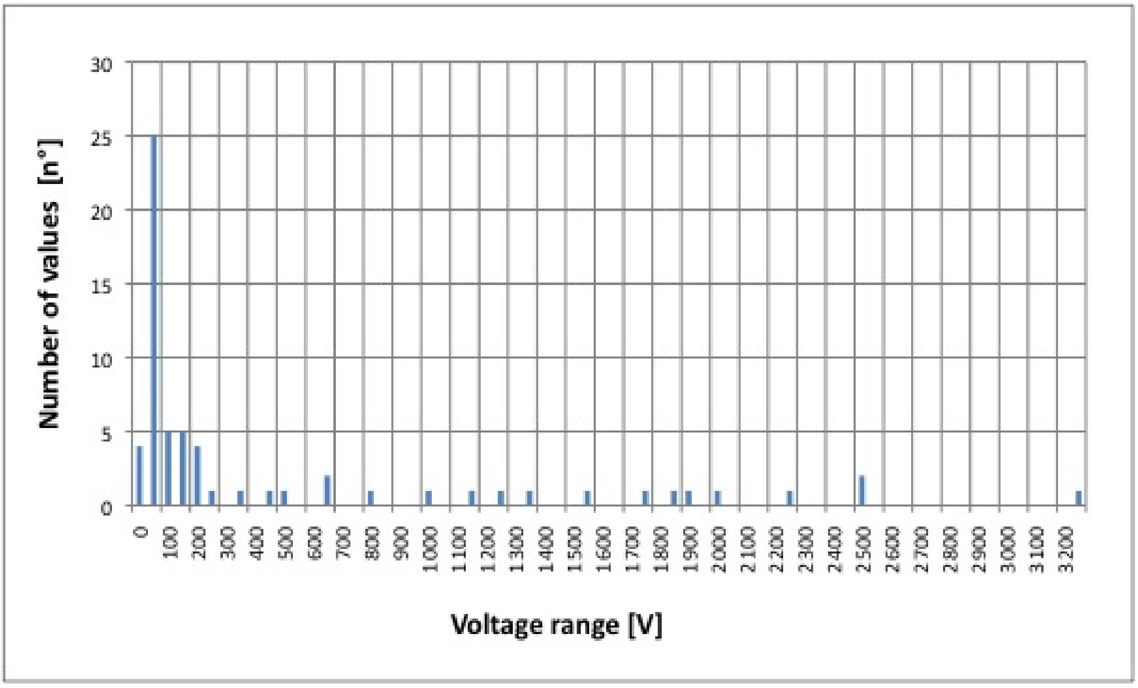

Figure 7.7: EPR statistic distribution on tower 15 of line L1

FAULT POSITION	EPR MAGNITUDE [V]					
L1	155,3	243,5	380,3	529,2	683,8	843,4	1009
L1	1183	1367	1565	1780	2016	2278	2571
L1	2900	3274	2583	1924	1293	695	271,3
Ze2	472,3						
L2	247,9	227,3	209,1	193	178,5	165,3	153,4
L2	142,5	132,4	123,1	114,5	106,4	98,9	91,84
L2	85,2	78,94	73,02	67,39	62	56,79	
Ze3	58,07						
L3	56,05	55,4	54,81	54,28	53,79	53,35	52,93
L3	52,55	52,18	51,83	51,5	51,19	50,89	50,61
L3	50,34	50,09	49,87	49,68	49,51	49,39	

Table 7.5: EPR values, obtained on tower 15 of line L1 changing the fault point along the network

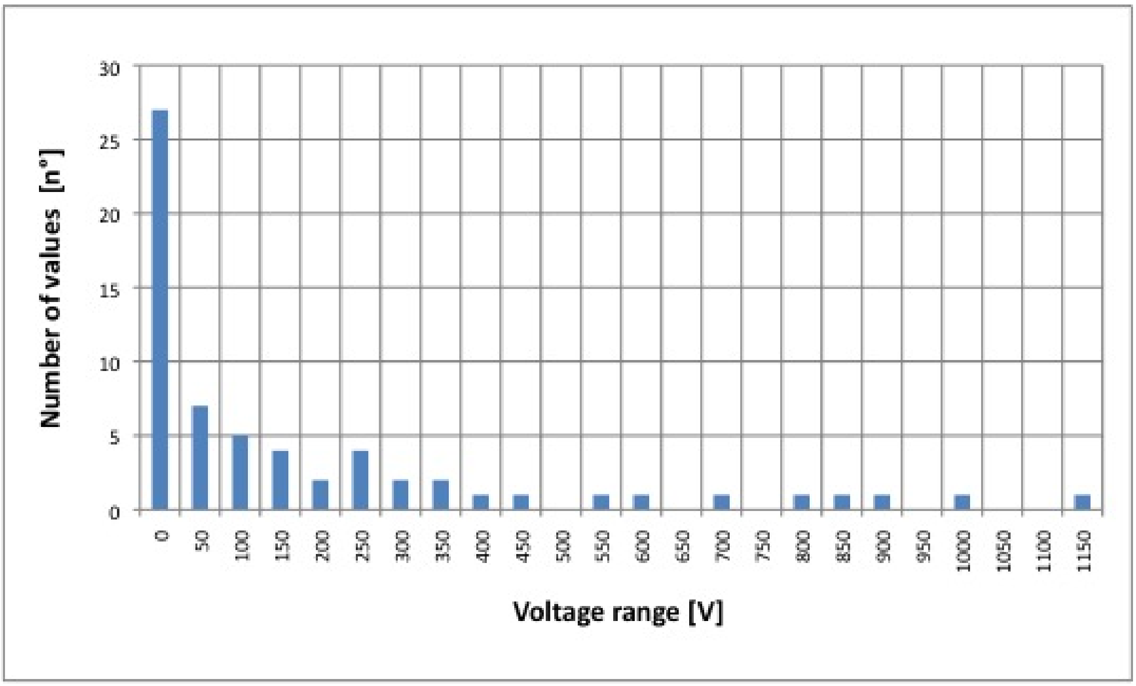

Figure 7.8: EPR statistic distribution on tower 19 of line L1

FAULT POSITION	EPR MAGNITUDE [V]						
L1	33,68	52,85	82,56	114,9	148,4	183,1	219,1
L1	256,8	296,8	339,8	386,5	437,7	494,5	558,1
L1	629,6	710,7	802,9	908	1028	1166	366,1
Ze2	857,8						
L2	322,4	284,5	251,7	223,2	198,4	176,6	157,4
L2	140,5	125,3	111,6	99,15	87,68	77,01	66,96
L2	57,41	48,24	39,37	30,74	22,34	14,3	
Ze3	10,81						
L3	13,71	13,2	12,75	12,37	12,05	11,77	11,54
L3	11,34	11,18	11,05	10,94	10,85	10,78	10,73
L3	10,69	10,66	10,65	10,65	10,65	10,64	

Table 7.6: EPR values, obtained on tower 19 of line L1 changing the fault point along the network

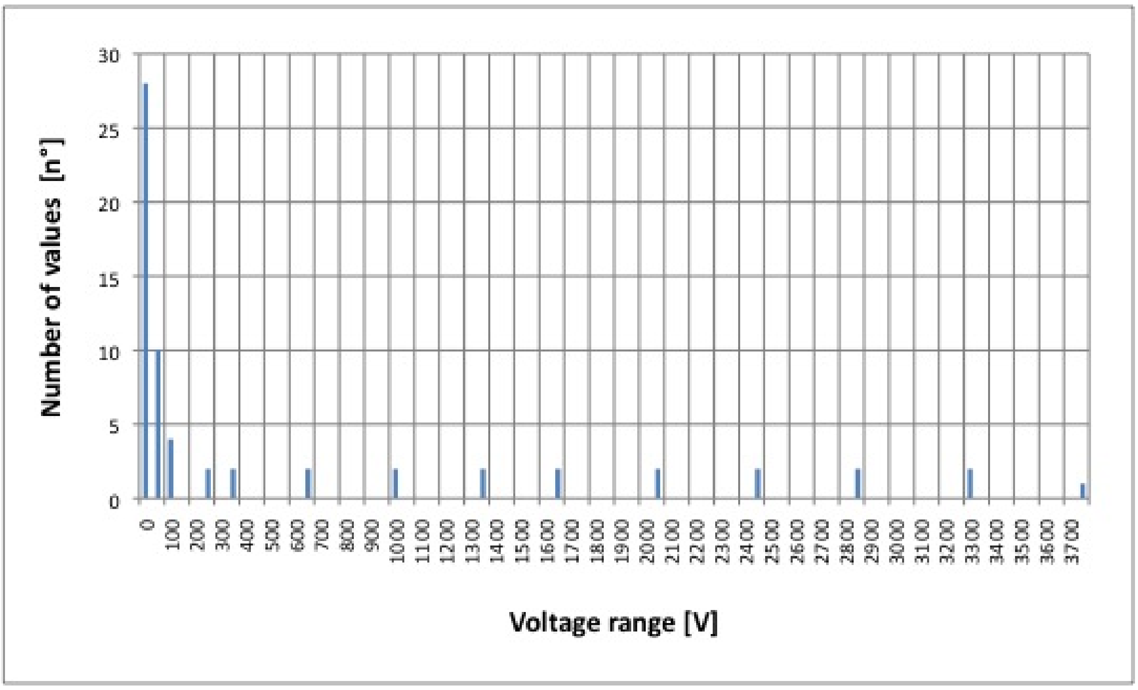

Figure 7.9: EPR statistic distribution on tower 10 of line L2

FAULT POSITION	EPR MAGNITUDE [V]						
L1	3,836	5,301	7,704	10,41	13,25	16,19	19,26
L1	22,48	25,9	29,57	33,55	37,94	42,8	48,26
L1	54,41	61,4	69,36	78,45	88,87	100,8	114,5
Ze2	275,4						
L2	371,4	687,9	1014	1351	1699	2064	2450
L2	2863	3309	3796	3309	2863	2450	2064
L2	1699	1351	1014	687,9	371,4	114,5	
Ze3	275,4						
L3	100,8	88,87	78,45	69,36	61,4	54,41	48,26
L3	42,8	37,94	33,55	29,57	25,9	22,48	19,26
L3	16,19	13,25	10,41	7,704	5,301	3,836	

Table 7.7: EPR values, obtained on tower 10 of line L2 changing the fault point along the network

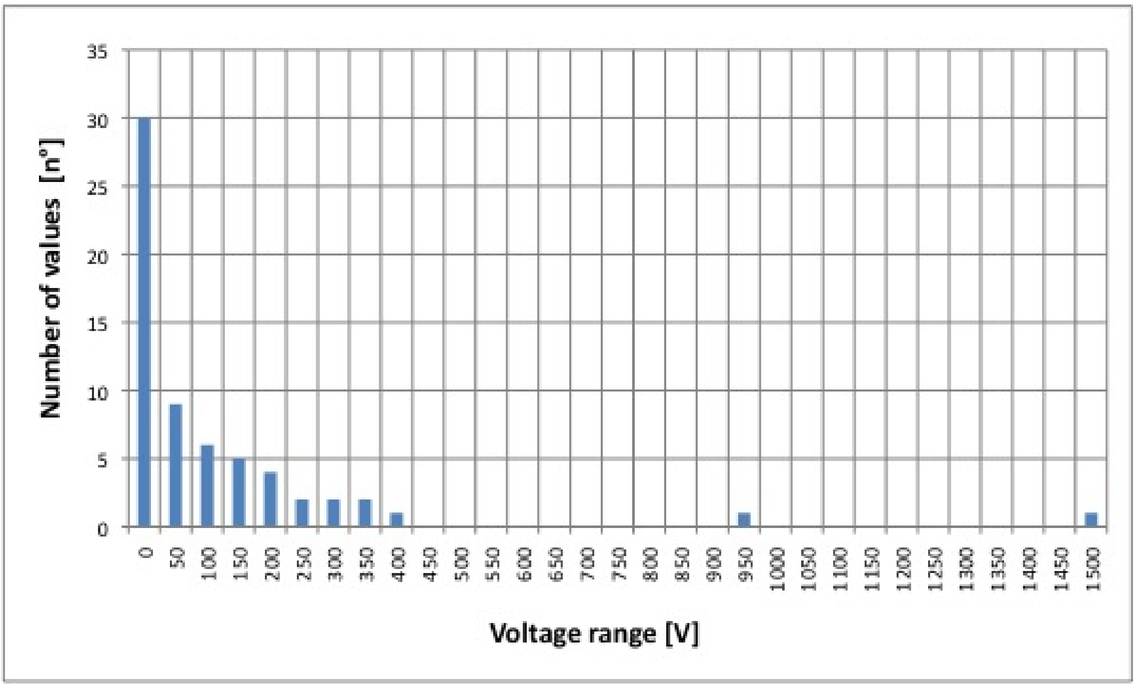

Figure 7.10: EPR statistic distribution on earth impedance $Ze2$ of substation 2

FAULT POSITION	EPR MAGNITUDE [V]					
L1	54,3	88,13	137,9	187,1	235,8	282,8	327,2
L1	371,7	416,1	461	506,9	554,5	604,4	657,4
L1	714,1	775,5	842,6	916,4	998,3	1090	1192
Ze2	2007						
L2	1069	959,9	864,6	779,7	703,7	635,2	572,9
L2	515,9	463,2	414	367,8	323,9	281,9	241,4
L2	201,9	163,1	124,7	86,68	49,53	22,14	
Ze3	13,55						
L3	20,08	19,57	18,46	17,41	16,45	14,95	13,43
L3	12,41	11,72	11,05	10,4	9,762	9,137	8,516
L3	7,893	7,258	6,02	5,911	5,82	5,76	

Table 7.8: EPR values, obtained on the earth impedance $Ze2$ of substation 2 changing the fault position along the network

7.2.3 Comments

As can we see in the charts, considering the tower footing EPR evaluation, all the trends are quite similar, with a rapid increment at the beginning until a peak point and a sudden decrement until the maximum range for each considered position.
Looking at the figures, the peak of the distributions is concentrate at extremely low voltage values; passing from tower 3 of line L1 to tower 10 of line L2, the peak translates from the right to the left, starting around 350 V until 50 V range values.
Regarding the minimum and maximum values, the lowest value of EPR, considering the towers, is present on the tower 10 of the second line L2 and the highest value is on tower 8 of the first line L1. Looking at the charts, moving away from the generator 1 towards the middle of the network, the peak concentration of the EPR values skips to the left to lower value.
One reason of this behaviour could be explained because near the generator there is less impedance which can limits the short-circuit current, indeed the impedance value is higher if the fault point is at the middle between substation 2 and 3 rather than close to the generator 1; the limit case is when it's considered the tower exactly at the middle of the network such as tower 10 of line L2, at this point the short–circuit current contribuition given by the two generators is exactly the same.
Looking at fig. 7.9, it shows a large amount of values between 0 and 50 V range, this proves that the earth potential rise is very low considering a tower in the middle which might describe the real behavior of tower footing resistance Earth Potential Rise on a meshed or more extended network where the generators are distributed in all the system. Evaluating these extremely low values we can say that, they can not be potentially dangerous for people who may standing close to the tower pylons or metal structure during the fault considering the permission touch voltage explained in chapter 2.
Looking at fig. 7.10, which describes the statistic distribution at substation earth impedance Ze_2, the trend is a sort of hyperbolic distribution; most of the values are concentrated between 0 and 50 V as seen for tower 10 on the line L2, with a decrement of number of values until 1500 V range. In this case the distribution is even better than the towers distribution where the peak is still at 0-50 V range but the maximum voltage range values are higher.
We can say that, on the earth substation impedances, the effects of short-circuit current regarding the earth potential rise and then the risk for the people connected to step and touch voltage is lower than the effects on tower footing resistance considering the total range values. Looking at minimum and maximum values it can be seen that, the minimum value variation follows the analysed positions; going from tower 3 close to the first generator to tower 10 of line L2 at the middle of the network, the minimum value decreases as the range of EPR peak value. Regarding the maximum value, its behaviour is completely different, starting from the initial position on tower 3 of line L1 the maximum value rises until the middle of the line and then it decrease until the end of it.
This kind of behaviour has a completely different trend compared with the tower footing voltage distribution seen in chapter 5; looking at the fig. 6.17 for a fixed faulted point the voltage is higher at the

beginning and at the end of the overhead line; considering instead the maximum values of earth potential rise changing the fault point they are at the middle of the considered overhead line which connects two substations.

7.3 SECOND CONFIGURATION

This configuration has been analysed changing soil and tower footing resistance parameters and short-circuit real power *Pcc* changing the generator impedances. In this case as we expect the magnitude of EPR values will be higher because of the higher value of the tower footing resistance and also due to the higher magnitude of short-circuit current.

7.3.1 Maximum and minimum value

As in the previous case, the values here reported below represent the maximum and minimum EPR magnitude in each considered point of analisys:

- **Vmax**=7199 [V] **Vmin**=500.6 [V] **TOWER 1, L1**
- **Vmax**=12739 [V] **Vmin**=415.8 [V] **TOWER 3, L1**
- **Vmax**=15844 [V] **Vmin**=344.3 [V] **TOWER 5, L1**
- **Vmax**=17352 [V] **Vmin**=103.4 [V] **TOWER 8, L1**
- **Vmax**=12346 [V] **Vmin**=97.27 [V] **TOWER 15, L1**
- **Vmax**=3766 [V] **Vmin**=27.4 [V] **TOWER 19, L1**
- **Vmax**=13891 [V] **Vmin**=22.51 [V] **TOWER 10, L2**
- **Vmax**=2007 [V] **Vmin**=13.5 [V] **EARTH IMPEDANCE Ze2**

7.3.2 Results

Here below there is a report of the charts and the tables relative to the second configuration. All the obtained values are relative to soil resistance $\rho = 1000\Omega m$ and tower footing resistance $RT = 20\Omega$; on the tables, the results have to be read from top to bottom and they are relative to the fault which changes the position from substation 1 to substation 4.

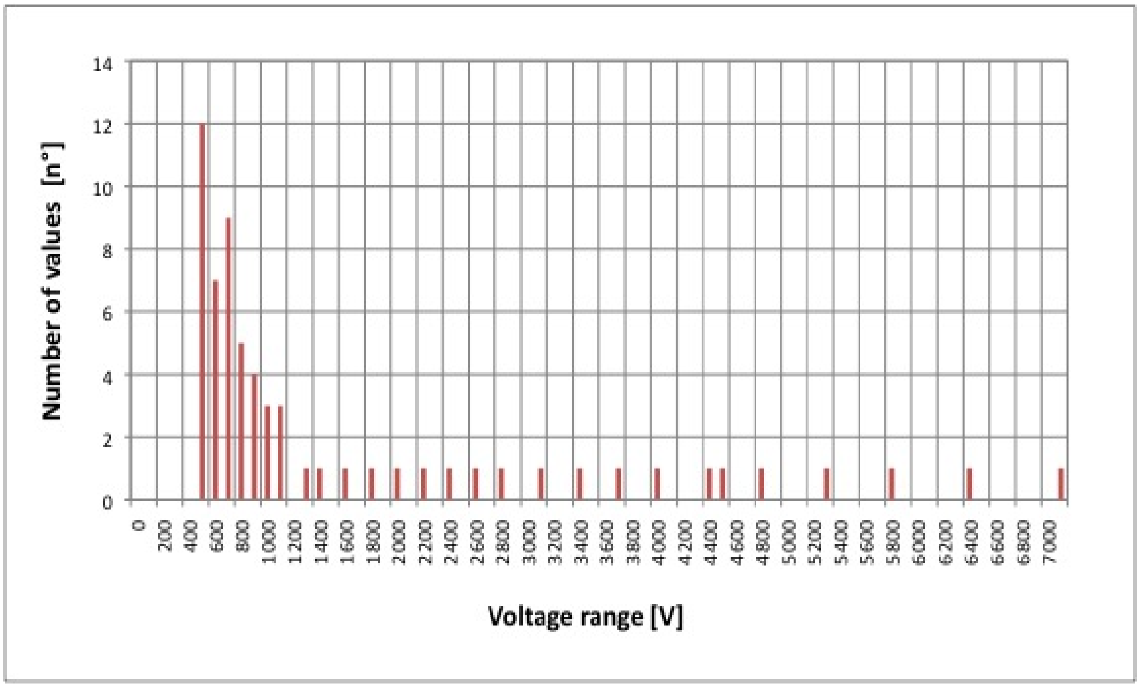

Figure 7.11: EPR statistic distribution on tower 1 of line L1

FAULT POSITION	EPR MAGNITUDE [V]						
L1	4437	7199	6457	5837	5300	4832	4419
L1	4052	3720	3419	3144	2889	2652	2431
L1	2223	2027	1841	1664	1495	1333	1179
Ze2	1111						
L2	1113	1092	1055	1021	990	961,5	935,2
L2	910,7	888	866,8	847,1	828,6	811,4	795,3
L2	780,5	766,9	754,5	743,3	733,5	725	
Ze3	726,4						
L3	705,9	687,8	671,7	656,3	642	628,4	615,6
L3	603,4	591,7	580,6	569,9	559,7	549,9	540,7
L3	532,2	524	516,7	510,2	504,8	500,6	

Table 7.9: EPR values, obtained on tower 1 of line L1 changing the fault point along the network

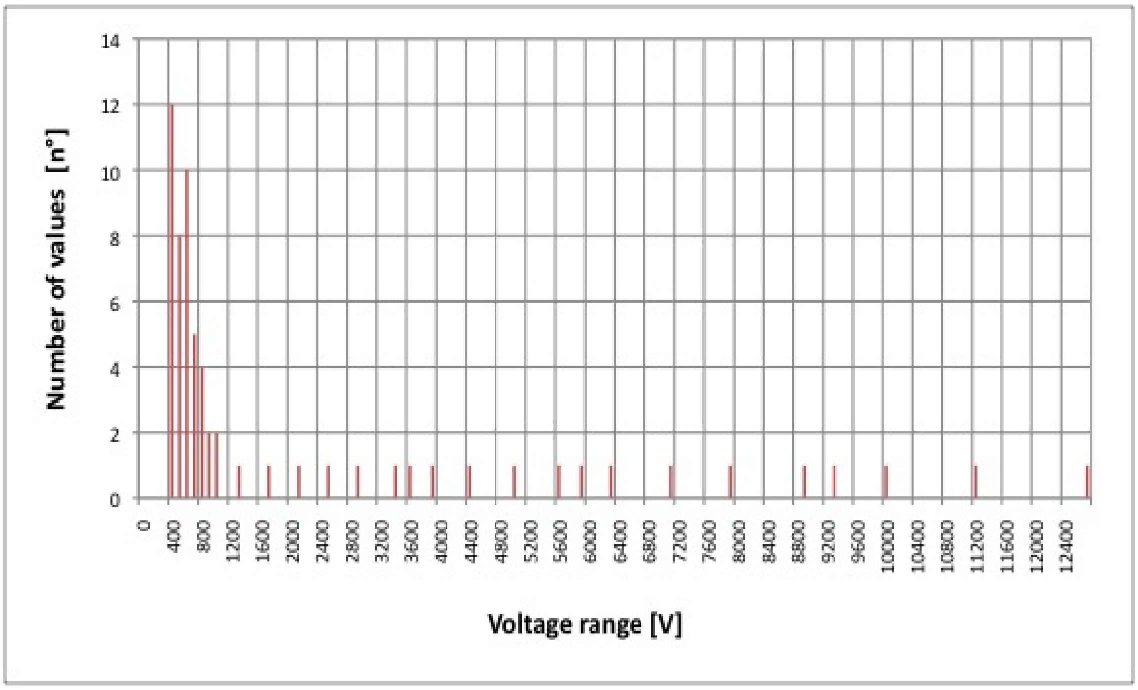

Figure 7.12: EPR statistic distribution on tower 3 of line L1

FAULT POSITION	EPR MAGNITUDE [V]						
L1	3685	5979	9354	12739	11276	10020	8932
L1	7977	7132	6374	5690	5066	4492	3960
L1	3463	2997	2557	2141	1748	1385	1066
Ze2	799,8						
L2	1017	972,2	932,8	896,7	864	834,2	806,9
L2	781,9	758,8	737,6	718	699,9	683,2	667,9
L2	653,8	640,9	629,3	618,8	609,5	601,4	
Ze3	604,9						
L3	585,5	570,5	557,1	544,4	532,5	521,3	510,7
L3	500,6	491	481,8	472,9	464,5	456,4	448,8
L3	441,6	435	429	423,7	419,2	415,8	

Table 7.10: EPR values, obtained on tower 3 of line L1 changing the fault point along the network

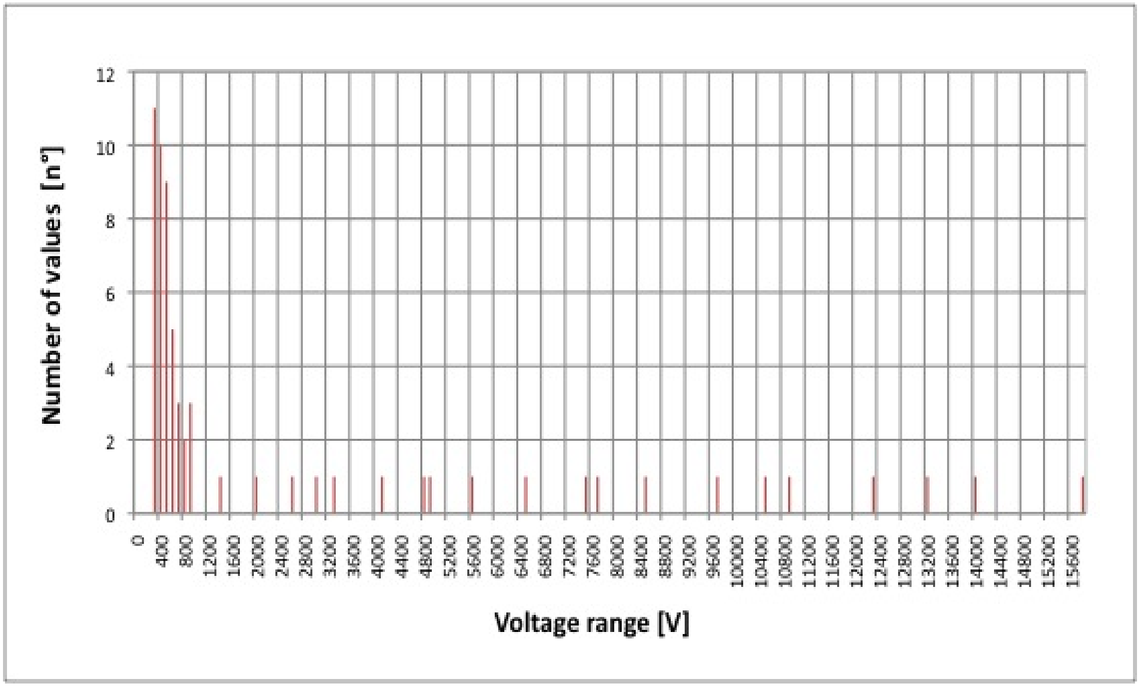

Figure 7.13: EPR statistic distribution on tower 5 of line L1

FAULT POSITION	EPR MAGNITUDE [V]						
L1	3052	4952	7747	10550	13244	15844	14002
L1	12391	10968	9700	8558	7520	6568	5688
L1	4865	4100	3375	2689	2045	1457	994,1
Ze2	500,2						
L2	941,2	903,2	850,6	811,7	776,4	744,2	714,9
L2	688	663,4	640,8	620,1	601,1	583,6	567,6
L2	552,9	539,5	527,3	516,2	506,2	497,3	
Ze3	502,5						
L3	484,1	471,7	460,7	450,2	440,4	431,1	422,3
L3	414	406	398,5	391,2	384,2	377,6	371,3
L3	365,4	360	355	350,7	347	344,3	

Table 7.11: EPR values, obtained on tower 5 of line L1 changing the fault point along the network

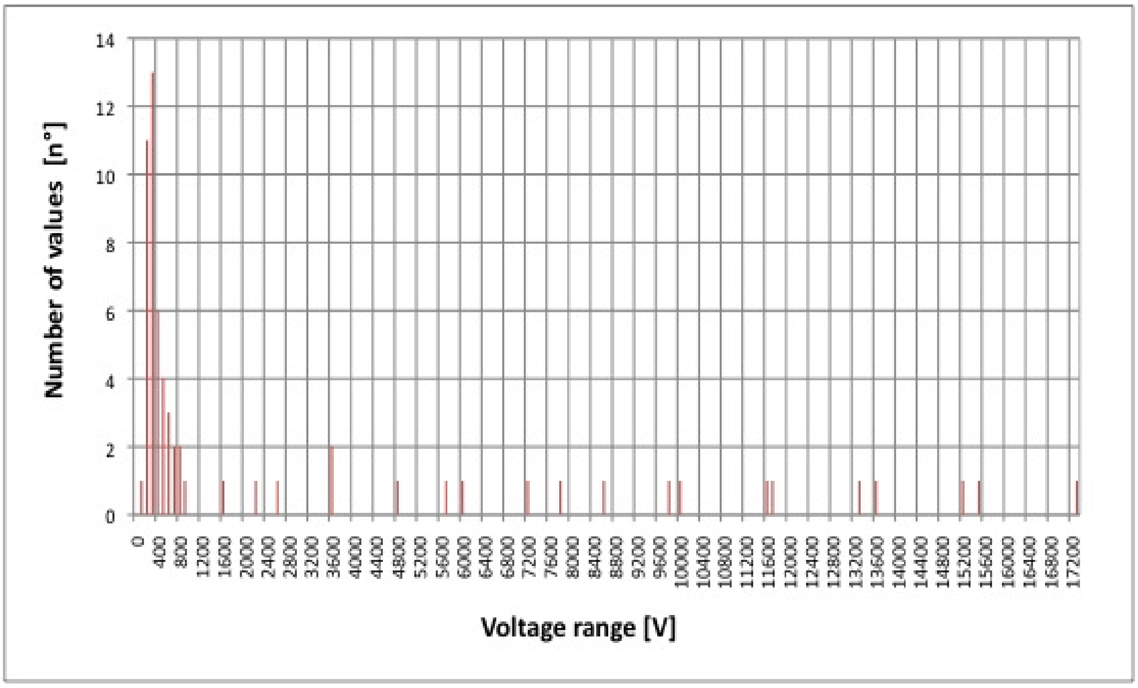

Figure 7.14: EPR statistic distribution on tower 8 of line L1

FAULT POSITION	EPR MAGNITUDE [V]						
L1	2266	3677	5753	7835	9835	11765	13646
L1	15500	17352	15249	13358	11643	10073	8625
L1	7276	6011	4816	3682	2609	1625	936,3
Ze2	103,4						
L2	878,4	825,7	778,6	735,4	696	659,9	626,8
L2	596,4	568,3	542,4	518,4	496,3	475,8	456,9
L2	439,3	423	407,9	393,9	380,7	368,4	
Ze3	374,9						
L3	358,6	349,4	341,1	333,3	326	319,2	312,7
L3	306,5	300,7	295,1	289,7	284,6	279,8	275,2
L3	270,9	266,9	263,3	260,2	257,6	229,7	

Table 7.12: EPR values, obtained on tower 8 of line L1 changing the fault point along the network

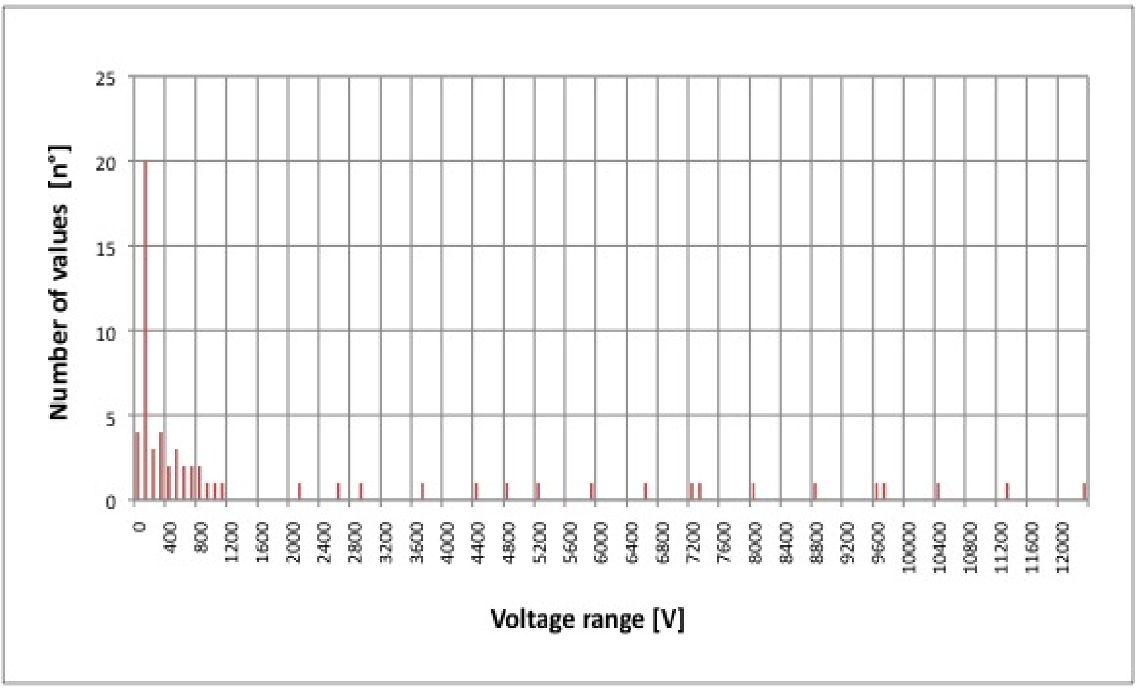

Figure 7.15: EPR statistic distribution on tower 15 of line L1

FAULT POSITION	EPR MAGNITUDE [V]						
L1	865,1	1121	2196	2991	3755	4491	5209
L1	5917	6624	7339	8070	8828	9623	10465
L1	11368	12346	9737	7250	4887	2601	943,8
Ze2	1062						
L2	866,3	797	735,7	680,1	629,5	583,2	540,5
L2	500,9	463,8	428,9	395,9	364,4	334,2	305,1
L2	276,9	249,4	222,5	195,8	169,1	142,3	
Ze3	142,7						
L3	137,9	133,9	130,3	127	123,9	121	118,4
L3	115,9	113,6	111,4	109,3	107,4	105,6	103,9
L3	102,3	100,9	99,7	98,66	97,84	97,27	

Table 7.13: EPR values, obtained on tower 15 of line L1 changing the fault point along the network

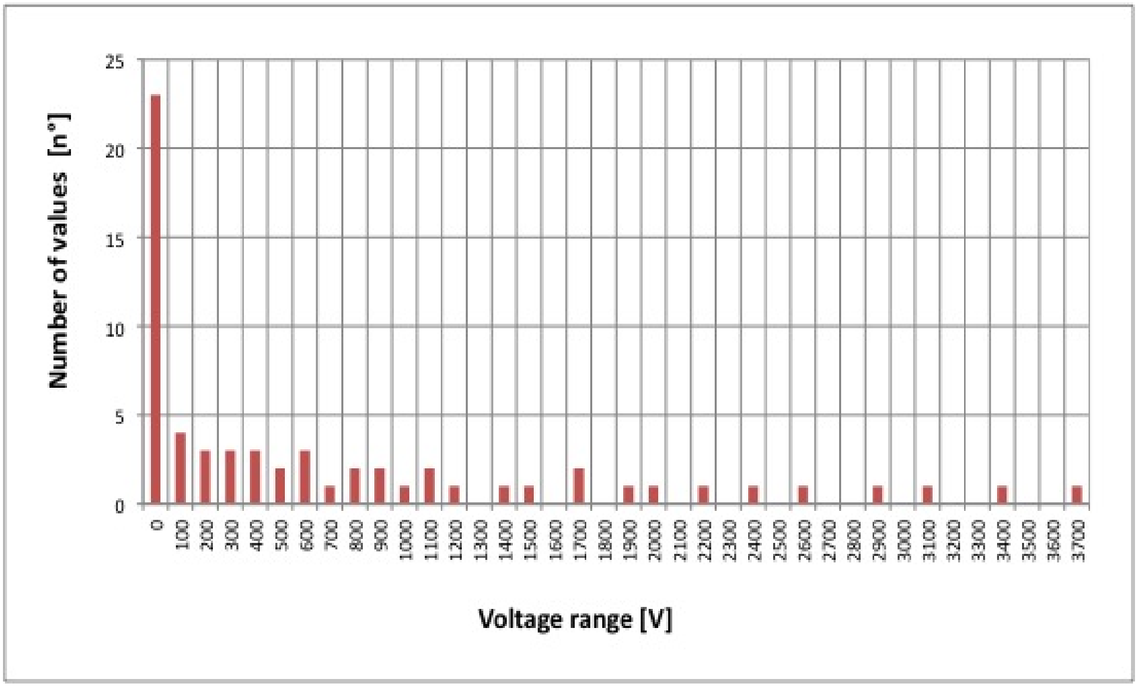

Figure 7.16: EPR statistic distribution on tower 19 of line L1

FAULT POSITION	EPR MAGNITUDE [V]						
L1	187,8	304,8	476,9	649,9	815,2	975,2	1131
L1	1285	1438	1593	1752	1917	2089	2272
L1	2468	2681	2913	3168	3451	3766	1115
Ze2	1799						
L2	1003	905,4	819,5	742,7	673,9	611,7	555
L2	503	454,7	409,7	367,2	326,8	288,1	250,6
L2	214,1	178,3	142,8	107,5	72,44	39,04	
Ze3	27,4						
L3	36,92	35	33,29	31,76	30,32	29,05	27,9
L3	26,87	25,93	25,08	24,32	23,64	23,02	22,5
L3	22,02	21,62	21,28	21	20,79	20,65	

Table 7.14: EPR values, obtained on tower 19 of line L1 changing the fault point along the network

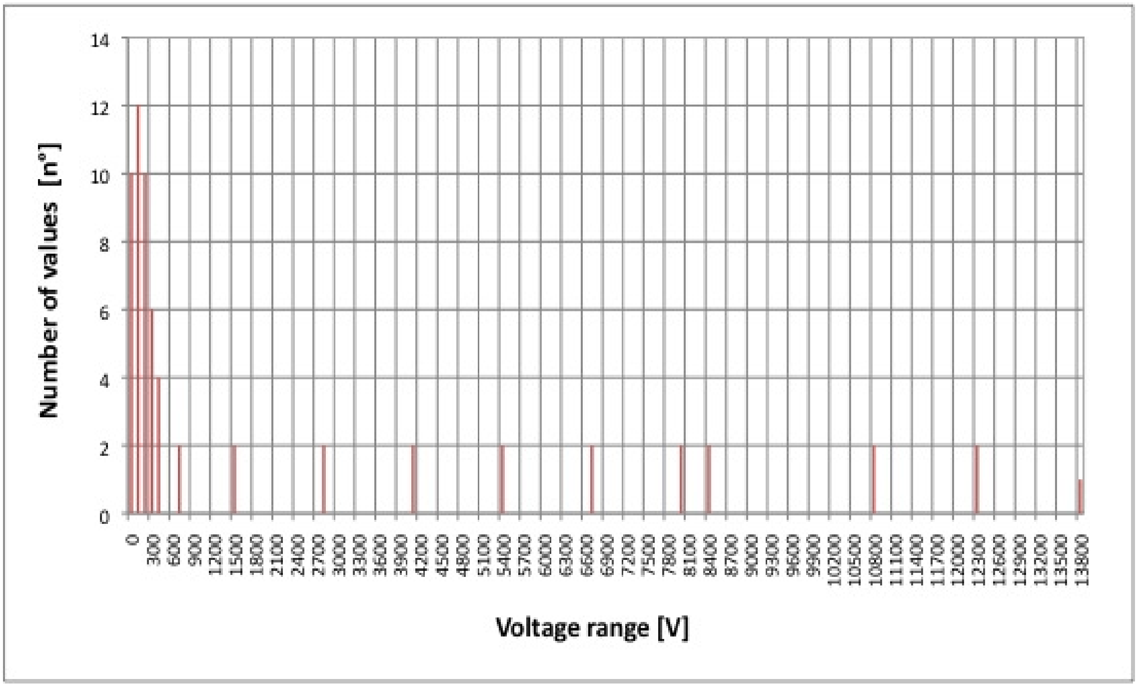

Figure 7.17: EPR statistic distribution on tower 10 of line L2

FAULT POSITION	EPR MAGNITUDE [V]						
L1	22,51	34,34	52,47	70,9	88,6	105,9	122,6
L1	139,2	155,7	172,3	189,4	207	225,6	245,2
L1	266,3	289	313,9	341,3	371,8	405,7	443,8
Ze2	752,5						
L2	1519	2809	4106	5404	6715	8050	9421
L2	10841	12326	13891	12326	10841	9421	8050
L2	6715	5404	4106	2809	1519	443,8	
Ze3	725,5						
L3	405,7	371,8	341,3	313,9	289	266,3	245,2
L3	225,6	207	189,4	172,3	155,7	139,2	122,6
L3	105,9	88,6	70,9	52,47	34,34	22,51	

Table 7.15: EPR values, obtained on tower 10 of line L2 changing the fault point along the network

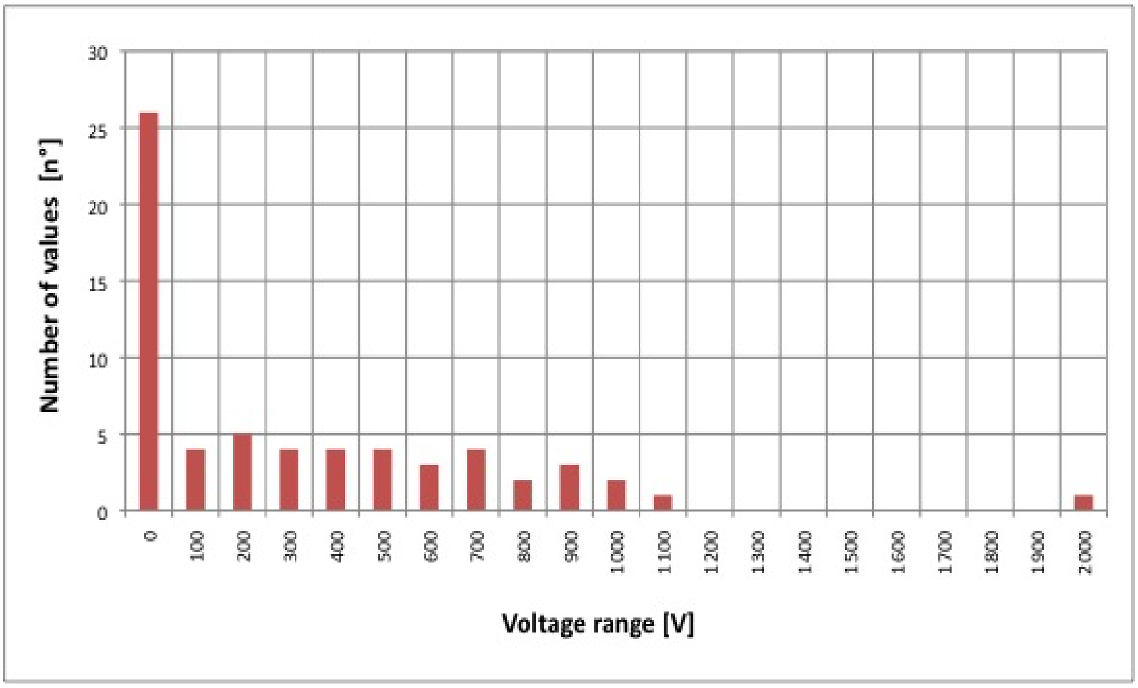

Figure 7.18: EPR statistic distribution on earth impedance $Ze2$ of substation 2

FAULT POSITION	EPR MAGNITUDE [V]						
L1	54,3	88,13	137,9	187,1	235,8	282,8	327,2
L1	371,7	416,1	461	506,9	554,5	604,4	657,4
L1	714,1	775,5	842,6	916,4	998,3	1090	1192
Ze2	2007						
L2	1069	959,9	864,6	779,7	703,7	635,2	572,9
L2	515,9	463,2	414	367,8	323,9	281,9	241,4
L2	201,9	163,1	124,7	86,68	49,53	22,14	
Ze3	13,55						
L3	20,08	19,57	18,46	17,41	16,45	14,95	13,43
L3	12,41	11,72	11,05	10,4	9,762	9,137	8,516
L3	7,893	7,258	6,02	5,911	5,82	5,76	

Table 7.16: EPR values, obtained on earth impedance $Ze2$ of substation 2 changing the fault position along the network

7.3.3 Comments

Comparing the charts between the different configurations, as expected, all the EPR values in this case are higher, either maximum and minimum value in all the considered points for the anlysis. The EPR distribution shape is quite similar on both configurations and this means that, the new values of the parameters, don't influence the trend but they influence only the magnitude, the peak point position and the voltage ranges.
The peak point in the second configuration is shifted on the right due to either the higher tower footing resistance and the higher short-circuit current values which contribute to increase the number of voltage values concentrated at higher ranges but, considering the risk of a possible damage, in statistic terms, we can say that is still quite low because the concentration of the values in all the points is around extremely low ranges. Obviously there are some values where the EPR magnitude is quite high and can be dangerous, but these values are rare or anyway single events which happen only when the fault is close to the considered position as on the towers near the faulted spans.
In conclusion, analysing both cases, first and second configuration, we can say that a short-circuit fault, which could happen along a transmission network, has a higher influence on the towers or earth substation impedance close to it.
Comparing the earth potential rise study between towers and substation we can say that the effects of a line-to-earth short-circuit produces more high values on the tower pylons rather than the substation earthing systems; considering the earth potential rise in all the network, the fault produces extremely low potential values which can not be considered dangerous in statistic terms for the person's safety also because there are even lower EPR values on the earth substation impedances where there might be higher danger for the personnel close to metal structure or electrical equipment.
The probabilistic study shows that a dangerous earth potential rise event has low probability to happen but there might be risk of electrocution with consequent damage for the people safety however.

Chapter 8

Current distribution on a meshed network

8.1 Introduciton

In this final chapter, a meshed network model with ATPDraw software as similar as possible to a real meshed network has been created looking for a start point for a possible future development.
The network represented in fig. 8.1 is composed by 10 substations with a nominal voltage of 275 kV and all of them are connected each other by one or more overhead lines with geometrical and electrical parameters used previously in the ATPDraw current distribution analysis with L2 tower pylon configuration shown in fig. 6.5; all the substation have the same value of earth impedance Ze=0,1 Ω and the side substations are feeded by three-phase sinusoidal generators.
The soil resistance value along the overhead lines which connect the susbstations is ρ=100 Ωm and the tower footing resistance of the tower pylons is RT=10 Ω.

All the considered substations are present in the UK network, as can be seen from the map which describes the substation disposition in NEPLAN represented in fig. 5.3; the considered substation are:

SUBSTATIONS
NEEPSEND
PISTMOOR
SHEFFIELD CITY
TEMPLEBOROUGH
WINCOBANK
BRINSWORTH
ALDWARKE
THURCROFT
WEST MELTON
THORPE MARSH

Table 8.1: Analysed substations

The overhead-lines which connect the substations each other were obtained from the NEPLAN model network and also compared with the Electric Ten Year Statment data; knowing the line length, the number of span were calculated with the hypothesis of single span length of 360 m.
The length characteristics are :

The scope of this simulation is to know the distribution of the earth fault current on the substation earthing systems when the fault, as a line-to-earth short-circuit, is placed in another substation within the network. This study was faced because all the substation protection equipment and parameters against the EPR and current flow through the earthing system might be overestimated; the amount of current wich flows through the earth substation impedances might be extremely lower than the set up values according with the standard design therefore, this study, was done to verify if the earth current flows

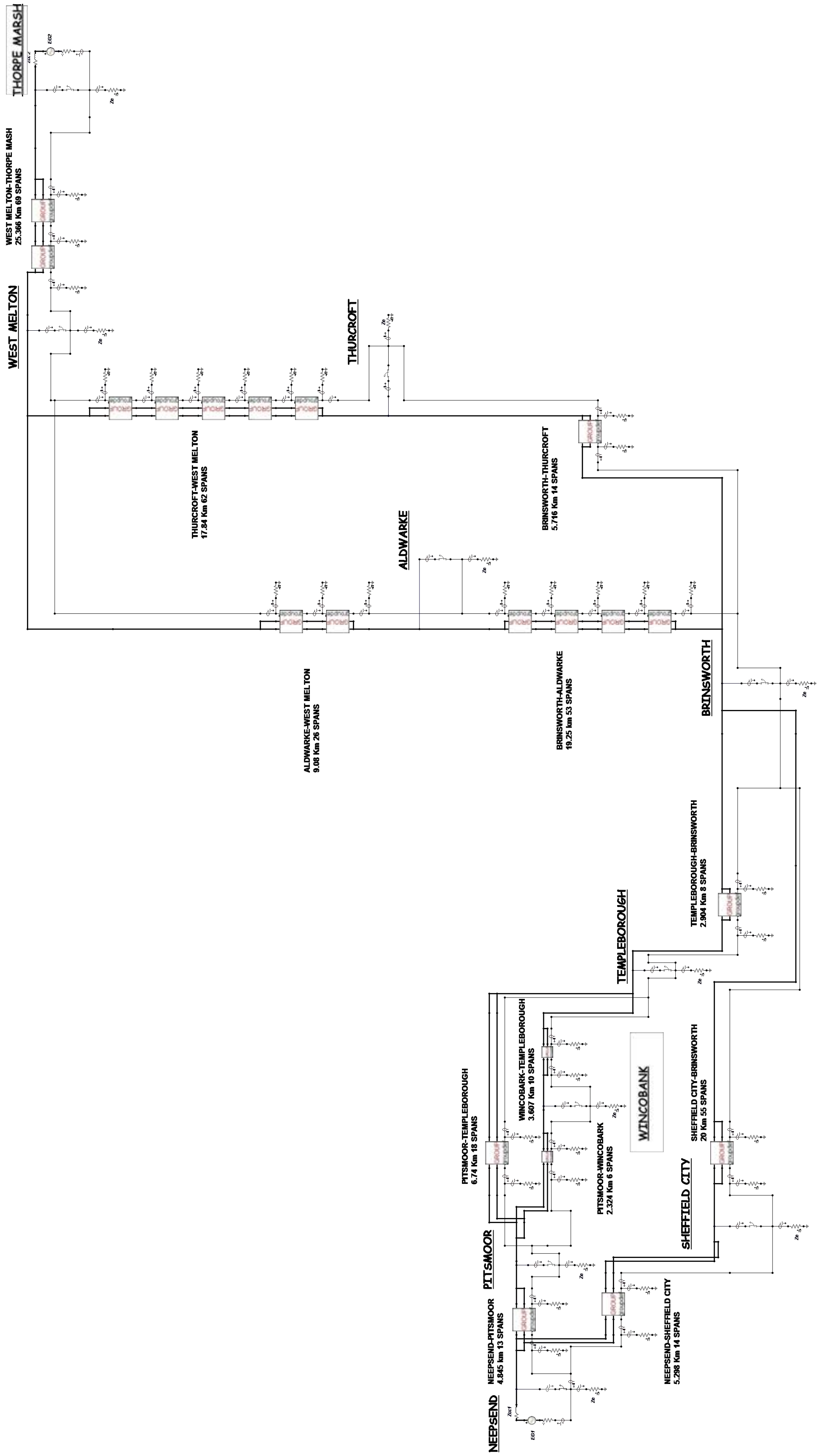

Figure 8.1: Meshed network composed by 10 substations with a nominal voltage of 275 kV, earth substation impedance $Ze = 0,1\Omega$ and two sides generators

LINE	**LENGTH** [km]	**SPANS** [$n°$]
NEEPSEND-PITSMOOR	4,845	13
NEEPSEND-SHEFFIELD CITY	5,298	14
PITSMOOR-TEMPLEBOROUGH	6,74	18
PITSMOOR-WINCOBANK	2,324	6
WINCOBANK-TEMPLEBOROUGH	3,607	10
SHEFFIELD CITY-BRINSWORTH	20	55
TEMPLE BOROUGH-BRINSWORTH	2,904	8
BRINSWORTH-ALDWARKE	19,25	53
BRINSWORTH-THURCROFT	5,716	14
ALDWARKE-WEST MELTON	9,08	26
THURCROFT-WEST MELTON	17,82	62
WEST MELTON-THORPE MARSH	25,366	69

Table 8.2: Line lengths and span number of the overhead-lines which connect the substations within the network

during a random substation fault within the network, may be dangerous for the people and than being reevaluated and then possibly reduced.
Since we want to get close to a real transmission network behaviour, considering the substations, the fault current magnitude in each of them, has been chosen with, more or less, the same value of the I_k maximum symmetrical short-circuit current obtained with NEPLAN simulation using the IEC 60909-0 standard changing the value of the short-circuit impedances of the side generators increasing or decreasing the short-circuit real power.
Once obtained the values of the current which we needed in the considered faulted substation all the current which flowed in the other substation earthing systems have been analysed and reported for each case in tables with magnitude and phase angle, taking into account that verse of the measured current has been considered positive when it flows from the substation to the soil.

8.2 Results

Considering the current with a phase angle between 0 and 180 degrees flowing down from the substation to the earth and the currents which have a phase angle between 0 and -180 degrees flowing up from the soil into the earth substation system, here below are reported all the substation faults and the relative current distributions in all the substation earthing systems.

NEEPSEND FAULT

The current value calculated with NEPLAN short-circuit analysis was 18263 A, in the ATPDraw network simulation the fault current value was 18298 A. The ratio between the amount of current which flows through the soil Igr and the fault current If is:

$$\frac{I_{gr}}{I_f} = \frac{2537.6}{18298} = 13\%$$

The currents on the substation earthing systems are reported in tab. 8.3.

SUBSTATION	CURRENT MAGNITUDE [A]	PHASE ANGLE [°]
PITSMOOR	47,34	-67,7
WINCOBANK	2,65	-146,9
SHEFFIELD CITY	43,48	-75,86
TEMPLEBOROUGH	0,707	168
BRINSWORTH	6,29	-164,8
ALDWARKE	0,126	-170
THURCROFT	0,167	-166
WEST MELTON	0,156	-173
THORPE MARSH	2681	-142

Table 8.3: Earth fault current distribution through the substation earthing systems when the fault is placed at NEEPSEND substation

PITSMOOR FAULT

The current value calculated with NEPLAN short-circuit analysis is 18438 A and in the ATPDraw network simulation the fault current value was 18673 A. The ratio between the amount of current which flows through the soil Igr and the fault current If is:

$$\frac{I_{gr}}{I_f} = \frac{11239}{18673} = 60\%$$

The currents on the substation earthing systems are reported in tab. 8.4.

SUBSTATION	CURRENT MAGNITUDE [A]	PHASE ANGLE [°]
NEEPSEND	5547	-143
WINCOBAnK	598	-40,3
SHEFFIELD CITY	152,2	99,8
TEMPLEBOROUGH	125,54	-101
BRINSWORTH	4,68	-176,84
ALDWARKE	0,144	-170
THURCROFT	0,147	172,5
WEST MELTON	0,177	-142,4
THORPE MARSH	3037	-142,4

Table 8.4: Earth fault current distribution through the substation earthing systems when the fault is placed at PITSMOOR substation

WINCOBANK FAULT

The current value calculated with NEPLAN short-circuit analysis is 18120 A, in the ATPDraw network simulation the fault current value was 18126 A. The ratio between the amount of current which flows through the soil Igr and the fault current If is:

$$\frac{I_{gr}}{I_f} = \frac{11325}{18126} = 62\%$$

The currents on the substation earthing systems are reported in tab. 8.5.

SUBSTATION	CURRENT MAGNITUDE [A]	PHASE ANGLE [°]
NEEPSEND	8370	-145
PITSMOOR	447,1	-30,12
SHEFFIELD CITY	143,4	98,8
TEMPLEBOROUGH	310,97	-56,92
BRINSWORTH	11,12	-140
ALDWARKE	0,14	-169,4
THURCROFT	0,263	-149,6
WEST MELTON	0,173	-173,7
THORPE MARSH	3036	-142

Table 8.5: Earth fault current distribution through the substation earthing systems when the fault is placed at WINCOBANK substation

TEMPLEBOROUGH FAULT

The current value calculated with NEPLAN short-circuit analysis is 18189 A, in the ATPDraw network simulation the fault current value was 18326 A.The ratio between the amount of current which flows through the soil Igr and the fault current If is:

$$\frac{I_{gr}}{I_f} = \frac{10891}{18326} = 59\%$$

The currents on the substation earthing systems are reported in tab. 8.6.

SUBSTATION	CURRENT MAGNITUDE [A]	PHASE ANGLE [°]
NEEPSEND	8259	-145,5
PITSMOOR	75,3	157,6
SHEFFIELD CITY	141,49	98,9
WINCOBANK	313,6	-55,5
BRINSWORTH	378	-45,649
ALDWARKE	0,132	-162,5
THURCROFT	6,69	-161
WEST MELTON	0,21	-175,6
THORPE MARSH	3272	-142,9

Table 8.6: Earth fault current distribution through the substation earthing systems when the fault is placed at TEMPLEBOROUGH substation

SHEFFIELD CITY FAULT

The current value calculated with NEPLAN short-circuit analysis is 16449 A, in the ATPDraw network simulation the fault current value is 16286 A. The ratio between the amount of current which flows through the soil Igr and the fault current If is:

$$\frac{I_{gr}}{I_f} = \frac{10115}{16286} = 62\%$$

The currents on the substation earthing systems are reported in tab. 8.7

SUBSTATION	CURRENT MAGNITUDE [A]	PHASE ANGLE [°]
PITSMOOR	144,73	107,5
WINCOBANKK	7,59	28,4
NEEPSEND	7761	-145,2
TEMPLEBOROUGH	1,55	-38,5
BRINSWORTH	0,48	59,1
ALDWARKE	0,05	-164
THURCROFT	0,137	-157
WEST MELTON	0,115	-168,47
THORPE MARSH	2544	-141,8

Table 8.7: Earth fault current distribution through the substation earthing systems when the fault is placed at SHEFFIELD CITY substation

BRINSWORTH FAULT

The current value calculated with NEPLAN short-circuit analysis is 22346 A, in the ATPDraw network simulation the fault current value was 22164 A. The ratio between the amount of current which flows through the soil Igr and the fault current If is:

$$\frac{I_{gr}}{I_f} = \frac{12502}{22164} = 56\%$$

The currents on the substation earthing systems are reported in tab 8.8

SUBSTATION	CURRENT MAGNITUDE [A]	PHASE ANGLE [°]
PITSMOOR	187	109,5
WINCOBANK	4,07	-111,4
SHEFFIELD CITY	171,1	99,6
TEMPLEBOROUGH	459,3	-44,79
NEEPSEND	9950	-144,7
ALDWARKE	1,42	72,18
THURCROFT	214,2	-75,4
WEST MELTON	0,26	-174,8
THORPE MARSH	3988	-142,9

Table 8.8: Earth fault current distribution through the substation earthing system when the fault is placed at BRINSWORTH substation

WEST MELTON FAULT

The current value calculated with NEPLAN short-circuit analysis is 21935 A, in the ATPDraw network simulation the fault current value was 21803 A. The ratio between the amount of current which flows through the soil Igr and the fault current If is:

$$\frac{I_{gr}}{I_f} = \frac{12783}{21803} = 58\%$$

The currents on the substation earthing systems are reported in tab. 8.9.

SUBSTATION	CURRENT MAGNITUDE [A]	PHASE ANGLE [°]
PITSMOOR	133,12	110,58
WINCOBANK	7,07	-142,1
SHEFFIELD CITY	122,3	102,4
TEMPLEBOROUGH	1,48	-31,4
NEEPSEND	7138	-142,1
ALDWARKE	46,87	-144,8
THURCROFT	0,296	0,26
BRINSWORTH	0,193	-140,7
THORPE MARSH	6685	-143,6

Table 8.9: Earth fault current distribution through the earth substation system when the fault is placed at WEST MELTON substation

ALDWARKE FAULT

The current value calculated with NEPLAN short-circuit analysis is 18229 A, in the ATPDraw network simulation the fault current value was 18559 A. The ratio between the amount of current which flows through the soil Igr and the fault current If is:

$$\frac{I_{gr}}{I_f} = \frac{11428}{18559} = 61\%$$

The currents on the substation earthing systems are reported in tab. 8.10.

SUBSTATION	**CURRENT MAGNITUDE [A]**	**PHASE ANGLE [°]**
PITSMOOR	128	110
WINCOBANK	6,8	31
SHEFFIELD CITY	117,6	102,2
TEMPLEBOROUGH	1,47	-31,5
NEEPSEND	4283	-144
WEST MELTON	39,98	-144
THURCROFT	0,09	-146
BRINSWORTH	1,19	-71
THORPE MARSH	4863	-143

Table 8.10: Earth fault current distribution through the substation earthing systems when the fault is placed at ALDWARKE substation

THURCROFT FAULT

The current value calculated with NEPLAN short-circuit analysis is 20,604 A, in the ATPDraw network simulation the fault current value was 20600 A. The ratio between the amount of current which flows through the soil Igr and the fault current If is:

$$\frac{I_{gr}}{I_f} = \frac{12717}{20600} = 62\%$$

The currents on the substation earthing systems are reported in tab. 8.11.

SUBSTATION	**CURRENT MAGNITUDE [A]**	**PHASE ANGLE [°]**
PITSMOOR	165,6	205,2
WINCOBANK	8,78	-31,4
SHEFFIELD CITY	172	101,1
TEMPLE BOROUGH	6,48	-145,9
NEEPSEND	8877,9	-143,5
ALDWARKE	0,156	162,2
BRINSWORTH	189	-74,48
WEST MELTON	0,155	9,41
THORPE MARSH	4050	-142,6

Table 8.11: Earth fault current distribution through the substation earthing systems when the fault is placed at THURCROFT substation

THORPE MARSH FAULT

The current value calculated with NEPLAN short-circuit analysis is 25276 A, in the ATPDraw network simulation the fault current value was 25279 A. the ratio between the amount of current which flows through the soil Igr and the fault current If is:

$$\frac{I_{gr}}{I_f} = \frac{2941}{25279} = 12\%$$

The currents on the substation earthing systems are reported in tab 8.12.

SUBSTATION	**CURRENT MAGNITUDE [A]**	**PHASE ANGLE [°]**
PITSMOOR	52,62	113
WINCOBANK	2,864	33,8
SHEFFIELD CITY	48,34	105,2
TEMPLEBOROUGH	0,68	-21,36
NEEPSEND	1510	-143,3
ALDWARKE	0,02	-89,6
THURCROFT	0,057	-11,49
WEST MELTON	0,05	-113,3
BRINSWORTH	0,123	-11,8

Table 8.12: Earth fault current distribution through the substation earthing systems when the fault is placed at THORPE MARSH substation

8.2.1 BRINSWORTH substation fault, graphic distribution

Considering only the BRINSWORTH substation fault, in fig. 8.2 is reported the graphic distribution of the earth fault currents and its values taken from table considering the flow directions hypothesis.

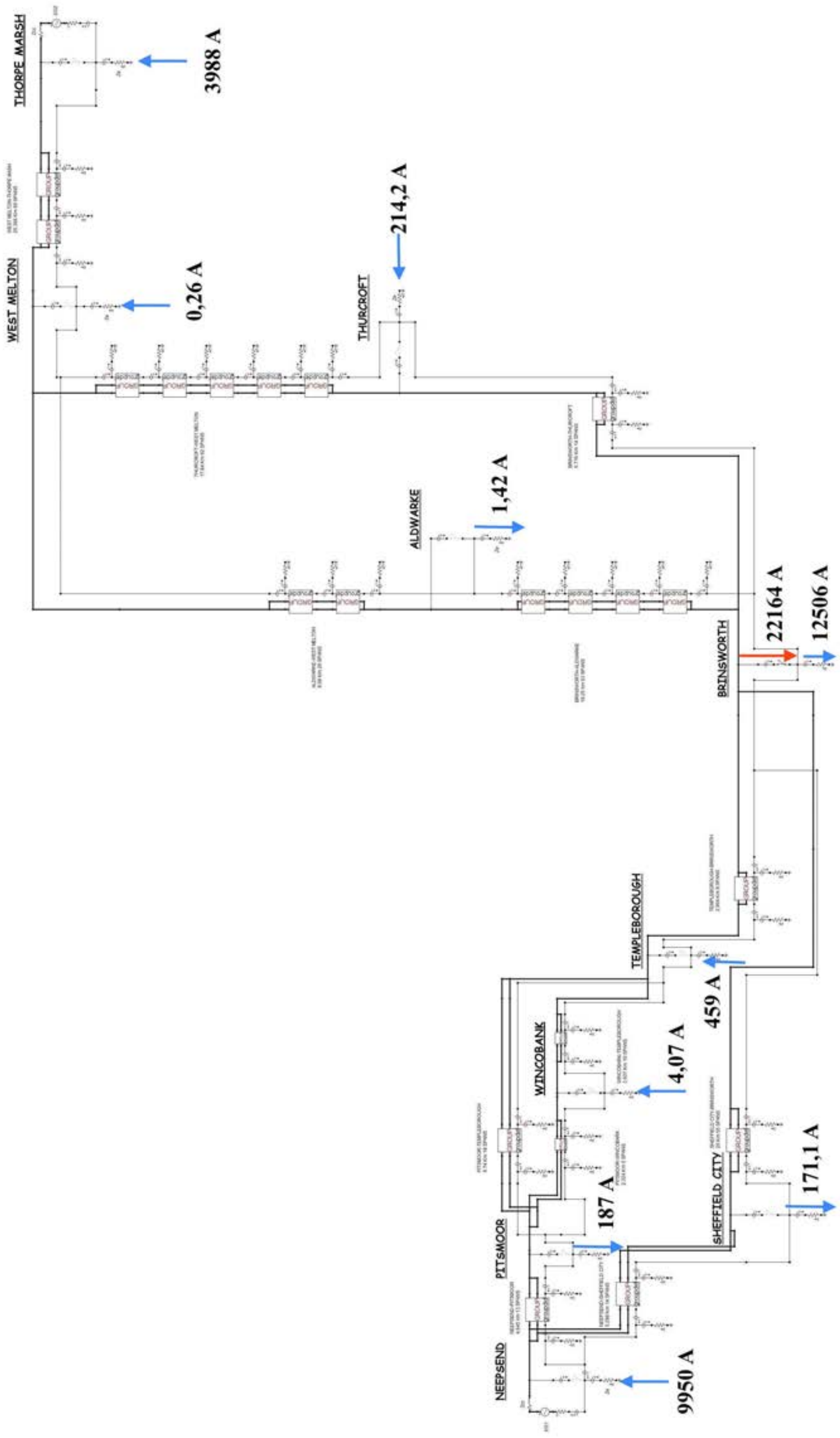

Figure 8.2: Current distribution on the substation earthing systems with the fault placed at BRINSWORTH substation

8.3 Comments

Looking at the values we can say that in all the substations the ratio between the ground current I_{gr} and the fault current I_f is, as seen on the previous chapters, still around 60% as expected. At the side substations the ratio is around the 13%; this difference can be explained by the fact that in cases where the short-circuit point is set nearby the generator substations, only a small amount of current flows through soil because it has to flow up immediately through the generator earthing system path which connect the earth impedance to the neutral point.
Regarding the obtained values we can say that changing the fault position, obviously the current flow through a particular substation earth impedance will change as well; the flow directions depends on which substation is faulted and how far away it is from the considered earthing systems.
Globally, looking at the results reported in the tables, the current values are quite low; if we consider the substations not feeeded by generators the maximum current is present on WINCOBANK earth impedance with a value of 598 A when the fault is set at PITSMOOR substation which is one of the closest.
Considering each substation fault it can be observed that the highest current value flows through the earthing system of the closest substation, this means that a part of fault current after split through the earth wires connected to the earthing system, enters for almost 60% through the earth impedance. After that the mostly part of the flow follows the overhead line which connects the closest substation and it flows up through the earthing system of the next substation. Looking at fig. 8.2 we can make many observations; the first is relative to the substations directly connected to the faulted point. The 53% of the fault current flows through the earth impedance and then it splits following the connected overhead lines distributing its magnitude in order to the closest substations.
As can be seen from the figure the closest connected substation is TEMPLEBOROUGH by an overhead line 2,904 km long where, through its earth impedance Ze flow 459 A; after that the next closest substation is THURCROFT where flow 214,2 A.
The last directed connected substation are, SHEFFIELD CITY, where a current of 171,2 A flows and ALDWARKE, with a current of 1,42 A. As can be noticed the current magnitude decreases its value going from the closest to the most distant connected substation following the overhead lines.

Chapter 9

Conclusions and possible further developments

In this thesis many kinds of studies and analysis have been faced; starting from the evaluation of the short-circuit current magnitude using the IEC standard in case of substation fault the obtained values reflect enough the real short-circuit values given by the National Grid on the Electric Ten Years Statement and they were compared with maximum short-circuit current values for a high voltage transmission system which gave us a quite similar values. The data also gave us an important knowledge of the magnitude of short-circuit current at different substation which was a first useful evaluation of the network, for a short circuit fault response analysis.

Continuing with the voltage study, the potential rise and the analysis of its distributon allowed us to know the influence of a fault as a line-to-earth short-circuit on the substation nodes and how the current spreads within the network. This particular study could be a very good start point for a further work consisting on developing a sort of network map distribution which can represent the voltage rise distribution area in each substation fault case starting from the fault point including all the nodes which assume a voltage during the line-to-earth short-circuit underneath 95% of the nominal voltage; this could be very helpful also for the system operator because, knowing the effects of a single substation fault on the voltages in all the busbars nodes, it can be possible to evaluate the part of the system affected mostly during a line-to-earth short-circuit placed at a substation.

The aim of this thesis was basically the study of earth fault current distribution on the transmission network and this aim was reached studying different network configurations; starting from a simple model and step by step, coming to a more complex network as a meshed system, we obtained many results as tower footing current and span current distribution along the earth wire, tower current phase angle and voltage; we have seen how the electric parameters as soil resistance, tower footing resistance, short-circuit power or line length influence the current and potential values and how they spreads along the lines giving a real view about the effects of a line-to-earth short-circuit on overhead line components either in case of substation fault and span fault. After that the earth potential rise study was one of the most important analysis; the statistic results gave an important indication about the range values where the potential distribution is concentrated.

As explained in the chapter comments we can say that the EPR, which is created by a current flow through metal structures as tower pylons and earth substation impedances, can be considered negligible in probabilistic terms as danger for people safety but it could always occurs during a line-to-earth short-circuit with high values and cause risk of electrocution. Earth substation standard designs support that, in case of fault, the expected current flow values through the soil and through earth substation impedances close and around to the fault area are high and not negligible but this study makes a really good re-evaluation of these distributions; the results indeed showed that the highest values are around the fault point but these values are within a range which can not be considered "high".

Knowledge of statistic representation in each point of the network of the earth potential rise might be a very useful tool to be used as a primary evaluation about the potential magnitude assumed by a pylon or a substation earthing system when a fault occurs in a random point of the transmission system, evaluating if those values might be potentially dangerous for people or electrical equipment; a future work which can be developed is a statistic map of the earth potential rise which represents the distribution curves of each pylons, substation or network node showing the earth potential range during a line-to-earth short-circuit which could occur in any part of high voltage transmission system and used to take adapt preventive measurements. Another possible development of this work could be the building of complete UK transmission network model in ATPDraw with all the lines, substations and generators setting real soil resistance and tower footing resistance parameters along each overhead line. An accurate analysis could be even improved using a better model as a double layer soil resistance distribution; having this model it would be easy to study the earth current distribution within the transmission earthing system and a further study about the potential rise which giving good results, can be useful for better design and study of the fault cases.

Bibliography

[1] F. Dawalibi "Ground Fault Current Distribution Between Soil and Neutral Conductors", IEEE Transactions, vol. PAS-99, no. 2, pp.452 -461, 1980.

[2] F. Dawalibi , D. Bensted and D. Mukhedkar "Soil Effects on Ground Fault Currents", IEEE Transactions, vol. PAS-100, no. 7, pp.3442 -3450, 1981.

[3] R. Verma and D. Mukhedkar "Ground Fault Current Distribution in Sub-Station Towers and Ground Wire", IEEE Transactions, vol. PAS-98, no. 3, pp.724 -730 1979.

[4] F. Dawalibi and D. Mukhedkar "Ground Fault Current Distribution in Power Systems-The Necessary Link", IEEE summer meeting.

[5] " Short-circuit currents in three-phase a.c. systems, Part: 0, Calculation of currents, IEC 60909-0, 2001.

[6] R.Caldon, M. Fauri, L. Fellin, A. Paolucci, R. Turri "Parallel path earthing systems in power distribution networks", Proc. of ERA Technology Conference "Earthing systems-Which path to follow?", Manchester, U.K., July 1993, pp. 3.4.1-3.4.10.

[7] J. Ma and F.P. Dawalibi "Correlation between worst case safety conditions and soil resistivity under power system fault conditions" Safe Engineering Services and technologies ltd. 1544 Viel, Montreal, Quebec, Canada, H3M 1G4, pp. 1-5.

[8] N. Ramezani, S.M. Shahrtash, "A complete procedure to determine earth fault current distribution and split factor for grounding grid design of HV substations",Iranian Journal of Science and Technology, Transaction B, Engineering, Vol. 32, No. B3, pp 205-221, 2008.

[9] National Grid, Electricity Ten Years Statement 2014, *http://www2.nationalgrid.com/UK/Industry-information/Future-of-Energy/Electricity-Ten-Year-Statement/.*

[10]Dr. Engineer E. Viel , PhD thesis, Earth fault current distribution on power systems, electrical division, School of engineering, University of Wales, Cardiff, December 2001.